The reproductive and physiological condition of a deep-sea mussel (*Bathymodiolus septemdierum* Hashimoto & Okutani, 1994) living in extremely acidic conditions

by

Giulia Rossi
B.Sc., University of Guelph, 2014

A Thesis Submitted in Partial Fulfillment
of the Requirements for the Degree of

MASTER OF SCIENCE

in the Department of Biology

Supervisory Committee

The reproductive and physiological condition of a deep-sea mussel (*Bathymodiolus septemdierum* Hashimoto & Okutani, 1994) living in extremely acidic conditions

by

Giulia Rossi
B.Sc., University of Guelph, 2014

Supervisory Committee

Dr. Verena Tunnicliffe, Department of Biology
Supervisor

Dr. Louise Page, Department of Biology
Departmental Member

Dr. Sarah Dudas, Department of Biology
Departmental Member

Abstract

Oceanic uptake of anthropogenic CO_2 emissions is causing wholesale shifts seawater carbonate chemistry towards a state of decreased carbonate ion concentration and reduced ocean pH. This change in water chemistry has potentially dire implications for marine organisms, especially those that build and maintain calcium carbonate structures. Our understanding of how ocean acidification may affect marine organisms is limited, as most studies have been short-term laboratory experiments. The CO_2 flux from hydrothermal vent fluids on NW Eifuku submarine volcano (Mariana Volcanic Arc) provides a natural setting to investigate the effects of acidification. Here, the vent mussel, *Bathymodiolus septemdierum*, lives in water with pH as low as 5.22. This study was designed to examine the consequences of a low pH environment on reproduction, calcification and somatic growth in *B. septemdierum*, since the presumed elevated cost of acid-base regulation may diminish available energy for these processes. Histological analysis reveals both females and males display synchronous gametogenesis across collection sites with spawning occurring between late winter and early spring. Mussels are functionally dioecious, although evidence of protogynous hermaphroditism was found– a first record for the genus. In comparison with mussels at near normal pH, we find no evidence that the pattern of gametogenesis is affected by low pH conditions. However, calcification is compromised: at a given shell volume, shells from NW Eifuku weigh about half those from sites with near normal pH mussels. The condition index (CI = body ash free dry weight/ shell volume) was assessed in mussels collected from four low pH sites on Northwest Eifuku and two control sites from Lau Basin and Nifonea Ridge; we show that low pH conditions negatively affect CI, especially when energy

availability is limited. *Bathymodiolus septemdierum* acquires energy from chemoautotrophic symbionts in the specialized gill epithelial cells. Using a gill condition index (GCI = gill ash free dry weight/ shell volume) and transmission electron microscopy to determine symbiont abundances in gill tissues, we show that NW Eifuku mussels with healthy gills and abundant symbionts have a higher CI than mussels from NW Eifuku with unhealthy gills. Optimal environmental sulphide concentrations appear to sustain higher symbiont abundances. While the survival of mussels on NW Eifuku is remarkable, it can come at a considerable cost to body and shell condition when during periods of energy limitation. *Bathymodiolus septemdierum* shows substantial resilience to low pH conditions when energy availability is sufficient due to energy budget adjustments that maximize fitness.

Table of Contents

List of Tables

List of Figures

Acknowledgments

It has been a great honour and privilege to have Dr. Verena Tunnicliffe as my supervisor. From beginning to end, Verena has showed me unwavering kindness and support. She pushed me forward and led the way to the next plateau, never ceasing to inspire me along the way. For her patience, guidance and inspiration, I am more thankful than words can say.

There are many other people I would like to thank, without whom this research would not have been possible. To my committee members, Dr. Louise Page and Dr. Sarah Dudas, thank you for all of your advice and support throughout this project and for guiding my research in the right direction. I would like to give a big thank you to Brent Gowen for his assistance in the lab and for teaching me the protocols for histology and transmission electron microscopy. Thank you to all those on the NOAA Submarine Ring of Fire 2014 cruise who facilitated sample collections, especially Chief Scientist, Dr. William Chadwick (University of Oregon/NOAA), and Dr. David Butterfield (University of Washington/NOAA) for water chemistry. I would also like and to thank Roxanne Beinart and Cherisse du Preez for taking the time to collect samples for me while at sea on the Falkor 2016 cruise. I am extremely grateful to all those in the Tunnicliffe and associated labs for being so supportive, providing feedback, and making this learning experience so memorable. I would like to especially thank Jonathan Rose for always lending a helping hand no matter what the situation, and Jackson Chu and Rachel Boschen for being the first to offer advice when I needed it most.

Most of all, my heartfelt appreciation goes to my family. To my mom, Mirella, thank you for your unwavering love and endless support, for being my anchor when life gets tough and for inspiring me to be the best I can be. To my brothers, Stefano and Gianluca, thank you for all your love and for making everyday so much brighter. To Jan, thank you for all your love and kindness, and for continually lifting my spirits with your zest for life. Last but not least, my deepest thanks to my partner, David, for his unconditional love and encouragement throughout this amazing adventure. Thank you for standing by my side through every tear and triumph.

Dedication

To my Mom

For her support, and constant love that sustains me.

Chapter 1 : General Introduction

Ocean acidification

Rising atmospheric carbon dioxide (CO_2) has become one of the most urgent environmental problems that we currently face. Prior to the industrial revolution, atmospheric CO_2 levels were approximately 280 parts per million (ppm). Presently, anthropogenic CO_2 emissions have caused atmospheric levels to exceeded 400 ppm (Wang et al., 2016). The ocean rapidly equilibrates with atmospheric CO_2 and is estimated to have absorbed about one third of all anthropogenic CO_2 emissions since 1760 (Kleypas et al., 2006). The following equation illustrates the flux of inorganic carbon between the atmosphere and ocean:

$$CO_{2\,(air)} \leftrightarrow CO_{2\,(water)} \qquad \text{Equation 1}$$

Dissolved CO_2 undergoes a hydrolysis reaction to form carbonic acid (H_2CO_3):

$$CO_2 + H_2O \leftrightarrow H_2CO_3 \qquad \text{Equation 2}$$

However, H_2CO_3 is a weak acid that dissociates almost immediately to form bicarbonate (HCO_3) and hydrogen (H^+) ions:

$$H_2CO_3 \leftrightarrow HCO_3^- + H^+ \qquad \text{Equation 3}$$

Under alkaline conditions (pH>7), the bicarbonate ion can also dissociate its hydrogen atom to yield H^+ and a carbonate ion (CO_3^{2-}). Moreover, when excess CO_2 is absorbed by the oceans (resulting in increased H^+ concentrations), this reaction reverses and CO_3^{2-} acts to buffer the excess CO_2:

$$HCO_3^- \leftrightarrow CO_3^{2-} + H^+ \qquad \text{Equation 4}$$

The relative proportion of each of these inorganic forms of carbon governs ocean pH. With a modern seawater pH of approximately 8, large amounts of HCO_3^- and CO_3^{2-} act to buffer the change in ocean pH caused by CO_2 absorption. In the long-term, continuing absorption of anthropogenic CO_2 will lead to a net decrease in the concentration of CO_3^{2-} ions in seawater ultimately reducing the ocean's buffering capability and resulting in ocean acidification. The pH of the surface ocean is already 0.1 unit below preindustrial values (~8.179), and is expected to decline by as much 0.4 units by 2100 (Gattuso et al., 2015).

Ocean Acidification: Problems for calcifying marine organisms

Ocean acidification poses a serious threat to marine organisms that produce calcium carbonate ($CaCO_3$) skeletons, shells, and internal structures like otoliths and statoliths. Marine organisms use calcium ions (Ca^{2+}) and CO_3^{2-} in seawater to precipitate $CaCO_3$ structures (Orr et al. 2005):

$$CO_3^{2-} + Ca^{2+} \leftrightarrow CaCO_{3\,(solid)} \qquad \text{Equation 5}$$

The concentration of Ca^{2+} is relatively constant throughout the water column, but the concentration of CO_3^{2-} changes considerably with depth. The deep ocean has inherently high CO_2 concentrations from respiration processes associated with the decomposition of falling organic matter. When the concentration of CO_2 is high, the excess H^+ from the dissociation of H_2CO_3 binds to CO_3^{2-} thereby decreasing its availability to calcifying organisms (Equation 4). Additionally, the excess CO_2 decreases ocean pH and ultimately dissolves any $CaCO_3$ supplied to the deep ocean from the die-off of calcareous surface plankton:

$$CaCO_3 + CO_2 + H_2O \leftrightarrow Ca^{2+} + 2HCO_3^- \qquad \text{Equation 6}$$

Therefore, as the ocean absorbs large amounts of anthropogenic CO_2, the challenges for calcifiers are two-fold, 1) the decreased availability of CO_3^{2-} reduces repair and formation rates of $CaCO_3$ structures and, 2) the dissolution of $CaCO_3$ weakens existing $CaCO_3$ structures.

Several recent studies investigate the effects of ocean acidification on various calcifying organisms. Although responses are variable and species specific, the general consensus is that calcifying organisms will be negatively affected as ocean acidification progresses. Ries et al. (2009) note a net decrease in calcification with increasing CO_2 partial pressure (pCO_2) in temperate corals, pencil urchins, hard clams, conchs, serpulid worms, periwinkles, bay scallops, oysters, whelks and soft clams. The same study revealed no response to elevated pCO_2 in blue mussels. Contrarily, Wood et al. (2008) found increased metabolic and calcification rates in the brittle star species, *Amphiura*

filiformis. However, this upregulation of metabolism and calcification comes at a considerable cost (muscle wasting) and is therefore unlikely to be sustainable during long-term exposure to low pH conditions (Wood et al., 2008).

Metabolic and reproductive effects in low pH conditions

Calcification is not the only challenge organisms face due to ocean acidification. Elevated environmental pCO_2 can induce excess CO_2 in body fluids and tissues; this phenomenon is hypercapnia (Michaelidis et al., 2005; Gazeau et al., 2013). Organisms lacking well-developed circulatory and respiratory systems, and that rely on favourable tissue-to-environment gradients for CO_2 excretion, are particularly susceptible to hypercapnia (Michaelidis et al., 2005). When environmental pCO_2 is elevated, CO_2 continues to rise in the intra- and extra-cellular compartments of the body until a new CO_2 gradient is reached that restores the favourable conditions for CO_2 excretion (Seibel & Walsh, 2003). This rise in internal CO_2 leads to an increase in H^+ that causes a reduction in pH, known as acidosis (Pörtner et al., 2004; Wicks & Roberts, 2012).

Passive buffering, whereby non-bicarbonate buffers bind to excess H^+, is the mechanism immediately available to organisms to mitigate changes in body pH (Seibel & Walsh, 2003; Melzner et al., 2009). However, passive buffering only masks the acidosis and does not act to restore acid-base balance to the body (Gazeau et al., 2013). In order to restore acid-base balance, the excess H^+ must be removed from the intra- and extra-cellular compartments of the body and bicarbonate must be accumulated (Seibel & Walsh, 2003; Pörtner et al., 2004; Fabry et al., 2008). These processes are made possible by membrane-bound ion transporters like Na^+/K^+ and H^+-ATPases that mediate active ion

exchange across epithelial membranes (Seibel & Walsh, 2003; Pörtner et al., 2004; Fabry et al., 2008).

Energy is required to maintain homeostasis in response to environmental stressors like ocean acidification (Pan et al., 2015). When decreases in body pH go uncompensated, changes in the energy budget of the organism may occur (Gazeau et al., 2013). For example, a greater proportion of energy may be allocated to restoring acid-base balance in the body that would otherwise go to processes like shell growth, somatic growth, immune response, protein synthesis, behaviour and reproduction (Gazeau et al., 2013). Recent work on the sea urchin, *Strongylocentrotus purpuratus*, indicates that the principle metabolic mechanism in response to elevated pCO_2 in urchin larvae is a change in the allocation of a set amount of ATP (Pan et al., 2015). Under acidic conditions, ion exchange and protein synthesis account for ~84% of the metabolic rate of urchin larvae, in comparison to 55% in control counterparts. This ~30% difference in the allocation of metabolic energy may reduce an organism's ability to respond to additional stressors (Pan et al., 2015). Moreover, metabolic depression is, in many cases, a strategy used by marine organisms to survive acidification (Guppy & Withers, 1999; Pörtner et al., 2004; Gazeau et al., 2013). Such a response is observed in *Mytilus galloprovincialis* where long-term hypercapnia (pH = 7.3) causes a permanent reduction in haemolymph pH, metabolic depression and increased nitrogen excretion (Michaelidis et al., 2005). In an effort to limit pH reduction in the body, mussels dissolve some shell $CaCO_3$ to increase bicarbonate levels in the haemolymph thereby slowing shell growth. Nitrogen excretion indicates protein degradation that can restrict both body growth and reproduction (Michaelidis et al., 2005). Understanding metabolic mechanisms in place to maintain

critical physiological functions in response to ocean acidification may provide insight into an organism's ability to cope with additional energy-demanding stressors like elevated ocean temperatures, parasitic infection, anthropogenic disturbances, and limited food availability. Although metabolic responses to ocean acidification are variable between species, the general agreement across the literature suggests that growth and performance of marine invertebrates will deteriorate in the face of an energy-demanding stressor like ocean acidification.

Hydrothermal vent environments: studying ocean acidification *in situ*

Hydrothermal vents are extraordinary ecosystems that, since their discovery in 1977, have revolutionized our understanding of life on Earth. Hydrothermal vents form in volcanically active areas of the sea floor – often at mid-ocean ridges where tectonic plates are spreading apart, or near subduction zones where tectonic plates are converging. Seawater percolates into the permeable ocean crust where it is subsequently heated by underlying magma. This heating process drives chemical reactions that remove constituents like oxygen, sulfates and magnesium while accumulating hydrogen sulphide (H_2S), hydrogen, and methane (CH_4). Further subsurface reactions leach metals (i.e. iron, copper, lead, zinc), silica and other compounds from the rocks, into the water. This mineral-rich (and usually acidic; pH<7) hydrothermal fluid that may exceed 400°C in temperature then returns to the ocean through openings in the seafloor (Delaney et al., 1984). As the hydrothermal fluid enters the cold, oxygenated waters of the deep ocean, another series of chemical reactions take place. Hydrothermal fluids contain metal sulphides such as pyrite, sphalerite, and chalcopyrite. These sulphides precipitate in response to the interaction between high-temperature vent fluid and ambient seawater and

eventually accumulate on the seafloor to form the characteristic polymetallic sulphide chimneys found at hydrothermal vent environments (Baross & Hoffman, 1985). Furthermore, the hydrothermal fluid contains compounds like hydrogen sulphide and methane that provide energy for chemoautotrophic bacteria through oxidation reactions (Jannasch, 1985). As primary producers, chemoautotrophic bacteria sustain diverse communities that can include organisms like snails, crabs, mussels, shrimp, clams, limpets, pycnogonids, and tubeworms.

The Mariana volcanic arc is located in the western Pacific Ocean in the region of Guam/Marianas Islands (Figure 1.1). The arc is formed as a result of the subduction of the Pacific plate beneath the Philippine plate, and extends from 13°N to 23°N (Embley et al., 2007). The Mariana region contains nine volcanic islands and more than 60 submarine volcanoes (Embley et al., 2007). At least 20 of these volcanoes are hydrothermally active making this one of the most active volcanic regions on Earth (Embley et al., 2007). During February and March 2003, the research vessel *Thomas G. Thompson* conducted a comprehensive survey of hydrothermal activity along the Mariana volcanic arc as part of the Submarine Ring of Fire project funded by NOAA's Ocean Exploration Program. It was on this cruise that hydrothermal activity was first discovered on Northwest Eifuku volcano, a small volcanic cone located along the arc at 21.49°N, 144.04°E (Figure 1.1, 1.2).

In March and April 2004, the remotely operated vehicle (ROV) ROPOS discovered the Champagne vent field (1604 m) located just below the summit of NW Eifuku (1563 m). Small chimneys at Champagne emit hot vent fluid containing 2.7 moles/kg of CO_2 – the highest reported concentration of CO_2 of any hydrothermal fluid

globally – and liquid droplets of CO_2 composed of ~98% CO_2, and ~1% H_2S (Figure 1.3) (Lupton et al., 2006). The hydrothermal fluid is composed of ~3000 mmol/kg CO_2, ~12 mmol/kg H_2S, <0.2 mmol/kg CH_4 and H_2, and 0.01 mmol/kg ^4He (Lupton et al., 2006).

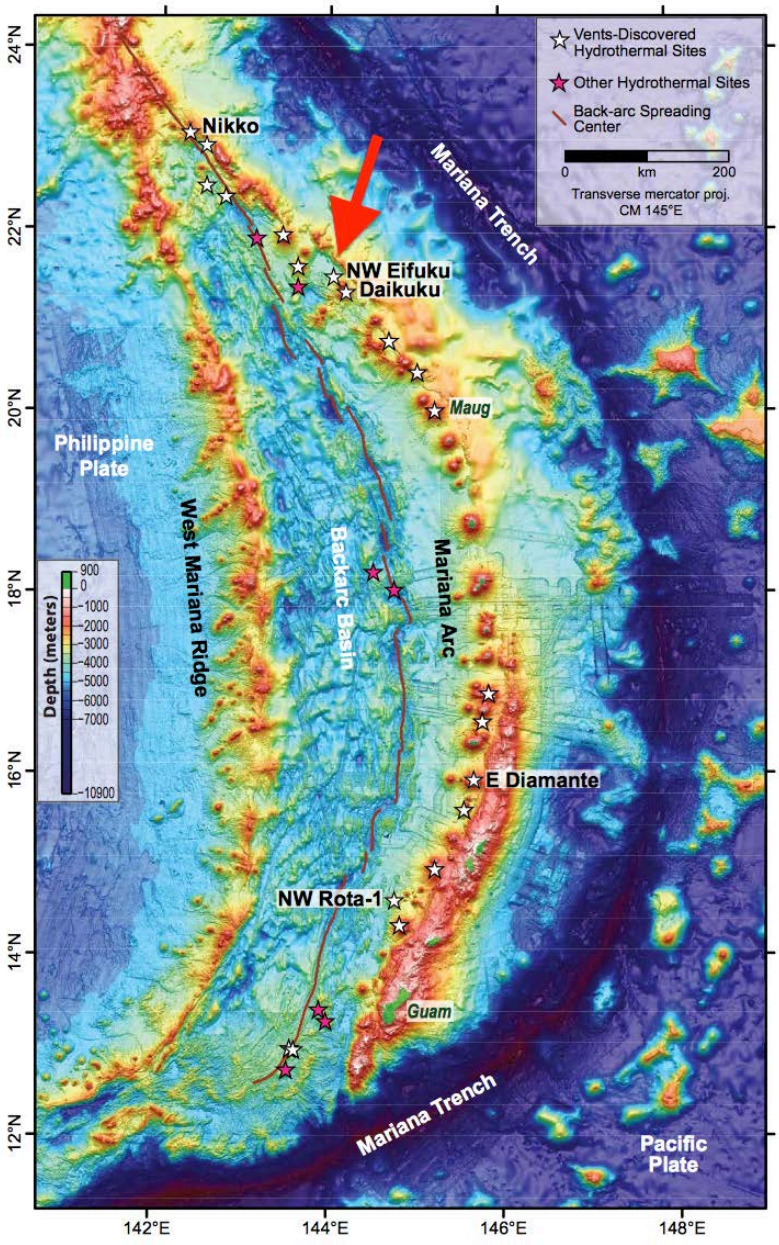

Figure 1.1. Bathymetric map of the Mariana arc. Solid green shading indicates islands. White stars indicate hydrothermal vent sites discovered on the Vents Exploration Project between 2003 and 2006. Red stars indicate other hydrothermal vent sites. The red arrow

is indicating the location of Northwest Eifuku. Image adapted from (Hammond et al., 2015).

As the concentration of CO_2 in the vent fluid is much higher than the expected solubility of CO_2 at the given temperature and pressure conditions at NW Eifuku (Wiebe & Gaddy, 1939; Takenouchi & Kennedy, 1964; Lupton et al., 2006) it is likely that vent fluid is picking up excess liquid CO_2 from a proposed pool that lies below a frozen hydrate layer just below the sea floor sediments. Hydrothermal activity at convergent plate boundaries is commonly rich in volatile compounds (e.g. CO_2, SO_2, CH_4) relative to hydrothermal activity at mid-ocean ridges (Gamo et al., 2006).

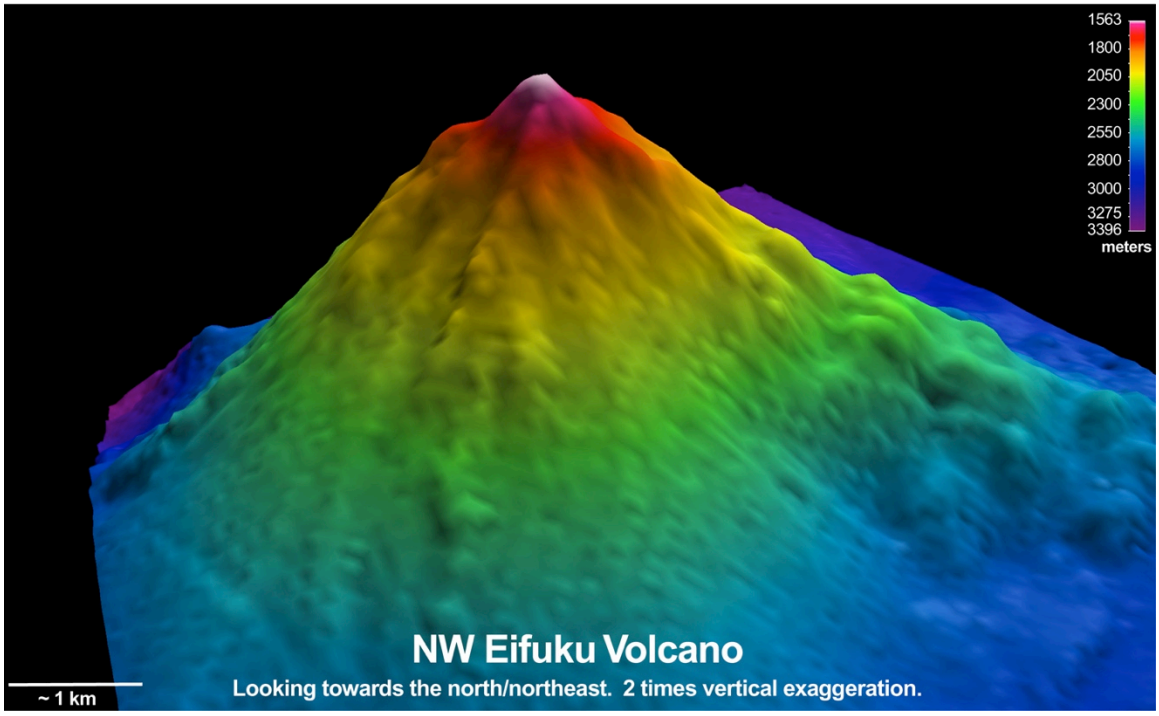

Figure 1.2. Three-dimensional map of NW Eifuku seamount. The vent field is located near the summit. Image courtesy of NOAA Vents Program.

Three principal processes contribute to the volatile nature of arc-back-arc hydrothermal fluids. The first is phase separation, which occurs when too much magmatic heat increases fluid temperatures to a pressure-dependant boiling point causing the fluid to

separate into liquid and vapour phases (Bischoff & Rosenbauer, 1988; Gamo et al., 2006). Arc-back-arc hydrothermal activity generally occurs at relatively shallow depths (<2000m) compared to mid-ocean ridges. Because the boiling point of seawater increases with increasing pressure, it is likely that phase separations occur more frequently at arc-back-arc systems resulting in a wider variation in the chemical composition of venting fluids (Gamo et al., 2006). The second process is the subsurface interaction between hot fluids and seafloor sediments accumulated over millions of years (Gamo et al., 2006). This hot fluid-sediment interaction can alter the chemical characteristics of the hydrothermal fluids especially when the sediments are largely composed of organic material. The third contributor to the volatility of arc-back-arc hydrothermal fluids is material supply from the subducting plate. The subducting plate supplies various components such as water, sediments, and organic matter that vary on both temporal and spatial scales (Gamo et al., 2006). Different combinations of these components result in a wide range of magma composition resulting in unique hydrothermal fluid characteristics (Gamo et al., 2006). Northwest Eifuku serves as an excellent example of the unique geochemistry of submarine volcanoes associated with convergent plate boundaries. Despite the high CO_2 conditions, bathymodioline mussels are among the dominant macrofauna at Northwest Eifuku as reported by Embley et al. (2006). The presence of mussels at NW Eifuku presents biologists with the unique opportunity to study the effects of extremely acidic conditions on marine organisms in a natural setting.

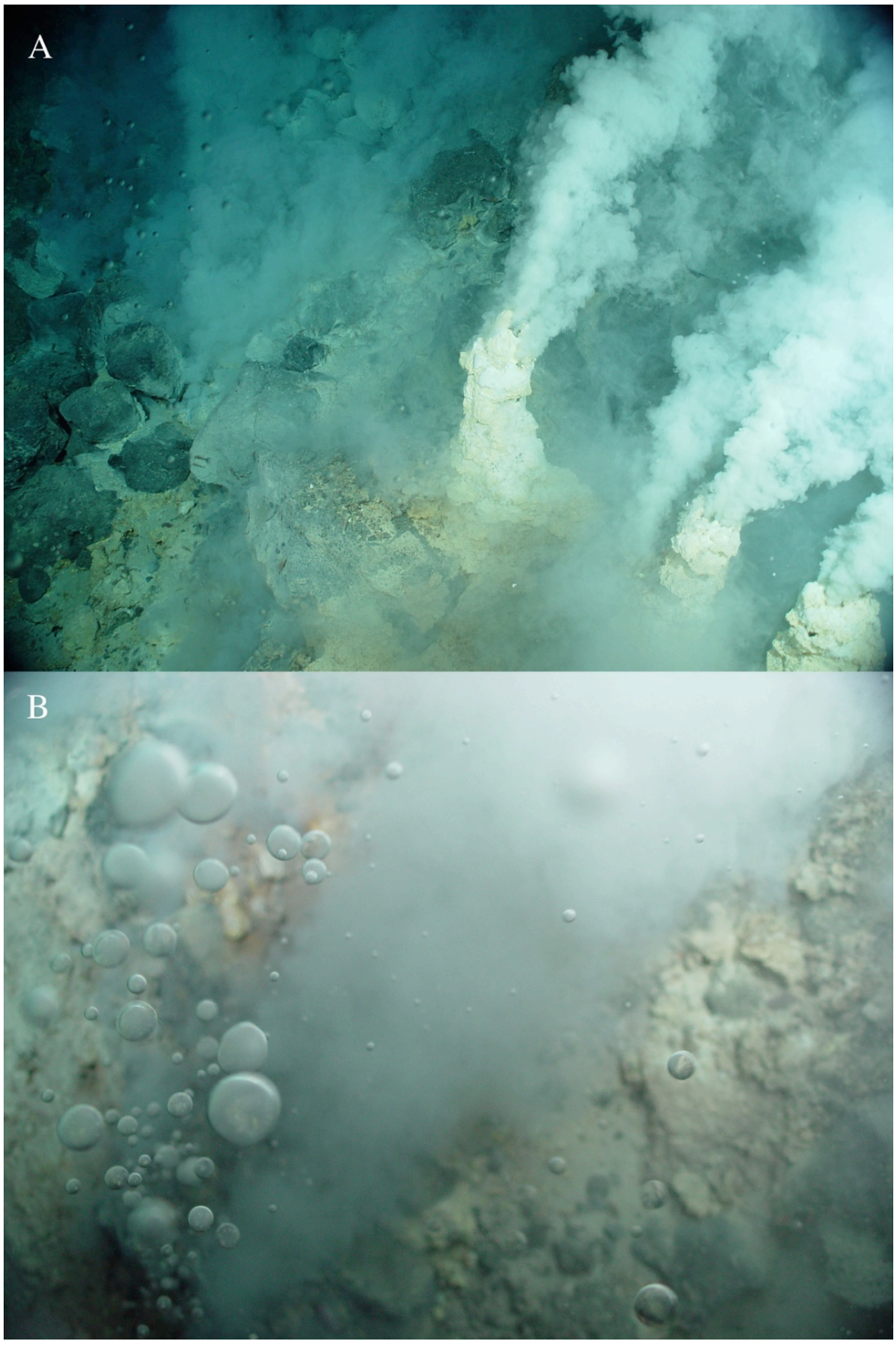

Figure 1.3. a) Photograph of Champagne vent field taken from ROPOS ROV illustrating liquid CO_2 droplets and hot vent fluid rising through sulphur chimneys. Field of view is about 2 m across, b) zoomed in photograph of liquid CO_2 droplets. Depth is ~1604 m. Images are courtesy of Submarine Ring of Fire 2006 Expedition, NOAA Vents Program.

Study organism: *Bathymodiolus septemdierum*

The genus *Bathymodiolus* in the family Mytilidae, was described by Kenk & Wilson (1985) when the first member, *Bathymodiolus thermophilus,* was discovered at the Galapagos Rift. To date, more than 20 new species of bathymodioline mussels have been described. The mussels from this genus inhabit several, if not most, chemosynthetic-based communities including hydrothermal vents and cold seeps in the deep sea. Bathymodioline mussels harbour chemosynthetic endosymbionts in their enlarged, filibranch gills from which they can derive a large part of their nutrition (Fisher et al., 1987). The bacterial symbionts in the gills can be methanotrophic (methane- oxidizing) or thiotrophic (sulphide- oxidizing) and, in some species, both types can co-occur (Distel et al., 1995). In addition, all bathymodioline mussels have retained highly reduced labial palps and gut compared to their shallow-water, non-symbiotic relatives (Page et al., 1991; von Cosel, 2002). The digestion of falling organic matter from photosynthetic origin (Dixon et al., 2006; Tyler et al., 2007), and/or free-living bacteria (Page et al., 1991; Dubilier et al., 1998) is thought to supplement the nutrition provided by the endosymbionts; this supposition is supported by the fact that the gills of many bathymodioline species have retained the ability to suspension feed at rates comparable to shallow mussels (Page et al., 1991; Pile & Young, 1999). The shells of most bathymodioline mussels are modioliform and usually brown in colour (Duperron, 2010). Adult shell length varies from ~40 to 360 mm depending on the species and the mantle between species shows different degrees of fusion (Duperron, 2010). Miyazaki et al. (2010) find that Bathymodiolus is paraphyletic, in which *Bathymodiolus (sensu lato) childressi* falls in a separate clade from other bathymodioline mussels.

The vent mussel, *Bathymodiolus septemdierum*, is a dominant member of the macrofauna at several hydrothermal vent sites in the western Pacific and Indian Ocean (Breusing et al., 2015). The biogeographic distribution of *B. septemdierum* is among the broadest of all hydrothermal vent fauna, but the full scope of the distribution was only recently realized. Researchers described four new species of bathymodioline mussels based on morphological characteristics, including *B. septemdierum* Hashimoto & Okutani, 1994, *B. brevior* Von Cosel & Metivier, 1994, *B. elongatus* and *B. marisindicus* Hashimoto, 2001. Subsequent work by Breusing et al. (2015) used multiple genes and allozymes from these putative species to identify two distinct metapopulations: *B. septemdierum* from the western Pacific Ocean, and *B. septemdierum marisindicus* from the Indian Ocean (Figure 1.5). All four species were subsumed as *B. septemdierum*. This distribution, the morphological differences between populations, and the survival in extremely acidic conditions suggests that *B. septemdierum* is highly adapted to a wide range of environments.

Bathymodiolus septemdierum relies on thiotrophic endosymbionts in the gills for nutrition, but like many other members of the genus, has retained the ability to suspension feed (Cosel & Métvier, 1994; Dubilier et al., 1998). Rather than occupying areas of high venting where temperatures exceed their upper temperature limit of 35°C (Henry et al., 2008), *B. septemdierum* tends to aggregate in regions of low temperature and hydrothermal fluid flux. There, *B. septemdierum* can obtain adequate sulphide to support symbiosis while remaining in temperatures ranging between 0.1 and 28.6°C above ambient seawater (~2.4°C; Podowski et al., 2010). This species is epibenthic and

the mussels use their byssal threads to form dense aggregates on hard substrates. These dense clusters of *B. septemdierum* form complex physical structures that enable diverse communities of fauna to survive (Turnipseed et al., 2004). The strong role that *B. septemdierum* plays in structuring hydrothermal vent communities indicates that it serves as a foundation species where present (Turnipseed et al., 2004).

Tunnicliffe et al. (2009) report *B. septemdierum* living at NW Eifuku volcano at densities exceeding 250 mussels m^{-2} (Figure 1.4). Due to proximity to the Champagne Vent, the pH among the extensive mussel beds is as low as 5.36 and mussel shell thickness is reduced compared to that of mussels living in higher pH conditions (Tunnicliffe et al., 2009). At a given shell length, mussel shells from NW Eifuku weigh about half that of shells from Monowai and Lau Basin where pH is 7.87 and 8.42, respectively. Using daily microgrowth bands in the shells (Schöne & Giere, 2005), Tunnicliffe et al. (2009) demonstrate that NW Eifuku daily increment widths are almost half that of shells from Monowai/Lau. Thus, shell thickness and shell growth rates in NW Eifuku mussels are restricted as a result of the extremely acidic conditions (Tunnicliffe et al., 2009). However, while the effects on calcification are now clear, there is no study examining the effects of high CO_2/low pH on other functions that influence physiological condition or fitness in *B. septemdierum*. As a foundation species, understanding the controls on the biology of *B. septemdierum* may be essential in determining the functionality of the entire community.

Figure 1.4. A photograph of dense *B. septemdierum* mussel beds, non-predatory anomuran crabs, and alvinocaridid shrimp at Near Fouling on NW Eifuku. ROV Jason arm is holding a scoop and preparing to collect mussels for this study. Scoop is ~50 cm wide.

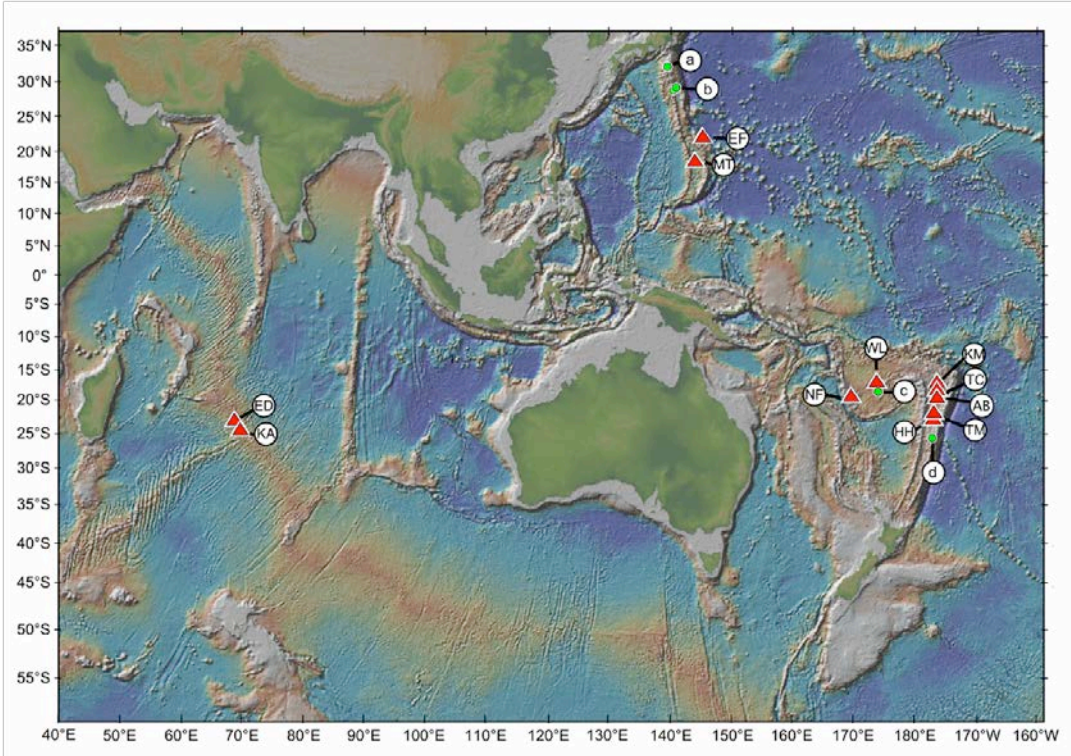

Figure 1.5. Biogeographic distribution of *B. septemdierum* in the western Pacific and Indian oceans. *B. septemdierum* occurs at both red and green vent sites. Study specimens from the present study were collected from the following sites: NW Eifuku (EF), Nifonea (NF), Tui Malila (TM), and ABE (AB). Image adapted from Breusing et al. (2015).

Research objectives

We use the *in situ* opportunity provided by the unique geochemistry at NW Eifuku to investigate the biology of *B. septemdierum* in extremely acidic conditions. The overall objectives of this research are to understand and identify the effects of low pH conditions on fitness sustaining processes like somatic growth and reproduction in *Bathymodiolus septemdierum*. The three specific goals include:

1) Determine the reproductive characteristics (e.g. reproductive mode, reproductive pattern) of *B. septemdierum* and present the first report of gametogenesis in this species. (Chapter Two)
2) Compare body and gill conditions across *B. septemdierum* populations from sites of varying pH. (Chapter Three)
3) Compare endosymbiont abundances across *B. septemdierum* populations from sites of varying pH. (Chapter Three)

Literature cited

Baross, J. A., & Hoffman, S. E. (1985). Submarine hydrothermal vents and associated gradient environments as sites for the origin and evolution of life. *Origins of Life and Evolution of the Biosphere, 15*(4), 327–345. https://doi.org/10.1007/BF01808177

Bischoff, J., & Rosenbauer, R. (1988). Liquid-vapor relations in the critical region of the system NaCl-H_2O from 380 to 415°C: A refined determination of the critical point and two-phase boundary of seawater. *Geochimica et Cosmochimica ACTA, 52*(8), 2121-2126.

Breusing, C., Johnson, S., Tunnicliffe, V., & Vrijenhoek, R. (2015). Population structure and connectivity in Indo-Pacific deep-sea mussels of the *Bathymodiolus septemdierum* complex. *Conservation Genetics*, 1–16. http://doi.org/10.1007/s10592-015-0750-0

Cosel, R. Von. (2002). A new species of bathymodiolinee mussel (Mollusca, Bivalvia, Mytilidae) from Mauritania (West Africa), with comments on the genus Bathymodiolus Kenk & Wilson 1985. Zoosystema, *24*(2): 259-271.

Cosel, R. Von, & Métvier, B. (1994). Three new species of Bathymodiolus (Bivalvia: Mytilidae) from hydrothermal vents in the Lau Basin and the North Fiji Basin, western Pacific, and the Snake Pit area, Mid-Atlantic Ridge. *Veliger, 37*, 374–392.Distel, D. L., Lee, H. K., & Cavanaugh, C. M. (1995). Intracellular coexistence of methano- and thioautotrophic bacteria in a hydrothermal vent mussel. *Proceedings of the National Academy of Sciences, 92*, 9598–9602

Delaney, J.R., McDuff, R.E., Lupton, J.E. (1984). Hydrothermal fluid temperatures of 400°C on the Endeavour Segment, northern Juan de Fuca. *Eos; Trans. Amer. Geophys. Union, 65*, 973.

Dixon, D. R., Lowe, D. M., Miller, P. I., Villemin, G. R., Colaço, A., Serrão-Santos, R., & Dixon, L. R. . (2006). Evidence of seasonal reproduction in the Atlantic vent mussel *Bathymodiolus azoricus*, and an apparent link with the timing of photosynthetic primary production. *Journal of the Marine Biological Association of the UK, 86*(6), 1363–1371. http://doi.org/10.1017/S0025315406014391

Dubilier, N., Windoffer, R., & Giere, O. (1998). Ultrastructure and stable carbon isotope composition of the hydrothermal vent mussels from the North Fiji Basin, western Pacific. *Marine Ecological Progress Series, 165*, 187-193.

Duperron, S. (2010). *The Vent and Seep Biota*. (S. Kiel, Ed.) (Vol. 33, pp. 137–167). Dordrecht: Springer Netherlands. http://doi.org/10.1007/978-90-481-9572-5

Embley, R. W., Baker, E. T., Butterfield, D. A., Chadwick Jr., W. W., Lupton, J. E., Resing, J. A., … Merle, S. G. (2007). Exploring the submarine ring of fire: Mariana Arc— Western Pacific. *Oceanography*, *20*(4), 68–79.

Embley, R. W., Chadwick, W. W., Baker, E. T., Butterfield, D. a, Resing, J. A, de Ronde, C. E. J., … Tamura, Y. (2006). Long-term eruptive activity at a submarine arc volcano. *Nature*, *441*(7092), 494–7. http://doi.org/10.1038/nature04762

Fabry, V. J., Seibel, B. A., Feely, R. A., & Orr, J. C. (2008). Impacts of ocean acidification on marine fauna and ecosystem processes. *Journal of Marine Science, 65*(3), 414-432.

Fisher, C., Childress, J., Oremland, R., & Bidigare, R. (1987). The importance of methane and thiosulfate in the metabolism of the bacterial symbionts of two deep-sea mussels. *Marine Biology*, *71*, 59–71.

Gamo, T., Ishibashi, J., Tsunogai, U., Okamura, K., & Chiba, H. (2006). Unique Geochemistry of Submarine Hydrothermal Fluids from Arc-Back-Arc Settings of the Western Pacific. *Back-Arc Spreading Systems: Geological, Biological, Chemical, and Physical Interactions (eds Christie DM, Fisher CR, Lee S-M, Givens S), American GeophysicalUnion,Washington,DC, 147–161*.

Gattuso, J.-P., Magnan, a, Billé, R., Cheung, W. W. L., Howes, E. L., Joos, F., … Turley, C. (2015). Oceanography. Contrasting futures for ocean and society from different anthropogenic CO_2 emissions scenarios. *Science*, *349*(6243), aac4722.

http://doi.org/10.1126/science.aac4722

Gazeau, F., Parker, L. M., Comeau, S., Gattuso, J. P., O'Connor, W. a., Martin, S., … Ross, P. M. (2013). Impacts of ocean acidification on marine shelled molluscs. *Marine Biology*, *160*(8), 2207–2245. http://doi.org/10.1007/s00227-013-2219-3

Guppy, M., & Withers, P. (1999). Metabolic depression in animals : physiological perspectives and biochemical generalizations. *Biological Review of the Cambridge Philosophical Society, 174*(1), 1-40.

Hammond, S., Embley, R., & Baker, E. (2015). The NOAA Vents Program 1983 to 2013: Thirty Years of Ocean Exploration and Research. *Oceanography*, *28*(1), 160–173. http://doi.org/10.5670/oceanog.2015.17

Hashimoto, J. (2001). A new species of Bathymodiolus (Bivalvia: Mytilidae) from hydrothermal vent communities in the Indian Ocean. *Japanese Journal of Malacology, 60*, 141–149.

Hashimoto, J., & Okutani, T. (1994). Four new mytilid mussels associated with deepsea chemosynthetic communities around Japan. *Japanese Journal of Malacology, 53*, 61–83.

Henry, M. S., Childress, J. J., & Figueroa, D. (2008). Metabolic rates and thermal tolerances of chemoautotrophic symbioses from Lau Basin hydrothermal vents and their implications for species distributions. *Deep Sea Research Part I: Oceanographic Research Papers*, *55*(5), 679–695. http://doi.org/10.1016/j.dsr.2008.02.001

Jannasch, H. (1985). The chemosynthetic support of life and the microbial diversity at deep-sea hydrothermal vents. *Proc. R. Soc. Lond.*, *225*, 277–297. https://doi.org/doi:10.1086/303379

Kenk, C., & Wilson, B. R. (1985). A new mussel (Bivlavia: Mytilidae) from hydrothermal vents in the Galapagos Rift zone. *Malacologia*, *26*, 253–271.

Kleypas, J., Feely, R., Fabry, V. J., Langdon, C., Sabine, C. L., & Robbins, L. L. (2006). Impacts of ocean acidification on coral reefs and other marine calcifiers: a guide for future research. Report of a workshop held 18–20 April 2005, St Petersburg, FL, sponsored by NSF, NOAA, and the US Geological Survey. 88 pp.

Lupton, J., Butterfield, D., Lilley, M., Olson, E., Baker, E., Roe, K., & Greene, R. (2006). Submarine venting of liquid carbon dioxide on a Mariana Arc volcano. *Geochemisty, Geophysics, Geosystems*, http://doi.org/10.1029/2005GC001152

Melzner, F., Stange, P., Trübenbach, K., Thomsen, J., Casties, I., Panknin, U., … Gutowska, M. A. (2011). Food supply and seawater pCO_2 impact calcification and internal shell dissolution in the blue mussel *Mytilus edulis*. *PloS One*, *6*(9), e24223. http://doi.org/10.1371/journal.pone.0024223

Michaelidis, B., Ouzounis, C., Paleras, A., & Pörtner, H. O. (2005). Effects of long-term moderate hypercapnia on acid – base balance and growth rate in marine mussels *Mytilus galloprovincialis*. *Marine Ecological Process Series*, *293*, 109–118.

Miyazaki, J.I., De Oliveira Martins, L., Fujita, Y., Mat-sumoto, H., & Fujiwara, Y. (2010) Evolutionary process of deep-sea Bathymodiolus mussels. *PLoS one, 5*, e10363, doi:10.1371/journal.pone.0010363

Page, H. M., Fiala-Medioni, a., Fisher, C. R., & Childress, J. J. (1991). Experimental evidence for filter-feeding by the hydrothermal vent mussel, *Bathymodiolus thermophilus. Deep Sea Research Part A. Oceanographic Research Papers*, *38*(12), 1455–1461. http://doi.org/10.1016/0198-0149(91)90084-S

Pan, T.-C. F., Applebaum, S. L., & Manahan, D. T. (2015). Experimental ocean acidification alters the allocation of metabolic energy. *Proceedings of the National Academy of Sciences of the United States of America*, *112*(15), 4696–701. http://doi.org/10.1073/pnas.1416967112

Pile, A., & Young, C. (1999). Plankton availability and retention efficiencies of cold-seep symbiotic mussels. *Limnology and Oceanography*, *44*(7), 1833-1839.

Podowski, E., Ma, S., Luther, G., Wardrop, D., & Fisher, C. (2010). Biotic and abiotic factors affecting distributions of megafauna in diffuse flow on andesite and basalt along the Eastern Lau Spreading Center, Tonga. *Marine Ecology Progress Series*, *418*, 25–45. http://doi.org/10.3354/meps08797

Portner, H. O., Langenbuch, M., & Reipschlager, A. (2004). Biological Impact of Elevated Ocean CO2 Concentrations: Lessons from Animal Physiology and Earth History. *Journal of Oceanography*, *60*(4), 705–718. http://doi.org/10.1007/s10872-004-5763-0

Ries, J. B., Cohen, a. L., & McCorkle, D. C. (2009). Marine calcifiers exhibit mixed responses to CO_2-induced ocean acidification. *Geology*, *37*(12), 1131–1134. http://doi.org/10.1130/G30210A.1

Schöne, B. R., & Giere, O. (2005). Growth increments and stable isotope variation in shells of the deep-sea hydrothermal vent bivalve mollusk *Bathymodiolus brevior* from the North Fiji Basin, Pacific Ocean. *Deep Sea Research Part I: Oceanographic Research Papers*, *52*(10), 1896–1910. http://doi.org/10.1016/j.dsr.2005.06.003

Seibel, B. A., & Walsh, P. w. (2003). Biological impacts of deep-sea carbon dioxide injection inferred from indices of physiological performance. *Journal of Experimental Biology*, *206*(4), 641–650. http://doi.org/10.1242/jeb.00141

Takenouchi, S., & Kennedy, G. (1964). The binary system H_2O-CO_2 at high temperatures and pressures. *American Journal of Science*, *262*, 1055–1074.

Tunnicliffe, V., Garrett, J. F., & Johnson, H. P. (1990). Physical and biological factors affecting the behaviour and mortality of hydrothermal vent tubeworms (vestimentiferans). *Deep Sea Research Part A. Oceanographic Research Papers*, *37*(1), 103–125. http://doi.org/10.1016/0198-0149(90)90031-P

Turnipseed, M., Jenkins, C. D., & Van Dover, C. L. (2004). Community structure in Florida Escarpment seep and Snake Pit (Mid-Atlantic Ridge) vent mussel beds. *Marine Biology*, *145*(1), 121–132. https://doi.org/10.1007/s00227-004-1304-z

Tyler, P., Young, C. M., Dolan, E., Arellano, S. M., Brooke, S. D., & Baker, M. (2007). Gametogenic periodicity in the chemosynthetic cold-seep mussel *"Bathymodiolus" childressi*. *Marine Biology*, *150*(5), 829–840. http://doi.org/10.1007/s00227-006-0362-9

Von Cosel, R., & Metvier, B. (1994). Three new species of Bathymodiolus (Bivalvia: Mytilidae) from hydrothermal vents in the Lau Basin and the North Fiji Basin, western Pacific, and the Snake Pit area, Mid-Atlantic Ridge. *Veliger*, *37*, 374–392.

Wang, Q., Cao, R., Ning, X., You, L., Mu, C., Wang, C., … Zhao, J. (2016). Effects of ocean acidification on immune responses of the Pacific oyster *Crassostrea gigas*. *Fish and Shellfish Immunology, 49*, 24–33. http://doi.org/10.1016/j.fsi.2015.12.025

Wicks, L. C., & Roberts, J. M. (2012). Benthic invertebrates in a high- CO_2 world. *Oceanography and Marine Biology: An Annual Review, 50*, 127–188.

Wiebe, R., & Gaddy, V. (1939). The solubility in water of carbon dioxide at 50, 75 and 100, at pressures to 700 atmospheres. *Journal of the American Chemical Society, 947*(4), 1933–1936. http://pubs.acs.org/doi/abs/10.1021/ja01871a025

Wood, H. L., Spicer, J. I., & Widdicombe, S. (2008). Ocean acidification may increase calcification rates, but at a cost. *Proceedings. Biological Sciences / The Royal Society, 275*(1644), 1767–73. http://doi.org/10.1098/rspb.2008.0343

Chapter 2 : The reproductive biology of deep-sea mussel (*Bathymodiolus septemdierum*) living in extremely acidic conditions

Introduction

Reproduction in Low pH Conditions

In response to CO_2-driven acidification, changes in the energy balance of marine invertebrates may negatively affect biological processes such as growth and reproduction. The energy budget of a living organism follows the "law of conservation of energy" for which the energy obtained through food sources is equal to the energy used for growth, reproduction, maintenance metabolism and excretory loss (Sibly & Calow, 1986). When limited food availability or energy-demanding stressors like acidification challenge an animal, studies suggest that energy allocation to maintenance generally takes precedence over growth and reproduction (e.g. Calow, 1983, Sokolova et al., 2012, Range et al., 2011, Pan et al., 2015). Energy metabolism therefore plays a fundamental role in determining the survival, fitness and stress tolerance of marine species and populations confronted with CO_2-driven acidification.

Several studies investigate the effects of high pCO_2 on invertebrate reproduction. Siikavuopio et al. (2007) report that gonad growth is reduced by 67% when the green sea urchin, *Strongylocentrotus droebachiensis*, is exposed to pH 6.98 for 56 days. The marine shrimp, *Palaemon pacificus*, cultured at pH 7.9 for 30 weeks, shows reduced fecundity compared to the control (Kurihara, 2008). When Range et al. (2011) rear juvenile grooved carpet clams (*Ruditapes decussates*) at pH 8.13, 7.84 and 7.46, no spawning events occur in the most acidic treatment, which also demonstrates reduced mortality.

The authors suggest that delayed reproductive development in the most acidic treatment is an energy saving strategy that facilitates the reduced mortality.

Despite the increasing threat of ocean acidification, data on reproduction in marine bivalves under low pH conditions, especially in natural conditions, are lacking. In the present study, we use a deep-sea marine mytilid with sustained survival at CO_2-rich vents as a model species to investigate the effects of extremely low pH conditions on reproduction. Results should provide further insight on how reproduction of coastal species will respond to continuing ocean acidification.

Gametogenesis in *Bathymodiolus*

In general, marine mussels reproduce by releasing gametes into the surrounding water where fertilization takes place (Bayne et al., 1983). Following fertilization is a period of planktotrophic larval development that ends when the larvae metamorphose to juveniles as they settle on benthic substrates (Bayne et al., 1983). Coastal mussels are typically iteroparous, reproducing annually, although more frequent spawning can occur (Bayne et al., 1983). The reproductive cycle usually tracks an energy storage cycle where mussels synthesize lipid and carbohydrate reserves during periods of nutrient surplus and use the reserves for gametogenesis during periods of nutrient limitation (Bayne et al., 1983).

Deep-sea species at chemosynthetic habitats have a strong dependence on *in situ* production and inhabit depths where few cyclical environmental cues exist; one hypothesis is that they should display continuous gametogenesis (Tyler et al., 2007). However, environmental cues in the deep sea can include the downward flux of seasonally available organic matter from surface waters (Khripounoff & Alberic, 1991)

or thermal fluctuations from tidal cycles (Tunnicliffe et al., 1990). Chemosymbiotic bivalves are mixotrophic, deriving energy from their endosymbionts and from additional sources like the flux of organic material from surface waters (Dufour & Felbeck, 2006). They inhabit upper bathyal regions where seasonal fluctuations in food availability may be notable (Le Pennec & Beninger, 2000). Dixon et al. (2006) provide evidence of a strong annual reproductive cycle in *Bathymodiolus azoricus* in which the main spawning event shows a correlation with a winter – spring bloom in primary production (northern hemisphere). In *Bathymodiolus childressi*, seasonal reproduction also appears to be correlated with surface production that peaks during the winter months (northern hemisphere) (Tyler et al., 2007). A downward flux of detritus during winter may provide a cue for gamete release, food for the planktotrophic larvae, and supplementary nutrition for adults recovering from energetically costly gamete production (Tyler et al., 2007).

Nothing is reported about gametogenesis in *B. septemdierum* despite the widespread nature of this species and the strong role it plays in structuring hydrothermal vent communities. Similarly, there are no studies on the effects of high CO_2 conditions on gametogenesis in deep-sea bivalves. *Bathymodiolus septemdierum* is a useful model species to study how reproduction in marine mytilids may respond to ocean acidification. As energy may be allocated to restoring acid-base balance at the expense of fitness-sustaining processes like reproduction (Gazeau et al., 2013), we expect that conditions of high CO_2 would have a consequence. We use the *in situ* opportunity provided by the unique geochemistry at NW Eifuku to investigate the reproductive biology of *B. septemdierum* in extremely acidic conditions. The objectives and hypotheses of this research are as follows:

1) To describe gametogenesis in *B. septemdierum* in comparison to other members of the genus.
2) To assess the seasonal pattern of gametogenesis in *B. septemdierum*. We present two hypotheses for the pattern of gametogenesis in *B. septemdierum*. i) Given the oligotrophic nature of the Marianas region, we hypothesize that gametogenesis is continuous and displays no annual cycle; alternatively ii) the pattern of gametogenesis in *B. septemdierum* parallels the annual cycle of other bathymodioline mussels.
3) To determine the effects of high CO_2 on reproduction in *B. septemdierum*. We hypothesize that mussels surviving in low pH conditions will show signs of compromised reproduction (i.e. premature spawning or poor gonadal condition).

Materials and Methods

Site Description and Collection Methods

Northwest Eifuku is a submarine volcano located along the Mariana volcanic arc (21°29.3' N, 144°02.5' E). At 1610 m depth, 80m south of the summit (1570 m), is a high temperature vent (Champagne) that discharges a buoyant plume of hydrothermal fluid that circulates around the summit delivering hydrogen sulphide to the extensive mussel beds, and associated crab and shrimp (Tunnicliffe et al., 2009). Minor low temperature venting occurs among the mussel beds surrounding Champagne (Tunnicliffe et al., 2009). In April 2004 mussels were collected using remotely operated vehicle (ROV) ROPOS from one site on NW Eifuku (Near Fouling; Table 2.1). At Near Fouling,

pH was determined from water samples collected with a multi-chambered manifold flushed with background seawater between samples (Tunnicliffe et al., 2009). In December 2014, mussels were collected using ROV Jason II (Figure 2.1) from 3 sites (Champagne, Pillar Top, Golden Lips; Table 1). All pH measurements from December 2014 collection sites were taken *in situ* using an AMT deep-sea pH sensor. All collection sites are separated by a maximum of ~100 meters (Figure 2.2). From each mussel, one valve was removed and the remaining valve and body were either fixed in 7% buffered formalin or frozen at -80°C shipboard.

Figure 2.1. ROV Jason II collecting mussels from Golden Lips, NW Eifuku, with scoop net. Scoop net is ~50 cm wide.

Table 2.1. Water characteristics for *B. septemdierum* collection sites in western Pacific Ocean; n/a = not available.

Vent	Site/Region	Coordinates	Date	Depth (m)	Temp (°C)	pH
Champagne	NW Eifuku, Mariana Volcanic Arc	21.4875, 144.0414	13-Dec-14	1,605	2.7	5.22
Golden Lips	NW Eifuku, Mariana Volcanic Arc	21.4876, 144.0413	13-Dec-14	1,606	2.7	5.78
Pillar Top	NW Eifuku, Mariana Volcanic Arc	21.4875, 144.0418	06-Dec-14	1,561	2.6	7.0
Near Fouling	NW Eifuku, Mariana Volcanic Arc	21.4878, 144.0417	10-Apr-04	1,576	2.5	5.88
ABE	East Lau Spreading Centre, Lau Basin	- 20.7626, 176.1918	25-Apr-16	2,130	maximum 15.3	no evidence of high CO_2
Nifonea	Nifonea Ridge, Vanuatu	-18.133, 169.517	13-Jul-13	1,873	n/a	no evidence of high CO_2

Nifonea volcano is located in the Vate Trough in the region of Vanuatu (18°10.2’ S, 169°30.0’ E). This large axial volcano rises 1 km higher than the adjacent sea floor and is ~14 km wide, spanning the entire width of the Vate Trough. The summit of the volcano is dominated by a large, horseshoe-shaped caldera that opens to the southeast. Hydrothermal activity near the northeast region of the caldera supports tubeworms, mussels and other vent fauna (Anderson et al., 2016). In July 2013, ROV Kiel collected mussels from Nifonea volcano (Table 2.1). Mussels were preserved in 95% ethanol. A pH measurement is not available for this site.

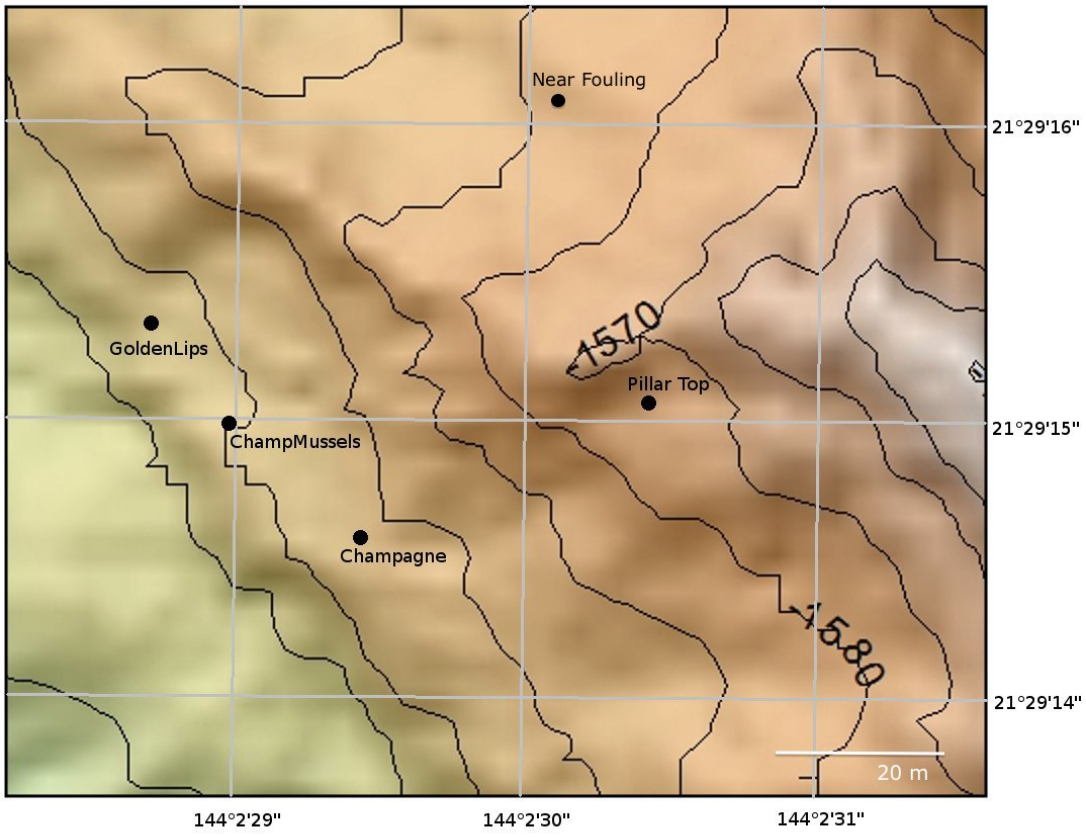

Figure 2.2. Bathymetric map of NW Eifuku summit indicating the locations of all collection sites and the Champagne Vent site.

Lau Basin is a back-arc spreading center in the region of Fiji that forms from the subduction of the Pacific plate beneath the Australian plate. Our collection site, ABE (20°45.75′ S, 176°11.51’ W), is located towards the northern end of this V-shaped basin. At ABE, there are three large areas of hydrothermal venting extending over 600m along a NE-SW trending fault (Flores et al., 2012). Hot fluid exits through large, tall chimneys but there are several peripheral areas with low to moderate temperature diffuse flow (Ferrini et al., 2008). The macrofaunal community is diverse, with abundant crab, squat lobsters, shrimp, anemones, snails, mussels and other vent fauna. In April 2016, ROV ROPOS placed a dome-shaped ‘flux integrator’ over a mixed patch of *B. septemdierum* and the vent snail, *Ifremaria nautilei,* to streamline diffuse flow for temperature measurements with an Eh/pH probe. A pH measurement is not available for this site. Mussels under the ‘flux integrator’ were subsequently collected (Table 2.1). Both valves were removed from each mussel and the body was fixed and stored in 7% buffered formalin shipboard.

Shell Measurements and Sex Determination

The shell length, width, and height from a single valve were measured for each individual. For specimens stored at -80°C only shells were available and sex was not determined. Small clips (~1mm^3) from the gonad and mantle of all available bodies were smeared and gametes observed under the light microscope to determine the sex.

Histology

A 5 mm cube of tissue was removed from the posterior gonad, anterior gonad and mantle/digestive gland of 6 female and 6 male mussels from each site, with the exception

of Golden Lips which included 5 females and 7 males, and ABE which included 2 females and 10 males. The tissues were subsequently dehydrated in a graded ethyl alcohol series and embedded in a JB-4 plastic resin solution. Transverse sections were cut (4 µm thick) and were stained with hematoxylin and eosin. Stages of gametogenesis were determined according to the staging scheme by Dixon et al. (2006) for *B. azoricus* with modifications to address residual gametes and include notable details observed in *B. septemdierum* (Table 2.2). The site gonadal index was calculated for each site in the following manner: the number of mussels at each stage was multiplied by the numerical value of that stage, the products were added, and the result was divided by the total number of individuals sampled (Seed, 1969). Histological analysis of mussels collected from Nifonea was not possible because samples were preserved in 95% ethanol. Mussels from low pH sites were assessed for evidence of compromised reproduction through, 1) visual inspection of reproductive tissues for signs of deterioration and, 2) examination of histological sections for evidence of premature spawning (i.e. spawning before gametes reach final maturation stage).

Circular equivalent diameter was determined for 40 oocytes that had been sectioned through the nucleus in each transverse section. Calculating the area of the oocyte using the longest and shortest diameter, and extrapolating diameter from this area measurement determined circular equivalent diameter. Oocyte size-frequency distributions were constructed for and for each site. These distributions were not normally distributed (Shapiro Wilk, $p<0.05$) and were analyzed using a Kruskal-Wallis test.

Table 2.2. Stages in the gametogenic cycle of *B. azoricus* by Dixon et al. (2006) and modifications to the *B. azoricus* scheme for *B. septemdierum*; ADG = adipogranular cells.

Stage	*Bathymodiolus azoricus (gametogenesis)* Dixon et al. (2006)	Stage	*Bathymodiolus septemdierum (oogenesis)*	*Bathymodiolus septemdierum (spermatogenesis)*
1	Adipogranular cells only, sexes undifferentiated.	1a	ADG cells only, sexually immature.	ADG cells only, sexually immature.
		1b	Residual oocytes may be present in sexually mature individuals within deflated acini or gonadal ducts. The majority of the reproductive tissue is comprised of ADG cells and most residual oocytes show signs of degradation.	Residual spermatozoa may be present in sexually mature individuals within deflated acini or gonadal ducts. The majority of the reproductive tissue is comprised of ADG cells.
2	Initiation of gametogenesis: spermatogonial or oogonial stage only.	2	Initiation of gametogenesis: oogonial (previtellogenic) stage only although residual oocytes may be present.	Initiation of gametogenesis: spermatogonia proliferate and differentiate into spermatocytes around the periphery of the acinus. Residual spermatozoa may be present.
3	Early gametogenesis: nothing beyond spermatid or early vitellogenesis.	3	Early gametogenesis: nothing beyond early vitellogenesis although residual oocytes may be present.	Early gametogenesis: spermatocytes begin to differentiate into spermatids and begin to occupy the lumen of the acinus. Residual spermatozoa may be present.
4	Late gametogenesis: differentiated sperms or late vitellogenic oocytes.	4	Late gametogenesis: late vitellogenic oocytes. Only the basal region of the oocytes remains connected to the acinus wall. Residual oocytes may be present.	Late gametogenesis: spermatids take up most of the lumen and are connected by cytoplasmic material that forms a whorl pattern within the acini. Spermatogonia and spermatocytes only occupy the periphery of the acinus.
5	Gamete maturation: ripe spermatozoa occupy 70% of the follicle in males; oocytes fully fill the follicles. The amount of adipogranular tissue is much reduced, to approximately 3% in females and 10% in males.	5	Gamete maturation: mature oocytes are released from acinus wall and fill the acinus. The amount of adipogranular tissue is greatly reduced.	Gamete maturation: spermatids differentiate into ripe spermatozoa and gamete density in the acinus greatly increases. Spermatogonia and spermatocytes now only form a thin layer around the periphery of the acinus. The amount of adipogranular tissue is greatly reduced.
6	Spawning: gamete density is greatly reduced with some follicles partly empty. Gonadal ducts visible in the intact mantle.	6	Spawning: gamete density is greatly reduced with some follicles partly empty. Gonadal ducts visible in the intact mantle. Residual oocytes may be present.	Spawning: gamete density is greatly reduced with some follicles partly empty. Gonadal ducts visible in the intact mantle. Residual spermatozoa may be present.
7	Post spawning: massive haemocyte infiltration resulting in enzymic degradation of residual or effete gametes. Parts of the mantle now appear extremely thin, almost transparent in places.	7	Post spawning: massive haemocyte infiltration resulting in enzymic degradation of residual or effete gametes. Parts of the mantle now appear extremely thin, almost transparent in places. Residual oocytes may be present.	Post spawning: massive haemocyte infiltration resulting in enzymic degradation of residual or effete gametes. Parts of the mantle now appear extremely thin, almost transparent in places. Residual spermatozoa may be present.

Results

Site Characterization and Collection Size Structure

Northwest Eifuku collection sites (Pillar Top, Golden Lips, Champagne and Near Fouling) share similar characteristics. Imagery shows that mussels are densely clustered across the rock-covered sea floor and along the steep contours of the summit. In many areas, the mussel beds are so dense that the substratum cannot be seen, though the mussels avoid areas of strong hydrothermal fluid flux. At all sites, non-predatory anomuran crabs and alvinocaridid shrimp are distributed throughout the mussel beds. Temperature measurements (~2.6°C) are similar among the mussel beds. The pH is variable across collection sites with values ranging from 5.22 to 7.00 (Table 2.1).

Nifonea is characterized by pillow-lavas and fractures that emanate diffuse hydrothermal fluids. Mussel beds are dense where present, but have a patchy distribution across the sea floor often aggregating in cracks between the pillow-lavas. Imagery shows the macrofaunal community at Nifonea is markedly more diverse than NW Eifuku consisting of animals like tubeworms, anemones, barnacles, crab, zooanthids and squat lobsters. There is no evidence of high CO_2 at the site of mussel collection; in close proximity to our mussel sample, we see shells of dead mussels with exposed calcium carbonate. Such exposed calcium carbonate does not occur on NW Eifuku as shells rapidly dissolved after mussel death due to the high CO_2 conditions at this volcano.

The sea floor at ABE is rocky and covered with scattered macrofaunal communities. Mussels tend to aggregate in isolated patches along with *I. nautilei.* Imagery indicates that Galatheid crabs, squat lobsters, barnacles, and alvinocaridid shrimp are also present. The maximum temperature at the location of mussel collection is

15.3°C. There is no evidence of high pCO_2; previous regional pH measurements are >7.8 and dead mussel shells are present <50 cm away from the collection. Available water characteristics from each site are summarized in Table 2.1.

Sex ratio and Size-sex Distributions

Shell length distributions from each site are predominately left-skewed (Figure 2.3) and the largest mussel is 157 cm long. The smallest average shell length is found at Champagne, while the largest average shell length is found at Near Fouling (Table 2.3). All individuals are sexually mature. The smallest mussel from our collections is 29 mm in length and male, while the smallest observed female is 73 mm. Of the mussels preserved allowing sex determination, (n=151) 75% of individuals smaller than 100 mm in length are male and 73% of individuals larger than 100 mm in length are female. Male: female (M: F) ratios vary considerably between sites with the lowest M: F ratio at Golden Lips, and the highest at ABE where males greatly outnumber females (Table 2.3, Figure 2.3). Evidence of successive sex change is present only in ABE mussels where mussels display a sex change from female to male. In 27% of ABE mussels, residual oocytes are observed in spawning canals and around the periphery of acini in functionally male mussels (Figure 2.4). The ABE mussels exhibiting sex change range from 81-102 mm in length. In all other mussels, only one type of gamete is present throughout the reproductive tissues.

Table 2.3. Male: female ratio, shell minimum length, shell maximum length, shell average length, mean oocyte diameter ± standard error, and gonadal indices from *B. septemdierum* from western Pacific collection sites. Sample size is shown as N(n), where N is the sample size used in shell length measurements, and n is the sample size used to determine male: female ratios. Gonadal indices were determined using *B. septemdierum* analyzed histologically; (m) indicates male gonadal index, and (f) indicates female gonadal index; n/a – not available.

Location	**Time of Collection (Month-Year)**	**pH**	**Sample Size N (n)**	**M: F Ratio**	**Min Shell Length (mm)**	**Max Shell Length (mm)**	**Average Shell Length (mm)**	**Mean Oocyte Diameter ± SE (µm)**	**Site Gonadal Index**
Pillar Top	Dec-14	7.00	33 (24)	0.71	51	142	112.8	40.09 ± 0.21	4.83 (m) 4.83 (f)
Champagne	Dec-14	5.22	38 (25)	1.27	39	118.5	86.5	41.47 ± 0.21	5.00 (m) 4.67 (f)
Golden Lips	Dec-14	5.78	45 (30)	0.30	78.5	124.5	109.2	33.34 ± 0.3	3.86 (m) 3.60 (f)
Near Fouling	Apr-04	5.88	27 (30)	0.25	29	157	121.3	33.09 ± 0.24	2.83 (m) 2.50 (f)
ABE	Apr-16	___	14 (15)	6.50	82	116	95.6	30.35 ± 0.37	2.33 (m) 2.50 (f)
Nifonea	Jul-13	n/a	27 (27)	0.93	87	140	111.5	n/a	n/a

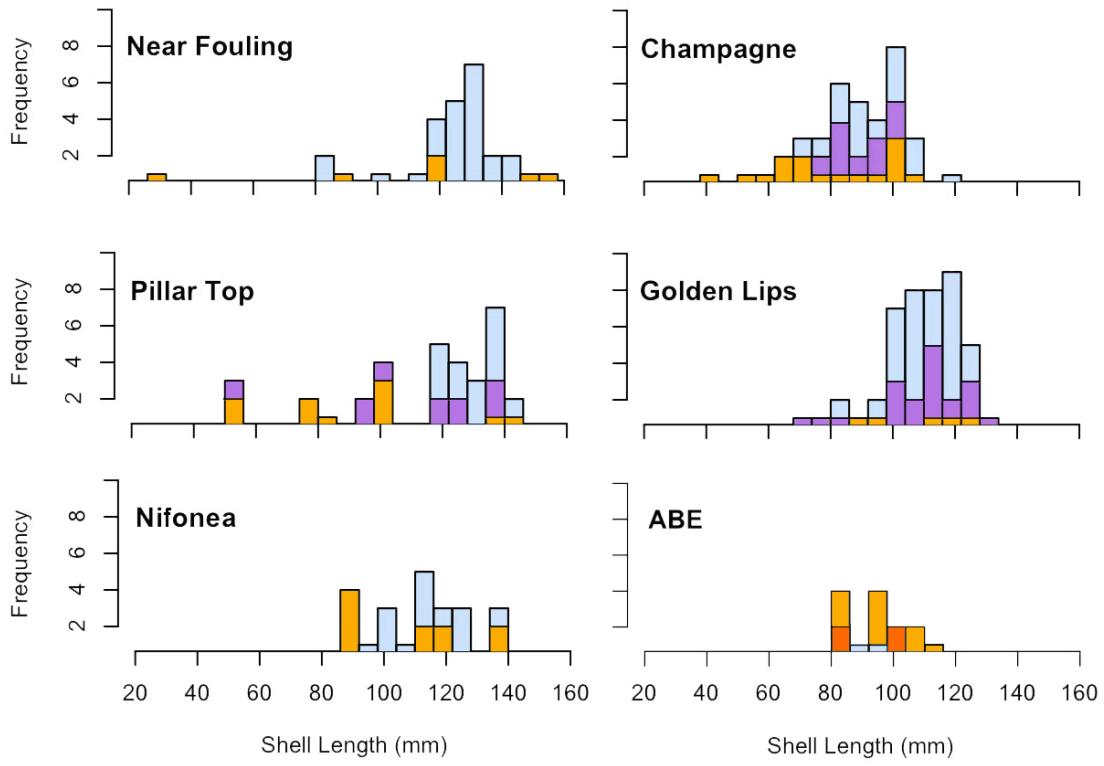

Figure 2.3. *Bathymodiolus septemdierum* size-sex distribution from all sample sites. Blue represents females, light orange represents males, dark orange represents males that contain residual oocytes, and purple represents mussels where sex could not be determined due to -80°C freezing of the body.

General Gonad Morphology

In both males and females, the gonad and mantle (dorsal to the attachment point of the gills to the mantle) consist of acini and gonadal ducts surrounded by interacinal tissue. The interacinal tissue is composed of adipogranular (ADG) cells but lacks vesicular connective tissue present in other mytilids. Lipid globules dominate the cytoplasm of ADG cells and there is a clearly visible nucleus. ADG cells act as storage cells that eventually convert to reproductive tissue.

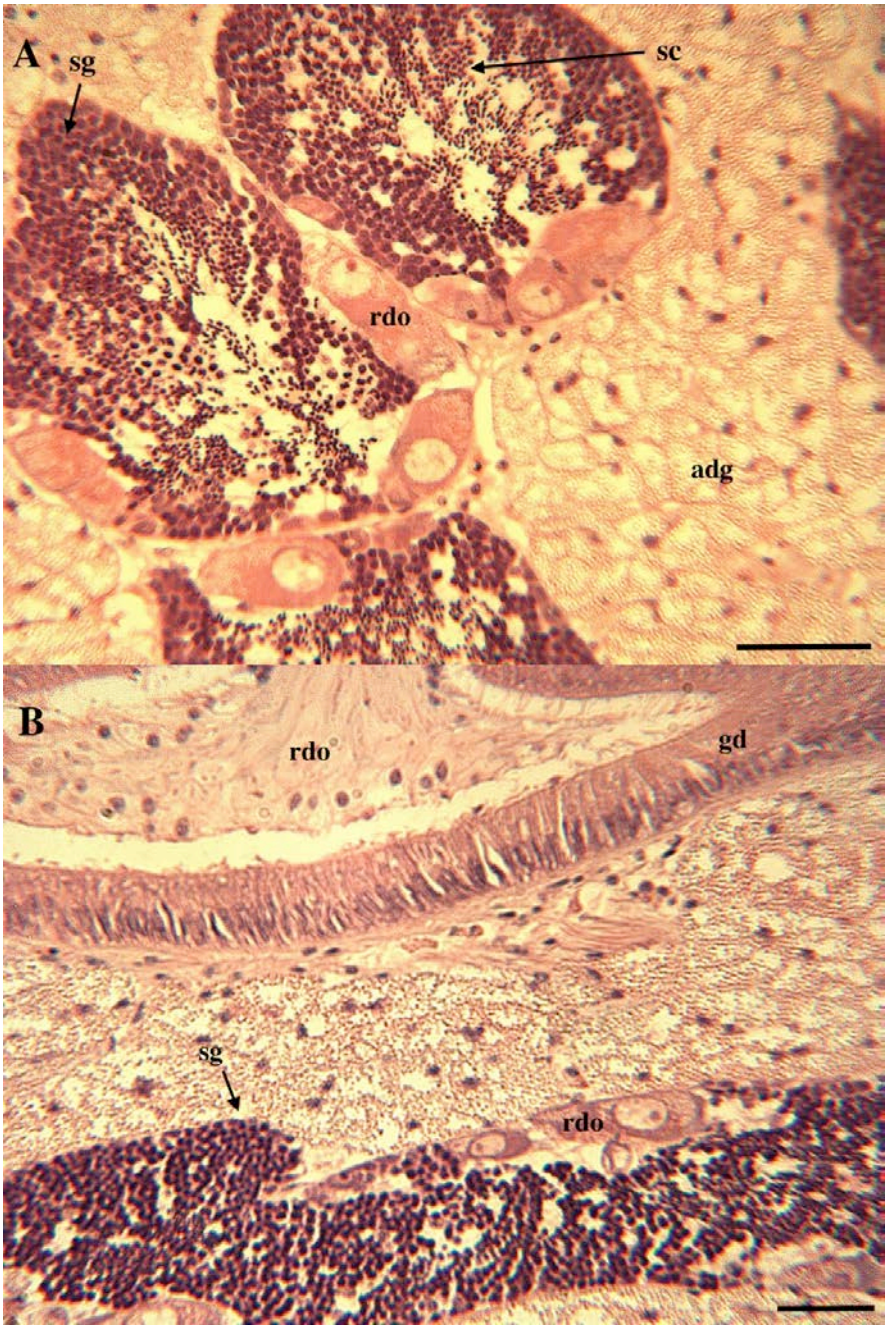

Figure 2.4. a) Functional ABE male in Stage 3 spermatogenesis with residual oocytes along the periphery of the acinus, b) the same male individual with residual oocytes in the gonadal duct and in the acinus. Labels include: adipogranular cells (adg), gonadal duct (gd), residual degrading oocyte (rdo), spermatocytes (sc), spermatogonia (sg). Scale bars represent 50 μm.

The acini are lined with undifferentiated germ cells that surround the lumen. The number of acini in the gonad and mantle increases as gametogenesis proceeds. The progression of

gametogenesis is uniform throughout the gonad and mantle. Gonadal ducts are more apparent in mussels in early gametogenesis that have recently undergone a major spawning event. It is unclear whether the number of gonadal ducts proliferates approaching a spawning event or if the canals are more difficult to see when acinus density is high. The gonadal ducts are composed of ciliated columnar cells and often contain residual oocytes or spermatozoa (Figure 2.5).

Oogenesis

Before gametogenesis begins, only adipogranular cells are present in the ovary and mantle. If individuals have previously undergone a spawning event, residual oocytes may be present in deflated acini or gonadal ducts before oogenesis begins (Stage 1). The majority of reproductive tissue is comprised of ADG cells and most residual oocytes show signs of degradation including a grainy appearance, close proximity to haemocytes, and disappearing nuclei (Figure 2.6 a.). Initiation of gametogenesis occurs when the undifferentiated germ cells lining the acinus give rise, by mitotic division, to previtellogenic oocytes (Stage 2). These oocytes are small in equivalent diameter (~5-15 µm) and remain attached to the acinus wall. In the ovary, follicle cells are often associated with the basal region of developing oocytes. Early vitellogenesis begins when oocytes become larger, early vitellogenic oocytes (~15-25 µm) (Stage 3; Figure 2.6 a.). In late vitellogenesis, only the basal region of the oocyte remains connected to the acinus wall by means of a broad stalk that eventually thins and detaches from the acinus wall (Stage 4; Figure 2.6 b.). Late vitellogenic oocytes are ~25-35 µm in diameter. Mature oocytes fill the acinus and the amount of adipogranular tissue is greatly reduced (Stage 5; Figure 2.6 c.). The mature oocytes are large in diameter (~35-55 µm) with clearly defined

nuclei. During spawning, the acini deflate and oocyte density is greatly reduced (Stage 6). After spawning, haemocytes enzymatically degrade most of the residual oocytes (Stage 7). Residual gametes may be present in all stages within acini or gonadal ducts.

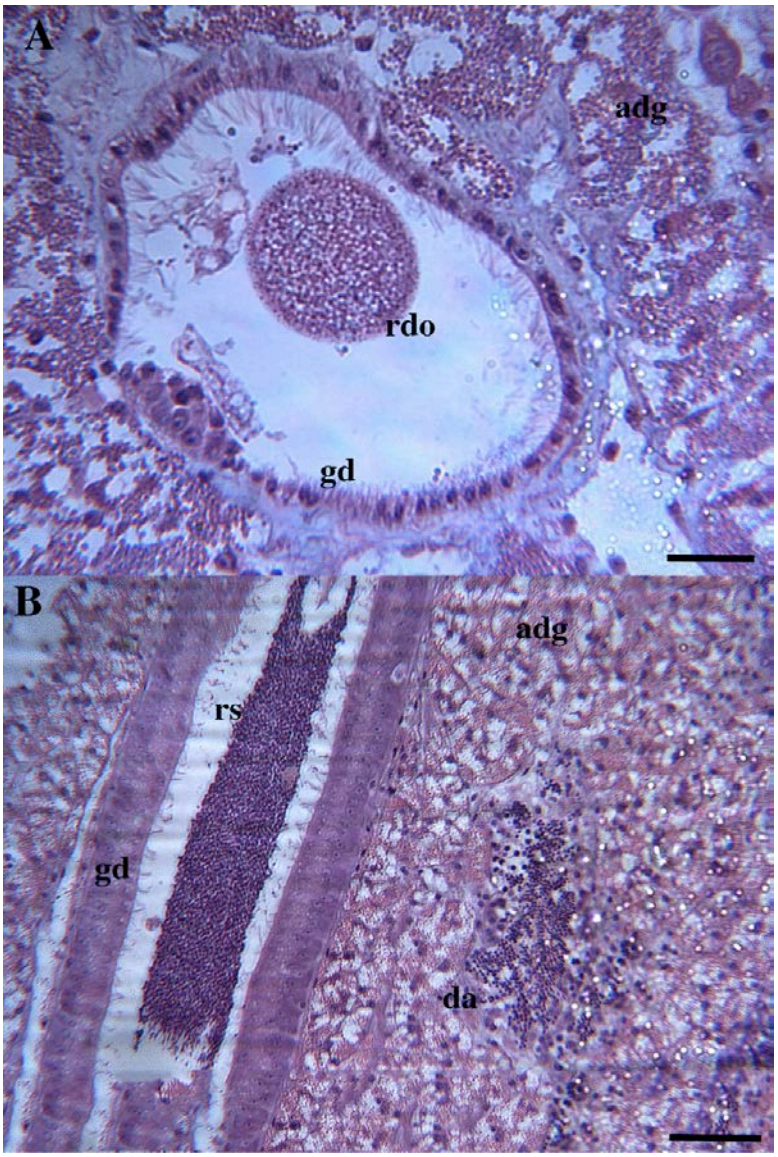

Figure 2.5. a) Near Fouling female in Stage 3 with residual degrading oocyte in gonadal duct, b) Golden Lips male in Stage 6 with residual spermatozoa in gonadal duct. Labels include: *adg* adipogranular cells, *da* deflated acinus, *gd* gonadal duct, *rs* residual spermatozoa, *rdo* residual degrading oocyte. Scale bars represent 20 µm.

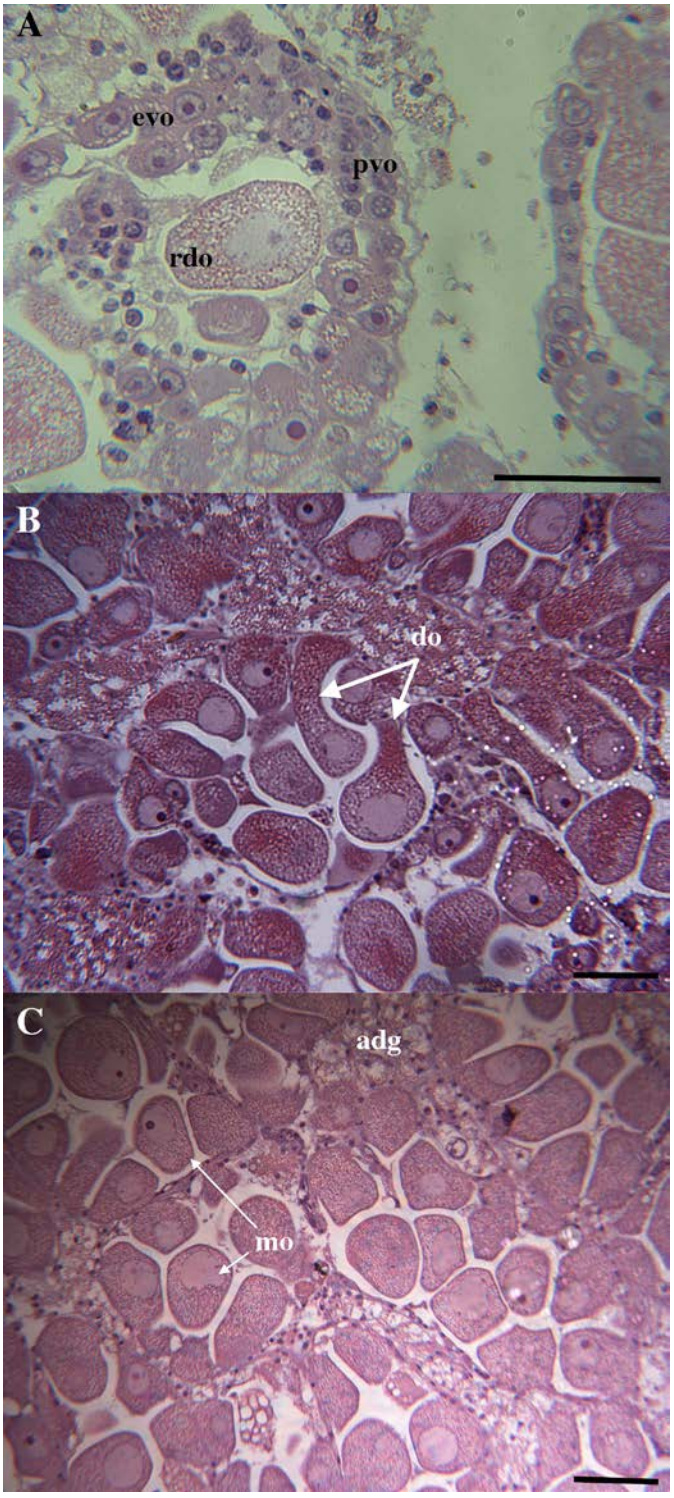

Figure 2.6. a) Near Fouling female in Stage 3 of oogenesis with previtellogenic oocytes and early vitellogenic oocytes on periphery of acinus with a residual degrading oocyte in the lumen, b) Golden Lips mussel in Stage 4 with oocytes disengaging from acinus wall, c) Champagne mussel in Stage 5 with several mature oocytes in the lumen, adipogranular tissue is greatly reduced. Labels include: adipogranular cells (adg), early vitellogenic

oocyte (evo), previtellogenic oocyte (pvo), disengaging oocyte (do), residual degrading oocyte (rdo), and mature oocytes (mo). Scale bars represent 50 μm.

Spermatogenesis

As in females, before gametogenesis begins, only adipogranular cells are found in the male testis and mantle (Stage 1). If individuals have previously undergone a spawning event, residual spermatozoa may be present in deflated acini or gonadal ducts before spermatogenesis begins. Initiation of spermatogenesis begins when spermatogonia proliferate and differentiate into spermatocytes around the periphery of the acinus (Stage 2; Figure 2.7 a.). Next, some spermatocytes differentiate into spermatids and both spermatocytes and spermatids begin to occupy the lumen of the acinus (Stage 3). As spermatogenesis proceeds, spermatids take up most of the lumen and are connected by cytoplasmic material appearing as whorls within the acini (Stage 4; Figure 2.7 b.); evident under high magnification that whorls are not composed of spermatozoa flagella. Spermatogonia and spermatocytes now only occupy the periphery of the acinus. Spermatids then differentiate into ripe spermatozoa, which can be identified by the presence of a cap-like acrosome, and gamete density in the acinus greatly increases. Spermatogonia and spermatocytes now only form a thin layer on the periphery of the acinus and the amount of adipogranular tissue is greatly reduced (Stage 5; Figure 2.7 c.). During spawning the acini deflate and spermatozoa density is greatly reduced (Stage 6; Figure 2.7 d.). After spawning, haemocytes enzymatically degrade most of the residual spermatozoa (Stage 7). Residual gametes may be present in all stages within acini or gonadal ducts.

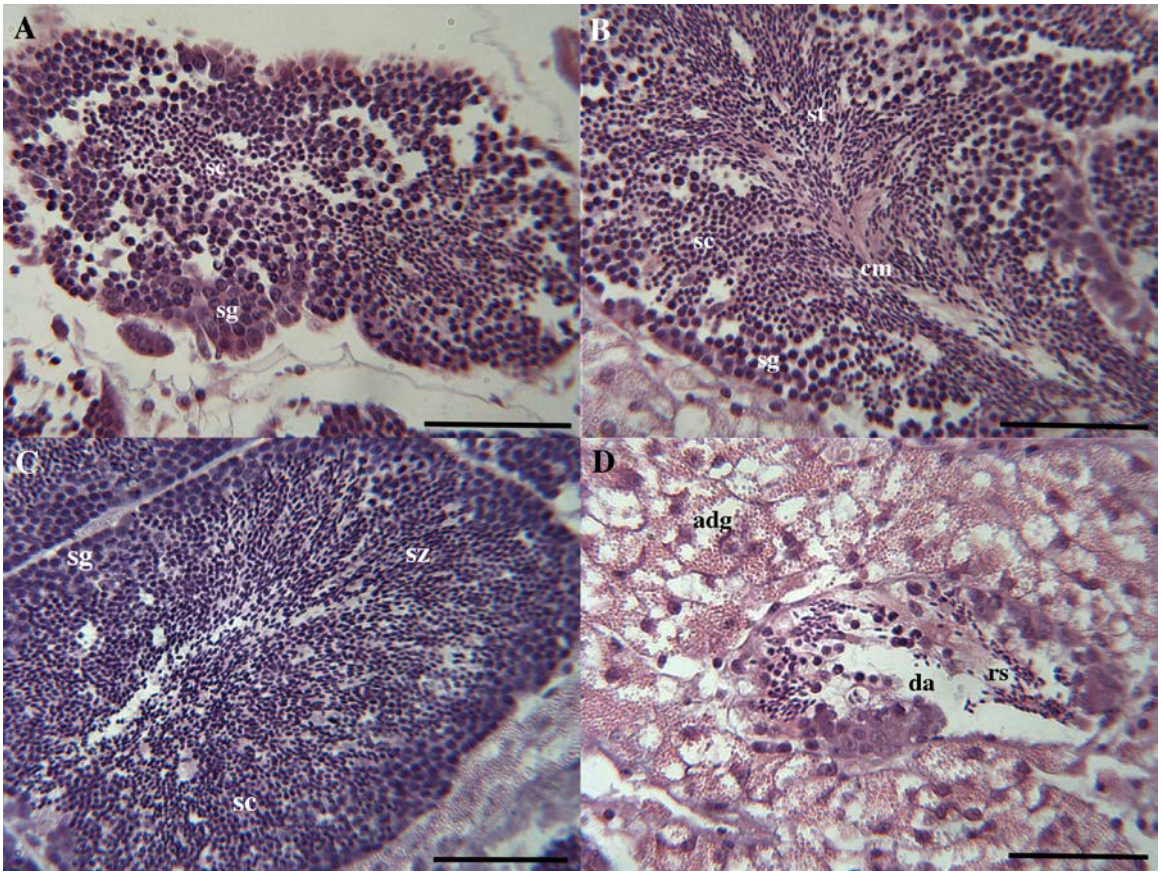

Figure 2.7. a) Near fouling male in Stage 2 with spermatogonia and spermatocytes occupying the majority of the acinus, b) Pillar Top male in Stage 4 with spermatids in the lumen connected by whorled cytoplasmic material within the acinus, c) Champagne male in Stage 5 where only a thin layer of spermatocytes and spermatozoa is found around the periphery of the acinus, and ripe spermatozoa occupy the lumen, d) Golden Lips male in Stage 6 with deflated acinus with few residual spermatozoa. Labels include: adipogranular cells (adg), spermatogonia (sg), spermatocytes (sc), spermatids (st), spermatozoa (sz), deflated acinus (da), residual spermatozoa (rs), and cytoplasmic material (cm). Scale bar represents 20 µm.

Periodicity of Gametogenesis and Reproductive Features at Low pH Sites

Periodicity of gametogenesis is reflected in gonadal indices and distribution of oocyte diameters summarized by size-frequency histograms (Figure 2.8, 2.9). The five collection sites showed significantly different oocyte diameters according to Kruskal-Wallis: $X^2 = 820.55$, $p<0.01$. Mussels collected in December from Champagne and Pillar

Top have gonadal indices that correspond to stages 4-5 (late gametogenesis/gamete maturation), and the largest oocytes (Figure 2.8, 2.9). Golden Lips mussels, also collected in December, temporally lag in gamete development with gonadal indices corresponding to stages 3-4 (early to late gametogenesis) and the mean oocyte diameter is ~19% smaller than the other two December sites (Table 2.3). December mussels display large gonads, thick proliferation of the gonad into the mantle and clearly visible spawning canals indicating that a spawning event is approaching (Figure 2.10). Mussels collected in April from both ABE and NWE Four are in the early stages of gametogenesis: gonadal indices correspond to stages 2-3 (initiation of gametogenesis/early gametogenesis)(Figure 2.8). Approximately 40% of all measured oocytes from the NWE Four and ABE samples are residual from a prior spawning event, and large in diameter (Figure 2.9). Non-residual oocytes are significantly smaller than oocytes in December counterparts (post hoc Wilcoxon test, $p<0.05$). April mussels have smaller gonads, almost transparent mantle tissue and poorly visible spawning canals (Figure 2.11). The reproductive tissues of mussels from low pH sites do not show visible signs of deterioration and there is no evidence of premature spawning. Moreover, there is no apparent relationship between pH and oocyte diameter, or gonadal index, as summarized in Table 2.3.

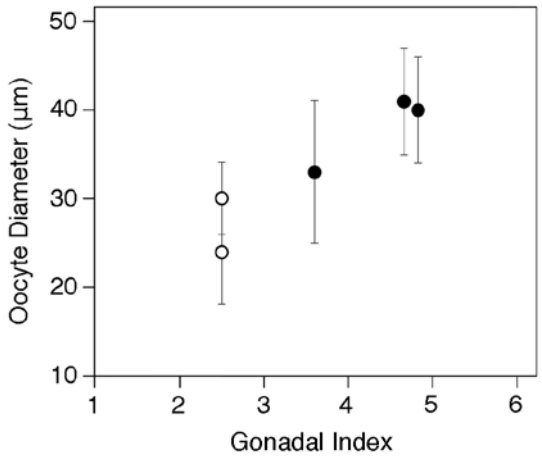

Figure 2.8. Stage corresponding to average oocyte diameter. Closed symbols represent the average oocyte diameter from female mussels collected in December (NW Eifuku). Open symbols represent the average oocyte diameter from female mussels collected in April (NW Eifuku and ABE). Data do not include residual oocyte sizes. Bars represent standard deviation.

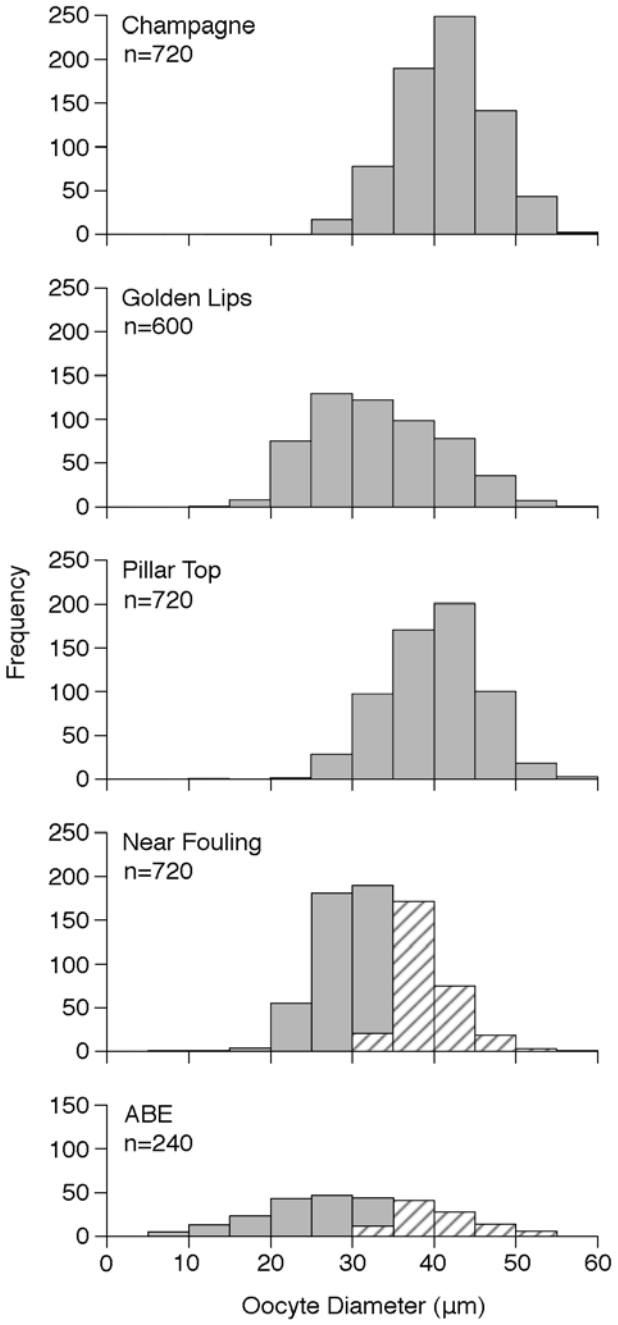

Figure 2.9. Oocyte size-frequency distributions from all collection sites. ABE has a small sample size because only 2 females were present in the collection. Hatched bars indicate residual oocytes.

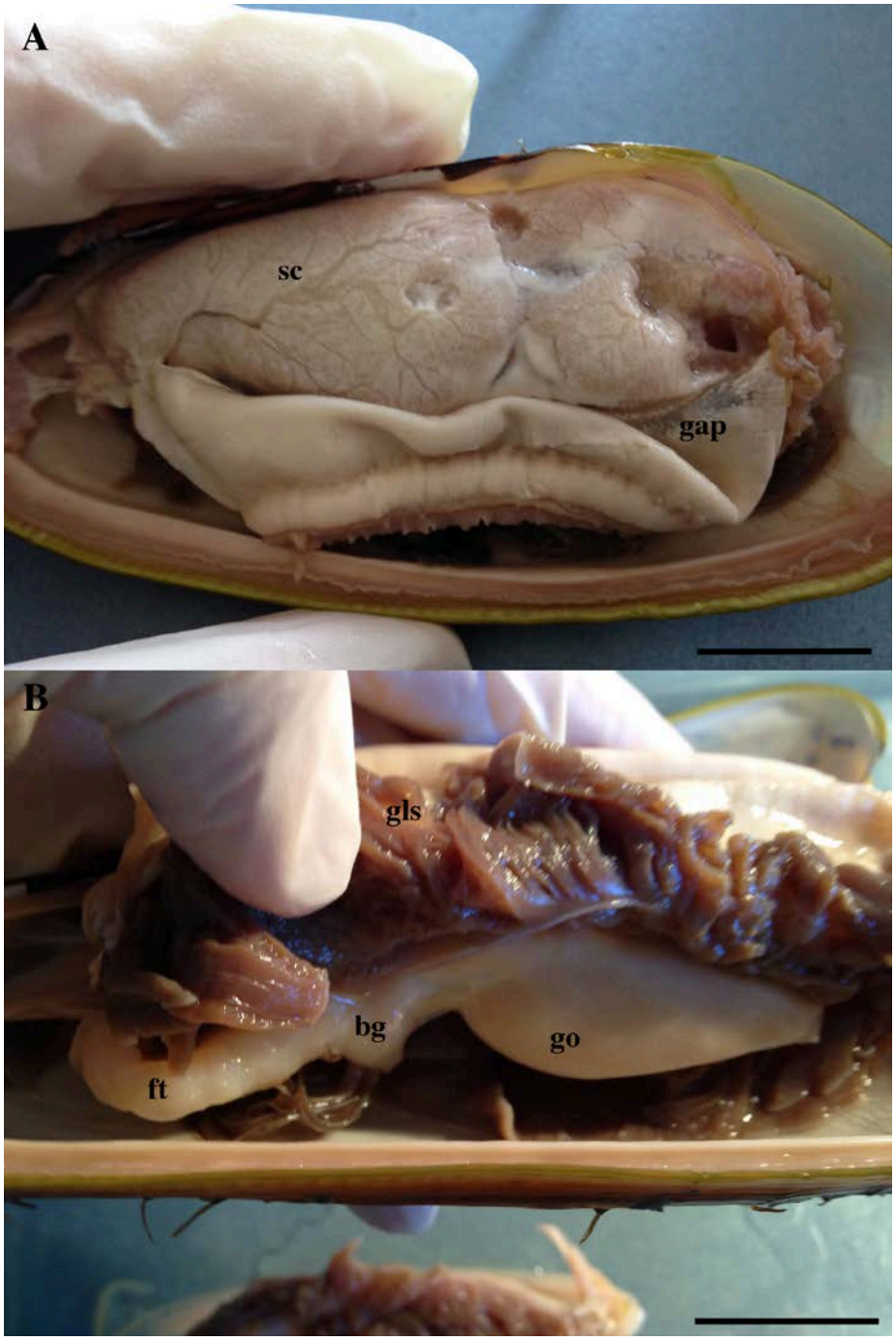

Figure 2.10. a) Dense proliferation of the gonad into the mantle of a Champagne mussel. There are evident spawning canals and a clear transition at the gill attachment point between reproductive and non-reproductive tissue, b) view beneath the gills of a Pillar Top mussel showing the large gonad. Labels include: gonad (go), spawning canals (sc), gill attachment point (gap), foot (ft), byssal gland (bg), and gills (gls). Scale bar represents approximately 2 cm.

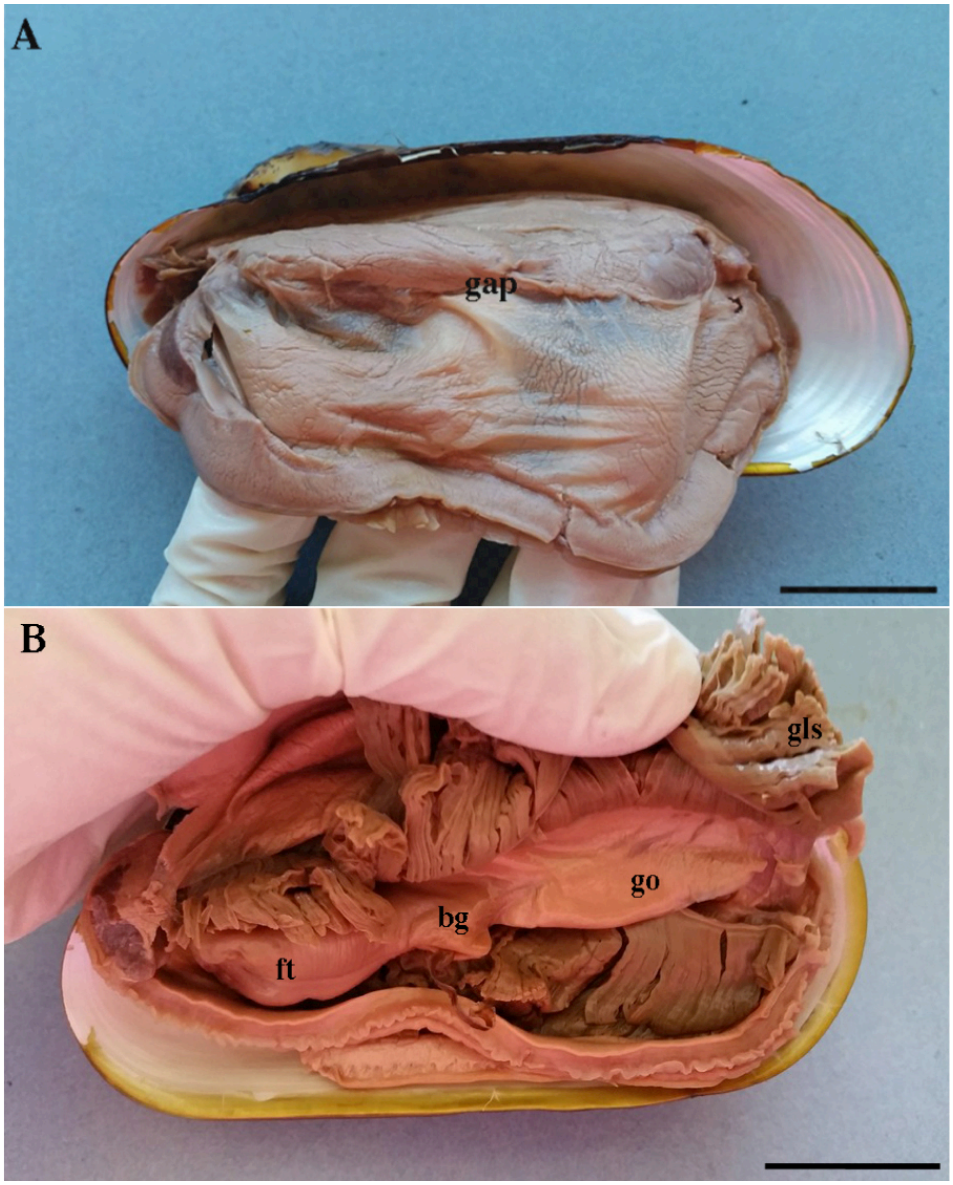

Figure 2.11. Very little proliferation of the gonad into the mantle of a Near Fouling mussel. There are few spawning canals and although there is a clear transition at the gill attachment point between reproductive and non-reproductive tissue, the area of reproductive tissue is greatly reduced, b) view beneath the gills of a Near Fouling mussel showing the small gonad. Labels include: gonad (go), gill attachment point (gap), foot (ft), byssal gland (bg), and gills (gls). Scale bar represents approximately 2 cm.

Discussion

Reproductive Mode

Bathymodiolus septemdierum is functionally dioecious but also displays hermaphroditism with sex change from female to male in a small number of individuals from our collections. The evidence of hermaphroditism includes residual oocytes in males with Stage 2-3 sperm development in some individuals. In contrast, Le Pennec & Beninger (1997) report protandry in the same species in the north Fiji Basin where female gametes appear in spent male acini. This male to female transition also occurs occasionally in *B. azoricus* (Dixon et al., 2006) with immature oocytes in the mantle tissue of functional males. It is only in our Lau Basin collection that some hermaphroditism (27%) is evident suggesting that the phenomenon is variable in both location and sex change direction. The smallest mussels sampled are mature males; maturity is possible as small as 29 mm while the smallest female is 73 mm in length. Thus, maturation size appears to differ between sexes as suggested for *B. thermophilus* where males mature at ~40 and females at ~60 mm. (Berg, 1985). Our smallest hermaphrodites are over 80 mm, indicating that sex change did not happen until after female maturation size.

As our study and that of Le Pennec & Beninger (1997) report opposite sex change directions, *B. septemdierum* appears to display alternative sexuality. Hermaphroditism is categorized into four groups (Coe, 1943; Kasyanov, 2001): 1) Functional hermaphroditism, where eggs and sperm develop simultaneously, 2) consecutive sexuality, where a single sex change event occurs, generally from male to female, 3) rhythmical consecutive sexuality, where the bivalve changes from one sex to the other

and maintains a rhythmical pattern throughout its life, and 4) alternative sexuality, where sex change can be triggered by season or environmental factors. Thus, in species like *B. septemdierum*, it is less likely genetics that determines germ cell development, but rather a response to external stimuli. Hermaphroditism is a common reproductive strategy, especially in animals that occur at low densities, have small, genetically isolated populations, and are sedentary as adults (Ghiselin, 1969; Charnov, 1982). It is not surprising therefore, that bivalves are commonly hermaphroditic (Coe, 1943).

Manifestation of sex can have a strong environmental component, whether it is biotic factors (e.g. food availability, parasites, symbionts) or abiotic factors (e.g. photoperiod, temperature). Males tend to dominate when environmental conditions are poor because producing eggs is energetically more expensive than producing sperm (Russell-Hunter, 1979). In the charru mussel (*Mytella charruana*), the sex ratio of mussels maintained in the laboratory changes toward a male-bias under starvation conditions within a month (Stenyakina et al., 2010). Dolgov (1991) relate protogynic sex change in the backlip pearl oyster (*Pinctada margaritifera*) to the stress of oil pollution. Gametogenesis in bivalves tends to begin when considerable lipid and carbohydrate reserves are present, and the quantity of energy reserves in an organism's reproductive tissues may subsequently influence gender determination. Coping with stressors like food scarcity, temperature, predation, habitat degradation or pathogens may compromise an organism's ability to acquire energy reserves thereby favouring the development of males.

Mussels from Lau Bain were collected from a mixed aggregation of *B. septemdierum* and *I. nautilei,* which occur at temperatures significantly higher than that

of homogenous aggregations of *B. septemdierum* (Podowski et al., 2010). Mixed aggregations of these two species generally indicate that *B. septemdierum* is surviving near its upper thermal tolerance (Podowski et al., 2010). Although the upper temperature limit of *B. septemdierum* is 35°C, temperatures of 19°C can only be tolerated for 2 hours (Henry et al., 2008). The temperature from the Lau Basin collection (maximum 15.3°C) is notably higher than that of NW Eifuku collections (~2.6°C) suggesting that thermal stress may prompt the female to male sex change observed in *B. septemdierum.*

Periodicity of gametogenesis

While a partial description of gametogenesis in *B. septemdierum* is available (Le Pennec & Beninger, 1997), in *B. azoricus* and *B. childressi* it is well documented. Dixon et al. (2006) regularly collected *B. azoricus* specimens from the Menez Gwen vent field (Mid-Atlantic Ridge) which show a high degree of reproductive synchrony between males and females, as well as a synchronized and annual reproductive cycle (Dixon et al., 2006). The main spawning peak for *B. azoricus* occurs in late December - early January coinciding with a winter - spring bloom in primary production in the euphotic zone (Dixon et al., 2006). A relationship between particulate feeding levels of *B. azoricus* and large amounts of nutrient storage tissue in the mantle provide further evidence of a dependence on photosynthetic inputs by *B. azoricus* (Dixon et al., 2006). These patterns in *B. azoricus* closely resemble that of *Mytilus edulis*, which is known for optimizing the timing of gamete production and release against seasonally- varying food availability (Bayne, 1976).

An annual pattern of gametogenesis also occurs in *B. childressi* at seeps on the Louisiana slope. Tyler et al. (2007) note a strong degree of synchrony in gamete

development between males and females, and evidence that spawning occurs sometime between October and February when the flux of detritus to the bathyal zone is substantial. Although there is notable inter-annual variability, gametogenesis in *B. childressi* is generally in its early stages in the early months of the calendar year and later stages in the later months (Tyler et al., 2007).

Gonadal indices and oocyte size-frequency distributions of *B. septemdierum* from NW Eifuku and ABE provide evidence of discontinuous gametogenesis consistent with the annual reproductive cycle observed in other bathymodioline mussels (e.g. Tyler et al., 2007, Dixon et al., 2006, Kàdàr et al., 2006). Mussels collected in April are in early stages of gametogenesis while mussels collected in December are in later stages. We note variation in stage of gametogenesis among individuals from neighbouring sites collected in December, where mussels from Golden Lips display intermediate stages of gametogenesis and one individual has already begun to spawn. This variation suggests "leaky" reproduction, whereby a number of smaller spawning events occur around the central event. Primary productivity in the northern Marina region borders on ultraoligotrophic (Chl *a* <0.06 mg m^{-3}, measured in March 2010) (Suntsov & Domokos, 2013). Surface production likely has little influence on the reproductive pattern observed in *B. septemdierum* at NW Eifuku.

Similarly, Le Pennec & Beninger (1997) observe discontinuous spermatogenesis in *B. septemdierum* from the North Fiji Basin despite the oligotrophic nature of the region (Lemasson et al., 1990). Species occurring at hydrothermal vents and cold seeps often have similar reproductive patterns to species in the same taxa found in non-chemosynthetic environments regardless of continuous nutritional input from symbionts

(Tyler & Young, 1999, Eckelbarger & Watling, 1995). It is possible that phylogenetic history may play an important role in governing the reproductive patterns of vent and seep organisms including *B. septemdierum*.

Reproductive Features in Low pH Conditions

Low pH conditions have no evident effect on reproduction in *B. septemdierum* from NW Eifuku. Although there is no unambiguous definition of 'compromised' reproduction, we examined mussels for signs of premature spawning and poor physical gonadal condition. Premature spawning in marine invertebrates may be indicative of insufficient energy to maintain mature gametes (Petes et al., 2008), and poor gonadal condition may reflect energy allocation away from reproduction to sustain other biological processes (Siikavuopio et al., 2007). Mussels from all sites, including those of the lowest pH (Champagne), show apparently healthy reproductive tissues, and there was no indication of premature spawning. Gamete development is consistent with the proposed annual cycle with only some variability exhibited by mussels from Golden Lips. Mussels collected in April from NW Eifuku (pH 5.88) and the same month in Lau Basin (pH >7.8) show no difference in the degree of gamete development or gonadal condition.

Environmental conditions are considered suboptimal if an organism needs to increase energy expenditure to maintain homeostasis and ensure survival (Lannig et al., 2010). During exposure to low pH conditions, an organism may compensate for increased energy demands by increasing food intake. Pansch et al. (2014) find that Tjärnö barnacles (*Amphibalanus improvisus*) are able to withstand moderate levels of elevated pCO_2 when food is abundant but show reduced growth when food is scarce relative to barnacles given low food levels at normal pCO_2. Tolerance to low pH conditions in *B. septemdierum*

may, therefore, be a function of proximity to hydrothermal fluids that support nutrient production by gill symbionts.

Energetic trade-offs exist in all organisms and, under stressful conditions, energy may be allocated away from one biological process in support of another. Melzner et al. (2011) find that the integrity of inner shell surfaces is tightly coupled to the energy budget of *M. edulis*. Under high pCO_2 and limited food conditions, *M. edulis* has significant biological control over energy allocation whereby fitness-sustaining processes like somatic growth and reproduction take precedence over inner shell maintenance and repair (Melzner et al., 2011). Tunnicliffe et al. (2009) note that at a given shell length, mussel shells from NW Eifuku weigh about half that of shells from Monowai and Lau Basin where pH is 7.87 and 8.42, respectively. Using daily microgrowth bands in the shells (Schöne & Giere, 2005), they also demonstrate that NW Eifuku increment widths are almost half those in shells from high pH vents (including Lau). Thus, rates of shell thickening and enlargement in NW Eifuku mussels are compromised as a result of the extremely acidic conditions. We suggest that *B. septemdierum* is allocating energy away from shell formation and toward reproduction, and/or that excess energy demands imposed by low pH conditions are alleviated by adequate food availability. Ultimately, in the face of an energy demanding stressor like CO_2-driven acidification, understanding the energy budget of organisms living in such conditions provides the greatest insight on stress tolerance and fitness.

Literature cited

Anderson, M. O., Hannington, M. D., Haase, K., Schwarz-Schampera, U., Augustin, N., McConachy, T. F., & Allen, K. (2016). Tectonic focusing of voluminous basaltic eruptions in magma-deficient backarc rifts. *Earth and Planetary Science Letters*, *440*, 43–55. http://doi.org/10.1016/j.epsl.2016.02.002

Bayne, B. L. (1976). *Marine mussels: their ecology and physiology*. (B. L. Bayne, Ed.) (Vol. 10). Plymouth, UK: Cambridge University Press.

Bayne, B. L., Salkeld, P. N., Worrall, C. M. (1983). Reproductive effort and value in different populations of the marine mussel, *Mytilus edulis L*. *Oecologia*, *59*, 18–26.

Berg, C. J. (1985). Reproductive strategies of mollusks from abyssal hydrothermal vent communities. *Bulletin of the Biological Society of Washington*, *6*, 185–197.

Calow, P. (1983). Energetics of reproduction and its evolutionary implications. *Biological Journal of the Linnean Society*, *20*(2), 153–165. http://doi.org/10.1111/j.1095-8312.1983.tb00359.x

Charnov, E. L. (1982). The theory of sex allocation. *American Journal of Physical Anthropology*, *63*(4), 437–438. http://doi.org/10.1002/ajpa.1330630409

Coe, W. R. (1943). Sexual Differentiation in Mollusks. I. Pelecypods. *The Quarterly Review of Biology*, *18*(2), 154–164. http://doi.org/10.1086/394673

Dixon, D. R., Lowe, D. M., Miller, P. I., Villemin, G. R., Colaço, A., Serrão-Santos, R., & Dixon, L. R. . (2006). Evidence of seasonal reproduction in the Atlantic vent mussel *Bathymodiolus azoricus*, and an apparent link with the timing of photosynthetic primary production. *Journal of the Marine Biological Association of the UK*, *86*(6), 1363–1371. http://doi.org/10.1017/S0025315406014391

Dolgov, L. V. (1991). Sex expression and environmental stress in a mollusc, *Pinctada margaritifera*. *Invertebrate Reproduction & Development*, *20*(2), 121–124. http://doi.org/10.1080/07924259.1991.9672188

Dufour, S., & Felbeck, H. (2006). Symbiont abundance in thyasirids (Bivalvia) is related to particulate food and sulphide availability. *Marine Ecology Progress Series*, *320*, 185–194. http://doi.org/10.3354/meps320185

Eckelbarger, K.J., & L. Watling. (1995). Role of phylogenetic constraints in determining reproductive patterns in deep-sea invertebrates. *Invertebrate Biology 114*, 256–269.

Ferrini, V. L., Tivey, M. K., Carbotte, S. M., Martinez, F., & Roman, C. (2008). Variable morphologic expression of volcanic, tectonic, and hydrothermal processes at six

hydrothermal vent fields in the Lau back-arc basin. *Geochemistry, Geophysics, Geosystems*, *9*(7), http://doi.org/10.1029/2008GC002047

Flores, G. E., Shakya, M., Meneghin, J., Yang, Z. K., Seewald, J. S., Geoff Wheat, C., … Reysenbach, a-L. (2012). Inter-field variability in the microbial communities of hydrothermal vent deposits from a back-arc basin. *Geobiology*, *10*(4), 333–46. http://doi.org/10.1111/j.1472-4669.2012.00325.x

Gazeau, F., Parker, L. M., Comeau, S., Gattuso, J. P., O'Connor, W. a., Martin, S., … Ross, P. M. (2013). Impacts of ocean acidification on marine shelled molluscs. *Marine Biology*, *160*(8), 2207–2245. http://doi.org/10.1007/s00227-013-2219-3

Ghiselin, M. T. (1969). The Evolution of Hermaphroditism Among Animals. *The Quarterly Review of Biology*, *44*(2), 189–208. http://doi.org/10.1086/406066

Kádár, E., Lobo-da-Cunha, A., Santos, R. S., & Dando, P. (2006). Spermatogenesis of Bathymodiolus azoricus in captivity matching reproductive behaviour at deep-sea hydrothermal vents. *Journal of Experimental Marine Biology and Ecology*, *335*(1), 19–26. https://doi.org/10.1016/j.jembe.2006.02.016

Kasyanov, V. L. (2001). *Reproductive strategy of marine bivalves and echinoderms.* Enfield, USA: Science Publishers, Inc.

Khripounoff, A., & Alberic, P. (1991). Settling of particles in a hydrothermal vent field (East Pacific Rise 13°N) measured with sediment traps. *Deep Sea Research Part A. Oceanographic Research Papers*, *38*(6), 729–744. http://doi.org/10.1016/0198-0149(91)90009-5

Kurihara, H. (2008). Effects of CO2-driven ocean acidification on the early developmental stages of invertebrates. *Marine Ecology Progress Series*, *373*, 275–284. http://doi.org/10.3354/meps07802

Lannig, G., Eilers, S., Pörtner, H. O., Sokolova, I. M., & Bock, C. (2010). Impact of ocean acidification on energy metabolism of oyster, *Crassostrea gigas*- Changes in metabolic pathways and thermal response. *Marine Drugs*, *8*(8), 2318–39. http://doi.org/10.3390/md8082318

Lemasson, L., Charpy, L., & Blanchot, J. (1990). Biomasse et structure de tailles dans les eaux oligotrophes du Pacifique Sud-Ouest (croisière Proligo). *Oceanologica ACTA*, *10*, 369–381.

Le Pennec, M. & Beninger, P. G. (1997). Ultrastructural characteristics of spermatogenesis in three species of deep-sea hydrothermal vent mytilids. *Canadian Journal of Zoology*, *75*(2), 308–316. http://doi.org/10.1139/z97-039

Le Pennec, M. & Beninger, P. G. (2000). Reproductive characteristics and strategies of reducing-system bivalves. *Comparative Biochemistry and Physiology Part A: Molecular & Integrative Physiology*, *126*(1), 1–16. http://doi.org/10.1016/S0742-8413(00)00100-6

Melzner, F., Stange, P., Trübenbach, K., Thomsen, J., Casties, I., Panknin, U., … Gutowska, M. A. (2011). Food supply and seawater pCO_2 impact calcification and internal shell dissolution in the blue mussel *Mytilus edulis*. *PloS One*, *6*(9), e24223. http://doi.org/10.1371/journal.pone.0024223

Pan, T.-C. F., Applebaum, S. L., & Manahan, D. T. (2015). Experimental ocean acidification alters the allocation of metabolic energy. *Proceedings of the National Academy of Sciences of the United States of America*, *112*(15), 4696–701. http://doi.org/10.1073/pnas.1416967112

Pansch, C., Schaub, I., Havenhand, J., & Wahl, M. (2014). Habitat traits and food availability determine the response of marine invertebrates to ocean acidification. *Global Change Biology*, *20*(3), 765–77. http://doi.org/10.1111/gcb.12478

Petes, L. E., Menge, B. A., & Harris, A. L. (2008). Intertidal mussels exhibit energetic tradeoffs between reproduction ans stress resistance. *Ecological Monographs, 78*(3), 387–402.

Podowski, E., Ma, S., Luther, G., Wardrop, D., & Fisher, C. (2010). Biotic and abiotic factors affecting distributions of megafauna in diffuse flow on andesite and basalt along the Eastern Lau Spreading Center, Tonga. *Marine Ecology Progress Series*, *418*, 25–45. http://doi.org/10.3354/meps08797

Range, P., Chícharo, M. a., Ben-Hamadou, R., Piló, D., Matias, D., Joaquim, S., … Chícharo, L. (2011). Calcification, growth and mortality of juvenile clams *Ruditapes decussatus* under increased pCO_2 and reduced pH: Variable responses to ocean acidification at local scales? *Journal of Experimental Marine Biology and Ecology*, *396*(2), 177–184. http://doi.org/10.1016/j.jembe.2010.10.020

Russell-Hunter, W. D. (1979). *A Life of Invertebrates*. *The Quarterly Review of Biology* (Vol. 54). New York: Macmillan Publishing Company. http://doi.org/10.1086/411368

Schöne, B. R., & Giere, O. (2005). Growth increments and stable isotope variation in shells of the deep-sea hydrothermal vent bivalve mollusk *Bathymodiolus brevior* from the North Fiji Basin, Pacific Ocean. *Deep Sea Research Part I: Oceanographic Research Papers*, *52*(10), 1896–1910. http://doi.org/10.1016/j.dsr.2005.06.003

Seed, R. (1969). The ecology of *Mytilus edulis L.* (Lamellibranchiata) on exposed rocky shores. *Oecologia*, *3*(3), 277–316. http://doi.org/10.1007/BF00390380

Sibly, R. M., & Calow, P. (1986). *Physiological Ecology of Animals: An Evolutionary Approach* (p. 179). Blackwell Scientific, Oxford.

Siikavuopio, S. I., Mortensen, A., Dale, T., & Foss, A. (2007). Effects of carbon dioxide exposure on feed intake and gonad growth in green sea urchin, *Strongylocentrotus droebachiensis*. *Aquaculture*, *266*(1-4), 97–101. http://doi.org/10.1016/j.aquaculture.2007.02.044

Sokolova, I. M., Frederich, M., Bagwe, R., Lannig, G., & Sukhotin, A. a. (2012). Energy homeostasis as an integrative tool for assessing limits of environmental stress tolerance in aquatic invertebrates. *Marine Environmental Research*, *79*, 1–15. http://doi.org/10.1016/j.marenvres.2012.04.003

Stenyakina, A, Walters, L. J., Hoffman, E. a, & Calestani, C. (2010). Food availability and sex reversal in *Mytella charruana*, an introduced bivalve in the southeastern United States. *Molecular Reproduction and Development*, *77*(3), 222–30. http://doi.org/10.1002/mrd.21132

Suntsov, A., & Domokos, R. (2013). Vertically migrating micronekton and macrozooplankton communities around Guam and the Northern Mariana Islands. *Deep Sea Research Part I: Oceanographic Research Papers*, *71*, 113–129. http://doi.org/10.1016/j.dsr.2012.10.009

Tunnicliffe, V., Davies, K. T. A., Butterfield, D. A., Embley, R. W., Rose, J. M., & Jr, W. W. C. (2009). Survival of mussels in extremely acidic waters on a submarine volcano. *Nature Geoscience*, *2*(5), 344–348. http://doi.org/10.1038/ngeo500

Tunnicliffe, V., Garrett, J. F., & Johnson, H. P. (1990). Physical and biological factors affecting the behaviour and mortality of hydrothermal vent tubeworms (vestimentiferans). *Deep Sea Research Part A. Oceanographic Research Papers*, *37*(1), 103–125. http://doi.org/10.1016/0198-0149(90)90031-P

Turnipseed, M., Jenkins, C. D., & Van Dover, C. L. (2004). Community structure in Florida Escarpment seep and Snake Pit (Mid-Atlantic Ridge) vent mussel beds. *Marine Biology*, *145*(1), 121–132. https://doi.org/10.1007/s00227-004-1304-z

Tyler, P. A., & Young, C. M. (1999). Reproduction and dispersal at vents and cold seeps. *Journal of the Marine Biological Association of the UK*, *79*(2), 193–208. http://doi.org/10.1017/S0025315499000235

Tyler, P., Young, C. M., Dolan, E., Arellano, S. M., Brooke, S. D., & Baker, M. (2007). Gametogenic periodicity in the chemosynthetic cold-seep mussel "*Bathymodiolus" childressi*. *Marine Biology*, *150*(5), 829–840. http://doi.org/10.1007/s00227-006-0362-9

Chapter 3 : The shell, body and gill condition of deep-sea mussel (*Bathymodiolus septemdierum*) living in extremely acidic conditions

Introduction

Acidification in a Natural Setting

Several short-term laboratory experiments have effectively shown that many organisms – especially calcifiers – will be negatively affected by ocean acidification in the next 100 years (Feely et al., 2004; Orr et al., 2005). Two dominant stressors accompany ocean acidification: 1) a reduced availability of carbonate ions which can restrict calcification, and 2) an increased pCO_2 that can cause hypercapnia and changes in energy metabolism. However, understanding how laboratory results translate to field conditions is hindered by the difficulty of imitating ocean acidification *in situ*, especially for extended periods of time (Hall-Spencer et al., 2008). Natural CO_2 flux from hydrothermal vents can alter local ocean chemistry and create an excellent environment for studying CO_2-driven acidification in a natural setting. Although vent systems are not perfect predictors of future ocean conditions, some acidify seawater on sufficiently large spatial and temporal scales (Hall-Spencer et al., 2008) to assess biological processes such as growth and reproduction.

Northwest Eifuku volcano is a small cone on the volcanic Mariana arc (21.49°N, 144.04°E). Small chimneys at Champagne vent field (located just below the summit) emit hot vent fluid containing 2.7 moles/kg of CO_2 – the highest reported concentration of CO_2 of any hydrothermal fluid – and liquid droplets of CO_2 (Lupton et al., 2006). Although CO_2 is generally the most abundant dissolved gas found in hydrothermal fluids,

it is rarely found in liquid form (Lupton et al., 2006). NW Eifuku is therefore a valuable natural laboratory for studying the effects of high CO_2 concentrations on marine organisms (Tunnicliffe et al., 2009). The present study investigates the shell, body and gill condition of the vent-obligate mussel, *Bathymodiolus septemdierum*, living in the extremely acidic conditions at NW Eifuku volcano.

Shell Condition

CO_2-driven acidification causes wholesale shifts in seawater carbonate chemistry towards a state of decreased CO_3^{2-} concentration. This leads to reduced $CaCO_3$ saturation states for both aragonite (Ω_{arag}) and calcite (Ω_{calc}) as indicated by:

$$\Omega = [CO_3^{2-}][Ca^{2+}] / K'_{sp} \qquad \text{Equation 1}$$

where K'_{sp} is the solubility product dependent on temperature, salinity, pressure and the mineral form of $CaCO_3$ (calcite or aragonite). The depth at which $CaCO_3$ is neither supersaturated nor under-saturated is the saturation horizon. Below the saturation horizon, $\Omega < 1$ and $CaCO_3$ is susceptible to dissolution. Large-scale decreases in CO_3^{2-} concentration can therefore have profound impacts on shell growth, maintenance, and repair (Feely et al., 2004).

In laboratory experiments, calcification rates correlate well with Ω in a wide range of taxa including marine bivalves (e.g. Gazeau et al., 2007; Ries et al., 2009). However, disturbances to physiological processes (i.e. acid-base balance) caused by high seawater pCO_2 can affect calcification in a secondary fashion (Thomsen et al., 2015). When environmental pCO_2 is elevated, CO_2 rises in the intra- and extra-cellular

compartments of the body (hypercapnia). This rise in internal CO_2 leads to an increase in H^+ that elevates the cost for proton removal by means of active transport (Boron, 2004). Though mussels can regulate intracellular pH, the pH of extracellular compartments such as the haemolymph and extrapallial fluid remain largely unregulated (Michaelidis et al., 2005; Thomsen et al., 2010). Changes in haemolymph and extrapallial fluid pH are therefore thought to affect the shell-forming process either through, 1) inner shell dissolution in an effort to minimize acidosis with shell HCO_3^- or, 2) changes in intra- and extracellular ion composition, which can impact intracellular precipitation of amorphous calcium carbonate (ACC) (Michaelidis et al., 2005; Hüning et al., 2013). ACC is thought to be the precursor to both calcite and aragonite forms of $CaCO_3$ and is formed in specialized vesicles in mantle epithelial cells that require regulated intracellular pH (Addadi et al., 2003; Hüning et al., 2013). Under hypercapnic conditions, pH regulation in mantle epithelial cells can become too costly, and energy allocation to other fitness-sustaining processes may therefore take precedence over creating optimal conditions for calcification (Thomsen & Melzner, 2010).

Due to proximity to Champagne vent fluids, *B. septemdierum* at NW Eifuku lives in extremely low pH conditions and saturation states for both aragonite and calcite as low as 0.01; shells here are much thinner than sites near normal seawater pH (Tunnicliffe et al., 2009). These environmental conditions impose stress on *B. septemdierum* that may induce trade-offs among shell growth, somatic growth and reproduction.

Body Condition

The volumetric condition index (CI = tissue dry weight/ shell volume) is used as a measure of physiological condition in bivalves; it is an effective representative and

responsive tool for evaluating how organisms are affected by environmental conditions (Rheault & Rice, 1996) since tissue mass can vary within the confines of the shell based on habitat quality (Crosby & Gale, 1990). When habitat quality deviates from optimal, metabolic adjustments are made in an effort to support basal maintenance costs, often at the expense of an organism's carbohydrate and lipid reserves (Sokolova et al., 2012). The CI of marine bivalves fluctuates in response to a wide range of environmental factors such as temperature (Lagade & Muley, 2014), nutrient availability (Bayne & Thompson, 1970), parasitic infection (Mercado-Silva, 2005) and pCO_2 (Lannig et al., 2010). However, the impact of environmental conditions - especially stressors - on an organism's CI is neither simple nor uniform. Responses can vary across populations, and may be influenced by stress intensity, stress duration, energy availability, potential for adaptation, and supplementary stressors. In addition to environmental conditions, endogenous factors, such as gonadal mass, may also influence CI. The gonadal mass of animals in high quality habitats may contribute significantly to CI as gametogenesis progresses, while animals in low quality habitats may produce fewer gametes due to depleted energy reserves, effectively reducing their contribution to the organism's CI (Cardoso et al., 2007).

Hydrothermal vent environments display significant variability in physical and chemical conditions on both spatial and temporal scales. The CI of vent mussels offers only a snapshot of an organism's response to environmental conditions for the place and time of collection. However, the relationship between CI and a set of environmental characteristics can provide insight on an organism's physiological response to habitat

condition, and on the distribution pattern of vent mussels since CI cannot be reduced below a certain limit.

Endosymbiotic Bacteria and Gill Condition

The success of many invertebrates inhabiting chemosynthetic environments is largely attributed to their relationship with endosymbiotic bacteria. The primary role of the symbionts is to synthesize nutrients through chemosynthesis and supply these nutrients to the host; eventually the symbionts may be absorbed as an additional a source of nutrition (Jannasch, 1995). The bacterial symbionts in the gills of bathymodioline mussels can be methanotrophic or thiotrophic and, in some species, both types can co-occur (Distel et al., 1995). Only thiotrophic symbionts occur in *Bathymodiolus septemdierum* and they derive energy through the oxidation of hydrogen sulphide emitted from the vents (Nelson et al., 1995):

$$CO_2 + 4H_2S + O_2 \rightarrow CH_2O + 4S + 3H_2O \qquad \text{Equation 2}$$

More recently, partially oxidized sulphur compounds, such as thiosulfate ($S_2O_3^{2-}$), have been implicated in autotrophy in *B. septemdierum* (Beinart et al., 2015). However, thiosulfate is frequently produced from sulphide as a detoxification mechanism in vent organisms (Grieshaber & Volkel, 1998). It is therefore unclear if symbionts utilize thiosulfate produced by their host, or if thiosulfate can be taken up from the environment for energy production (Beinart et al., 2015).

Symbiont abundance plays a fundamental role in determining energy availability for the host, and many chemosynthetic organisms (including *B. septemdierum*; Fujinoki

et al., 2011) can increase symbiont abundances when environmental sulphide concentrations are favourable (Kádár et al., 2005; Dufour & Felbeck, 2006). While a wide range of environmental factors can modulate the CI of chemosynthetic mussels, enhanced energy uptake should increase resilience to environmental stressors – including high pCO_2 - and make the organism less likely to experience changes in condition index. Our study emphasizes the need to consider habitat characteristics carefully when formulating species responses to ocean acidification.

Understanding how the condition of *B. septemdierum* responds to the stress of extremely acidic conditions at NW Eifuku should provide further insight on how the condition of coastal species will respond to continuing ocean acidification. The objectives and hypotheses of this research are as follows:

1) To assess the effects of low pH on shell condition (weight: volume ratio) in *B. septemdierum.* We hypothesize that mussels living in a low pH setting will show reduced calcification compared than those in a high pH setting.

2) To assess the effects of a high pCO_2 environment on the body condition in *B. septemdierum*. We present two hypotheses for the body condition in *B. septemdierum*. i) Given the energetic costs associated with high pCO2, we hypothesize that mussels in a high pCO_2 setting will have a poorer body condition index than those in a low pCO_2 setting; alternatively ii) we hypothesize that there will be no high pCO_2 effect on body condition index as found in *B. septemdierum* reproduction (Chapter 2).

3) To assess gill condition, and determine bacteriocyte characteristics (i.e. symbiont type, abundance) in *B. septemdierum* from NW Eifuku using microscopy.

Materials and Methods

Collection Methods

Bathymodiolus septemdierum specimens were obtained by remotely operated vehicles from seven hydrothermal vent sites in the western Pacific Ocean on multiple expeditions between April 2004 and April 2016 (Table 3.1, Figure 3.1). The pH varies across NW Eifuku collection sites from 5.22 to 7.00; there is no evidence of high CO_2 at ABE or Nifonea. The temperature at the mussel collection sites ranged from 2.5 to 2.7°C with the exception of ABE where temperature was a maximum of 15.3°C.

Tui Malila is located about 140 km south of ABE in Lau Basin and hydrothermal activity extends about 350m from north to south (Flores et al., 2012). Hydrothermal venting occurs from several very small chimneys in addition to areas of diffuse flow. The sea floor is rocky and covered with diverse macrofaunal communities. Mussels tend to aggregate in isolated patches along with the vent snail, *Ifremeria nautilei.* Bythograeid crabs, squat lobsters, barnacles, and alvinorcaridid shrimp are also present. Although an exact pH measurement is not available, there is no evidence of high CO_2 at Tui Malila. See Chapter 2 for other site descriptions. Calcium carbonate saturation state is not available for any site.

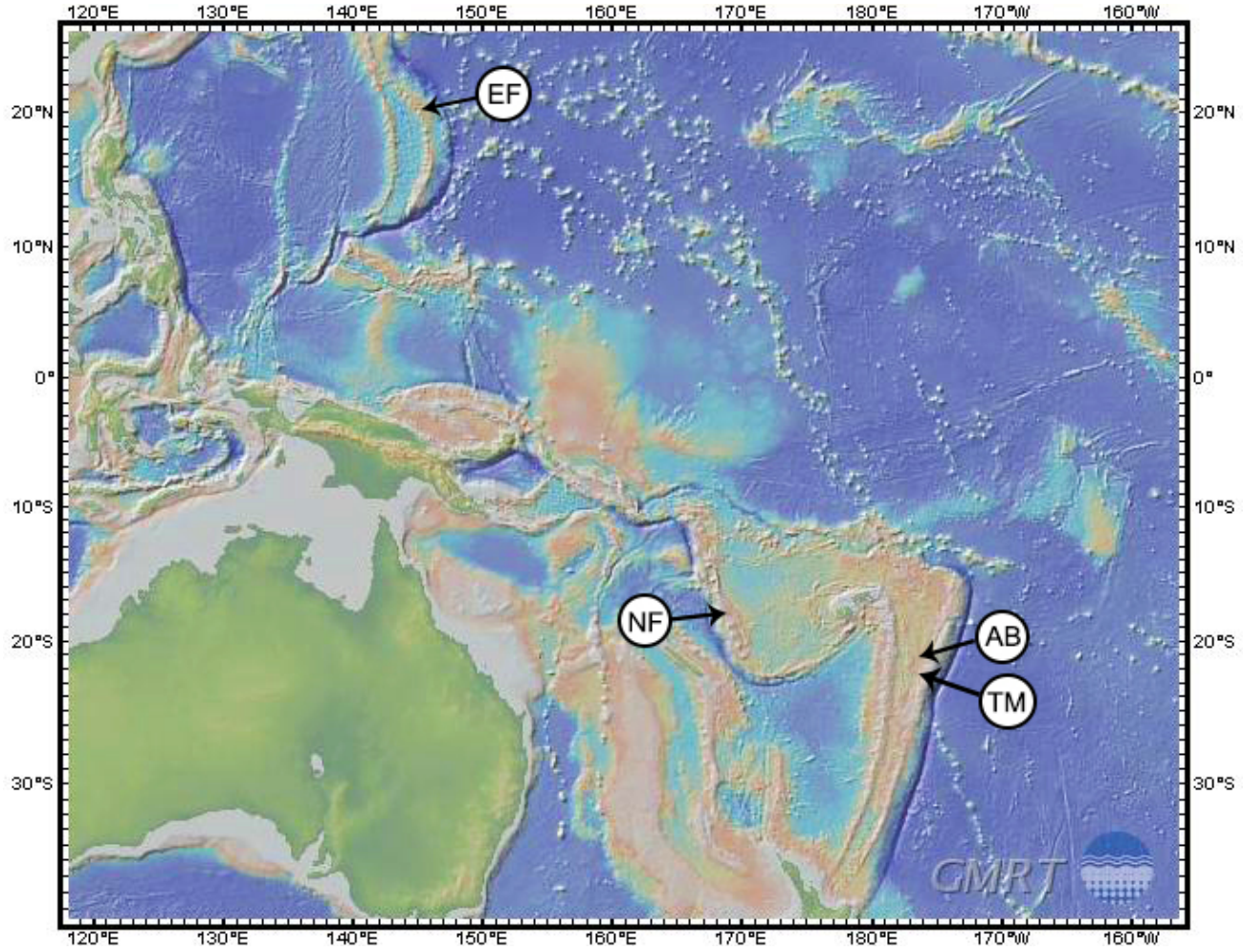

Figure 3.1. Bathymetric map of *Bathymodiolus septemdierum* collection sites in the western Pacific Ocean. Labels include: NW Eifuku (EF), Nifonea (NF), Tui Malila (TM), and ABE (AB).

Shell Condition

The relationship between shell weight and volume (W: V) was compared across sites of varying pH using one valve from each mussel. Only undamaged shells were used for this comparison. Shell volume was determined by recording the amount of water a valve could hold before overflow. Tui Malila mussels were only used for shell condition analysis.

Table 3.1. *Bathymodiolus septemdierum* collection site and sample characteristics for our study. [1] indicates hydrogen sulphide concentration from nearby site of similar pH reported by Tunnicliffe et al. (2009), [2] indicates range of hydrogen sulphide concentration observed in mixed *I. nautili* and *B. septemdierum* patch measured by Podowski et al. (2010), n/a ; not available

Vent	Site/Region	Coordinates	Date	Depth (m)	Temp (°C)	pH	[H_2S]	# mussels collected	ROV	Preservative
Pillar Top	NW Eifuku, Mariana Volcanic Arc	21.4875, 144.0418	06-Dec-14	1,561	2.6	7.00	>1[1]	33	JASON II	Formalin/ frozen
Champagne	NW Eifuku, Mariana Volcanic Arc	21.4875, 144.0414	13-Dec-14	1,605	2.7	5.22	151[1]	35	JASON II	Formalin/ frozen
Golden Lips	NW Eifuku, Mariana Volcanic Arc	21.4876, 144.0413	13-Dec-14	1,606	2.7	5.78	n/a	45	JASON II	Formalin/ frozen
Near Fouling	NW Eifuku, Mariana Volcanic Arc	21.4878, 144.0417	10-Apr-04	1,576	2.5	5.88	101	30	ROPOS	Formalin
ABE	East Lau Spreading Centre, Lau Basin	- 20.7626, 176.1918	25-Apr-16	2,130	maximum 15.3	no evidence of high CO_2	0-131[2]	15	ROPOS	Formalin
Nifonea	Nifonea Ridge, Vanuatu	-18.133, 169.517	13-Jul-13	1,873	n/a	no evidence of high CO_2	n/a	23	Kiel	Ethanol
Tui Malila	East Lau Spreading Centre, Lau Basin	-21.989, 176.568	22-Apr-16	1,888	n/a	no evidence of high CO_2	n/a	5	ROPOS	Formalin

Body and Gill Condition Indices

Body and gill condition indices were compared among 15 mussels from Near Fouling and Nifonea, nine mussels from ABE, and 12 mussels from Champagne, Pillar Top and Golden Lips. Gills were dissected from the body and ash free dry weights (AFDW) of both components were determined after drying at 60ºC and burning at 550ºC in a muffle furnace. Prior to drying, epifaunal limpets and parasitic scale worms were removed from Nifonea mussels so as not to contribute to the body weight. There were no parasites in NW Eifuku or ABE mussels to remove. Condition indices were determined using the following equations:

Body condition index (BCI) = (body AFDW / shell volume in ml)

Gill condition index (GCI) = (gill AFDW / shell volume in ml)

Total body condition index (CI) = (body AFDW + gill AFDW / shell volume in ml)

where shell volume for each mussel was determined by doubling the volume obtained from a single valve. Due to similarities between female and male condition indices, both sexes were grouped for each site. Bivalve biomass fixed in formalin and preserved in ethanol has not been found to vary significantly in dry weight over time (e.g. Gaston et al., 1996). The % water content of Pillar Top, Champagne and Golden Lips mussels was also determined from wet body weights measured prior to preservation compared to dry body weights. Wet weights were not available from mussels at the other collection sites.

Transmission Electron Microscopy

For electron microscopy analysis, 2 mussels each from Champagne, Golden Lips, and Pillar Top within 100-130 mm in length were selected. An anterior gill snip from each mussel was fixed in 2.5% glutaraldehyde and 0.1 M PBS. The gill snips were rinsed in the same buffer and post-fixed in 1% osmium tetroxide. The snips were subsequently dehydrated in ethanol series and propylene oxide and embedded in EMbed 812 resin. Ultrathin cross-sections of the mid-filament region of the snips were obtained with a diamond knife, and subsequently stained with uranyl acetate and lead citrate. The sections were examined and photographed using a JOEL JEM-2100F transmission electron microscope.

Statistical Analysis

The shell W: V, CI and GCI data were initially assessed for normality using the Shapiro–Wilk test, and for homogeneity of variance using Levene's test. If the data were non-parametric then a Kruskal Wallis and post hoc Wilcoxon test were used to determine differences among sites. A linear regression was performed to test the significance between % water weight and CI. Significance was designated at $p<0.05$ for all data analyzed.

Results

Shell Condition

Mussel shells from low pH sites (Near Fouling, Champagne, Pillar Top and Golden Lips) have a significantly lower weight to volume ratio (W: V) than shells from comparison sites (Nifonea, Tui Malila and ABE) as illustrated in Figure 3.2. (Kruskal

Wallis: X^2= 97.75, df=5, p<0.001; Wilcoxon: p<0.01). All sites exhibit a linear relationship between shell weight and volume, though Golden Lips mussels display lower shell W: V relative to the remaining low pH sites (Wilcoxon: p<0.01) while ABE mussels appear more heavily calcified.

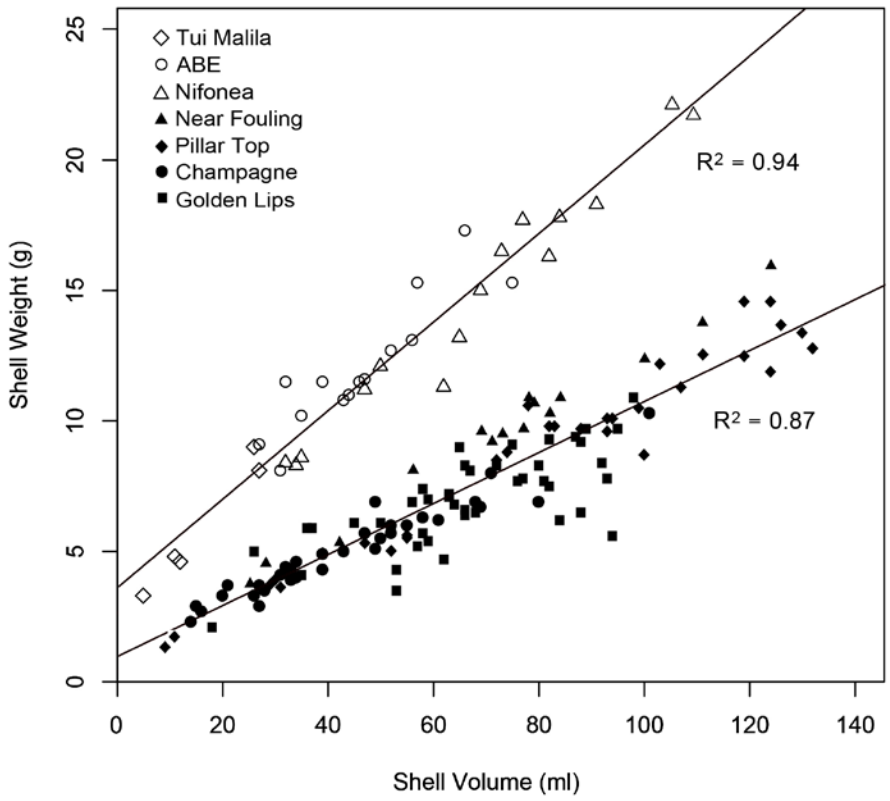

Figure 3.2. The relationship between shell weight (one valve) and shell volume (one valve) in *B. septemdierum* from all collection sites. Open symbols represent high pH sites and closed symbols represent low pH sites.

Condition Indices

The CI data failed to fit a normal distribution (p<0.05) and homogeneity of variance test (p<0.05). Overall, there is significant variation in CI from all collected mussels (X^2= 48.05, df=5, p-value<0.001). In particular, mussels from Champagne, Near

Fouling and Nifonea have a significantly higher CI than those of Pillar Top and Golden Lips mussels ($p<0.05$). ABE mussels also have a higher CI than Golden Lips mussels ($p<0.05$). The water content values of mussels from Pillar Top, Champagne and Golden Lips were 91.4 ± 1.3%, 89.7 ± 2.1% and 92.7 ± 1.7%, respectively. There is a significant relationship between condition index and % water content ($F=29.61$, $df=34$, $p<0.001$), where % water weight decreases with increasing condition index as summarized in Figure 3.3.

Similarly, the GCI data failed to fit a normal distribution ($p<0.05$) and homogeneity of variance test ($p<0.05$). There is significant variation across the GCI from all collected mussels ($X^2= 47.82$, $df=5$, p-value<0.001). Mussels from Champagne, Near Fouling, Nifonea have a significantly higher GCI than those of Pillar Top and Golden Lips mussels ($p<0.05$). The relationship between the CI and GCI is also noteworthy: when GCI is high, CI is also high and vice versa (Figure 3.4). CI and GCI results are summarized in Table 3.2. The total body AFDW to shell weight and shell volume relationships are shown Figure 3.5.

Table 3.2. Average gill condition index (GCI), and body condition index (CI) from each collection site. Subscript letters indicate significant differences between collection sites ($p<0.05$).

Vent	Site/Region	Water Content ± SD (%)	Average GCI ± SD (g/ml)	Average BCI ± SD (g/ml)
Pillar Top	NW Eifuku, Mariana Volcanic Arc	91.4 ± 1.3	$0.005 \pm 0.001_{a}$	$0.025 \pm 0.004_{a}$
Champagne	NW Eifuku, Mariana Volcanic Arc	89.7 ± 2.1	$0.010 \pm 0.002_{b}$	$0.045 \pm 0.009_{b}$
Golden Lips	NW Eifuku, Mariana Volcanic Arc	92.7 ± 1.7	$0.006 \pm 0.00_{c}$	$0.023 \pm 0.006_{a}$
Near Fouling	NW Eifuku, Mariana Volcanic Arc	n/a	$0.009 \pm 0.001_{b,d}$	$0.042 \pm 0.007_{b,c}$
ABE	East Lau Spreading Centre, Lau Basin	n/a	$0.006 \pm 0.003_{a,c}$	$0.034 \pm 0.019_{c}$
Nifonea	Nifonea Ridge, Vanuatu	n/a	$0.008 \pm 0.002_{d}$	$0.045 \pm 0.011_{b}$

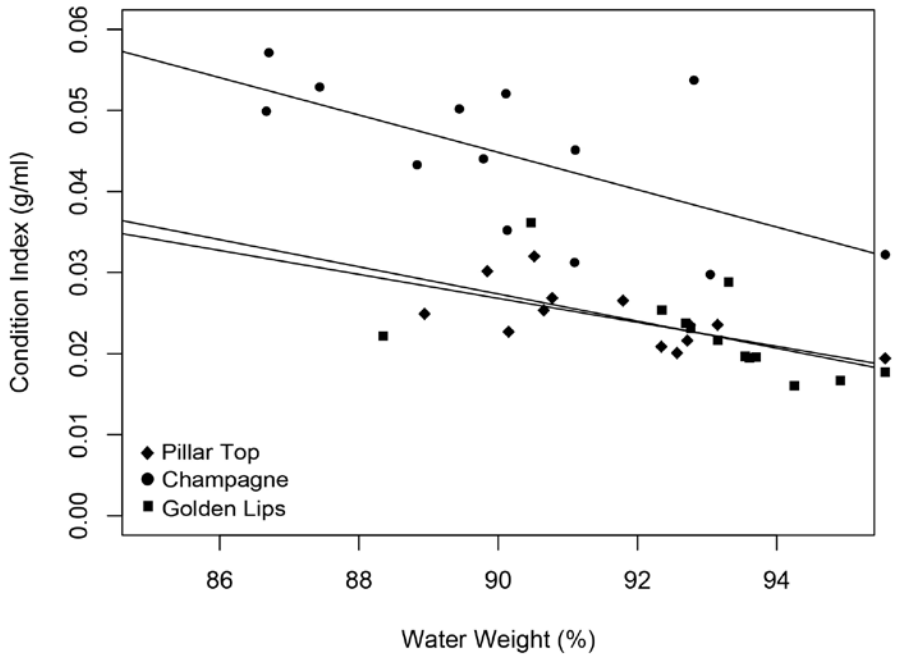

Figure 3.3. The relationship between condition index and % water content in Pillar Top, Champagne and Golden Lips mussels. Champagne mussels have a lower % water weight indicative of a better condition. Symbols on the outside of the plot indicate the line of best-fit trajectory for the respective site.

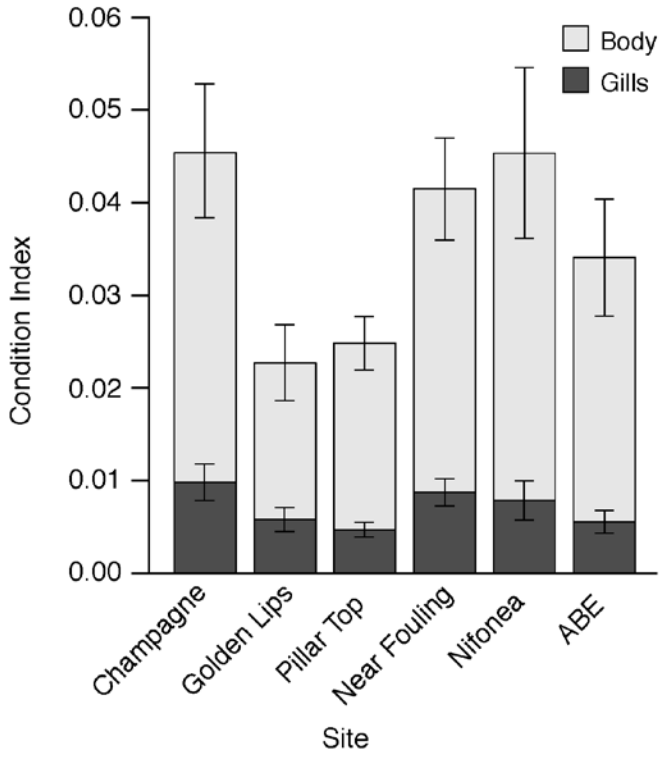

Figure 3.4. The proportion of the CI attributed to gill tissue and body tissue of mussels from all sites. Error bars represent standard deviation.

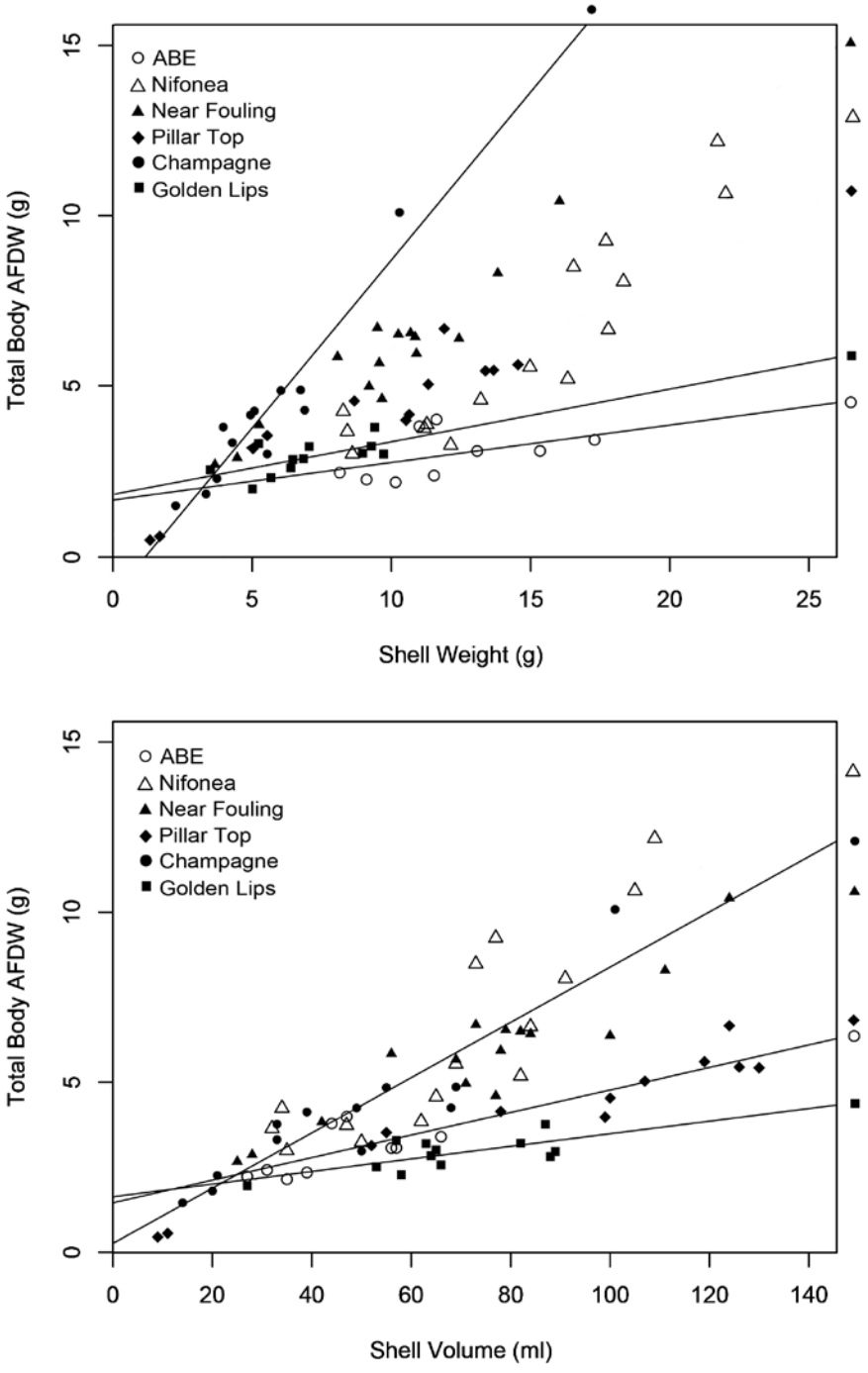

Figure 3.5. a) The relationship between total body AFDW and shell weight in *B. septemdierum* from all collection sites, b) the relationship between total body AFDW shell volume (i.e. CI). Open symbols represent high pH sites and closed symbols represent low pH sites. Symbols on the outside of the plot indicate the line of best-fit trajectory for the respective site; three plotted lines facilitate comparison.

Gill Structure

The overall structure of the gills in *B. septemdierum* is comparable to that described previously in other members of the genus (Fiala-Médioni et al., 2002; Fisher et al., 1987). The gills of *B. septemdierum* consist of inner and outer demibranchs composed of ascending and descending lamellae. The lateral zone of the gill filament has two types of gill epithelial cell. The first, bacteriocytes, harbour symbionts in bacterial vacuoles. The second are intercalary cells, which are characterized by an apical surface covered in cilia and microvilli and by the absence of symbiotic bacteria.

Bacteriocytes have a relatively smooth apical surface although a few microvilli are occasionally present. The cytoplasm near the apical region of the bacteriocyte is dominated by vacuoles containing symbiotic bacteria. Bacteriocytes can harbour hundreds of bacteria within the cell with a varying number of bacteria per vacuole. Champagne mussels have 1-12 bacteria per vacuole and the vacuoles are often interconnected (Figure 3.6). Mussels from Pillar Top and Golden Lips have mostly 1-2 bacteria per vacuole though as many as five per vacuole are observed (Figure 3.7). The thickness of this bacterial layer varies between individuals. Champagne mussels have a thick bacterial layer (~25μm; Figure 3.8 a.), while that of Pillar Top and Golden Lips is thinner (~12μm; Figure 3.8 b.). No open connection to the external seawater is evident in apically situated vacuoles although Dubilier et al. (1998) note this conduit in *B. septemdierum* from the North Fiji Basin.

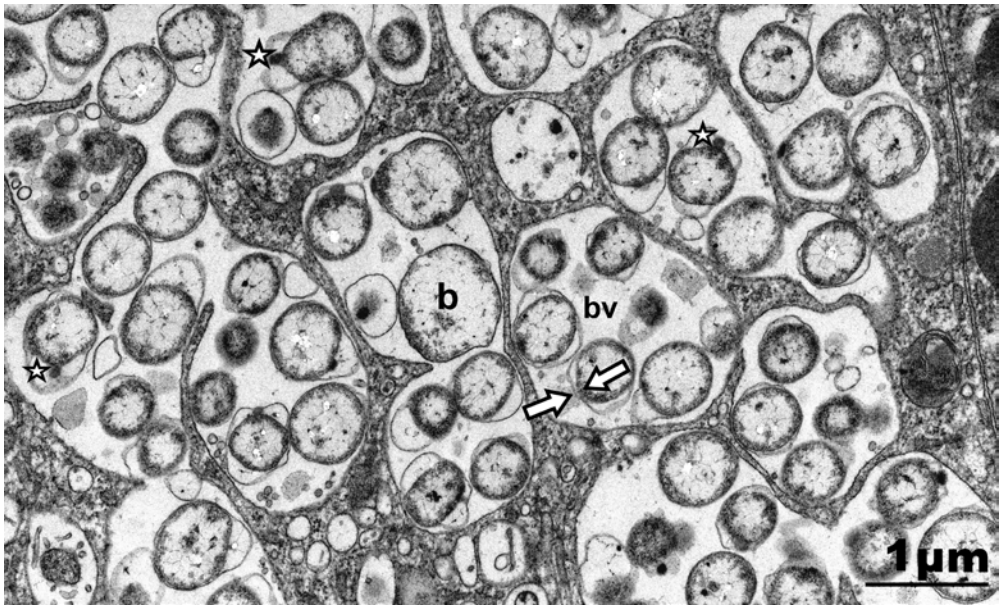

Figure 3.6. Ultrathin cross-section of Champagne mussel gill showing thiotrophic bacterial symbionts (b) in bacterial vacuoles (bv). Large arrows indicate the cytoplasmic and outer membrane typical of Gram-negative bacteria. Stars indicate electron-dense granules in the periplasmic space.

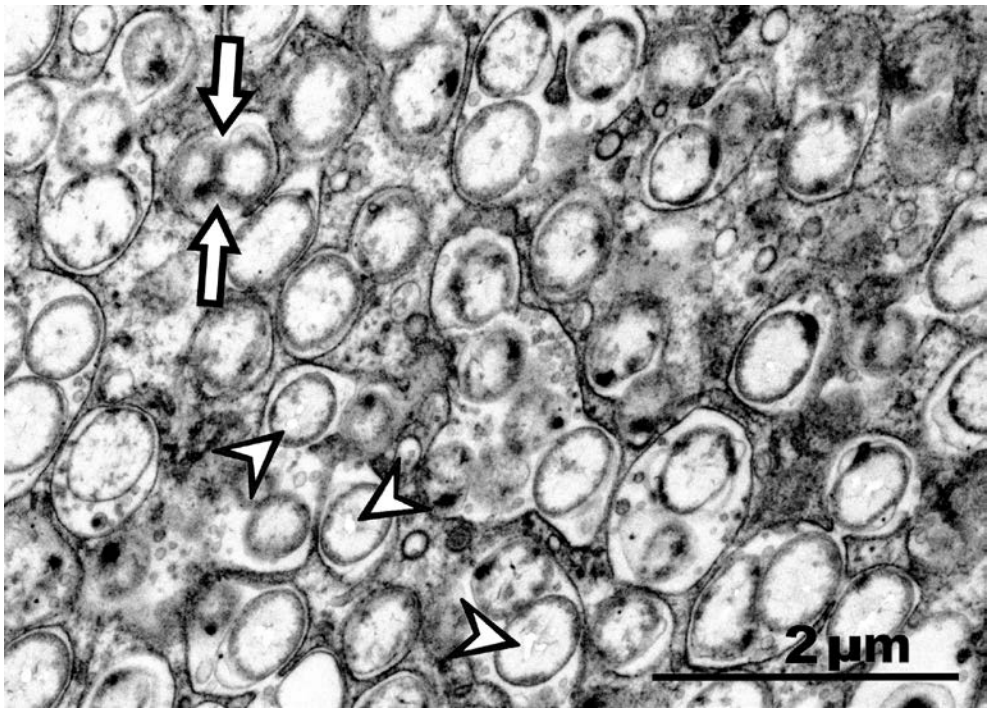

Figure 3.7. Ultrathin cross-section of Pillar Top mussel gill. Large arrows indicate dividing bacteria. Arrowheads indicate electron-transparent granules in the cytoplasm of bacteria.

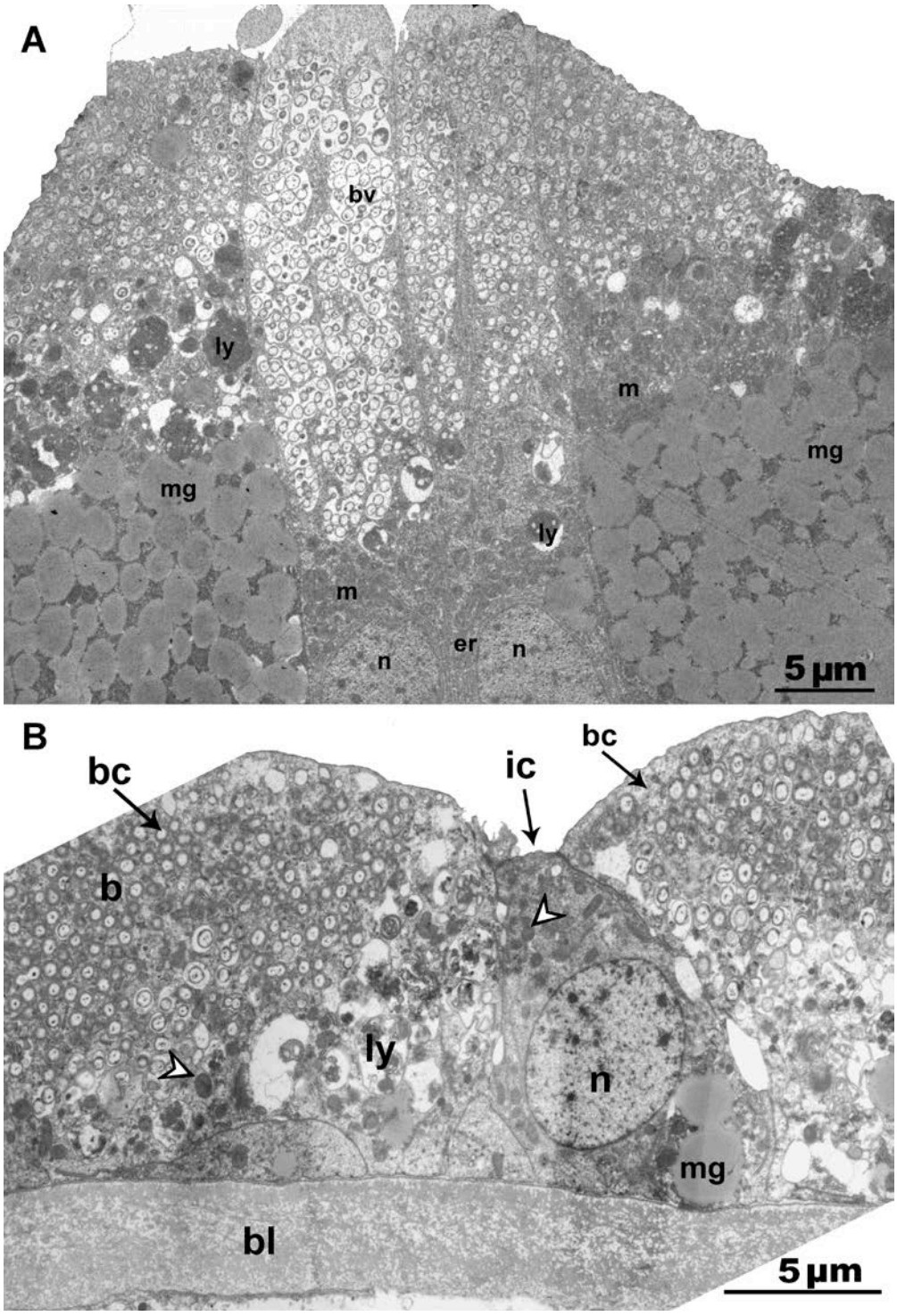

Figure 3.8. a) Ultrathin cross-section through several bacteriocytes of Champagne mussel. Labels include: bacterial vacuole (bv), mitochondria (m), nucleus (n), endoplasmic reticulum (er), mucous granules (mg), and lysosomes (ly). b) Ultrathin cross-section through Pillar Top mussel gill indicating bacteriocytes (bc) and intercalary (ic) cell types. Arrowheads indicate mitochondria. Labels include: basal lamina (bl), mucus granules (mg), nucleus (n), lysosomes (ly) and symbiotic bacteria (b).

Only coccoid-shaped thiotrophic symbionts are present in *B. septemdierum* gills ranging from 0.25 to 0.75 μm in diameter. All observed bacteria have a cytoplasmic and outer membrane typical of Gram-negative bacteria and lack intercytoplasmic membranes characteristic of methanotrophic bacteria. Rather, within the cytoplasm of several bacteria are electron-transparent granules that may represent sulphur granules washed out during TEM preparation as observed in other chemosynthetic bivalves (Dufour, 2005; Caro et al., 2007; Duperron et al., 2008). Electron-dense granules are frequently found in the periplasmic space. Dividing bacteria are only observed in one Pillar Top individual and one Champagne individual.

Beneath the bacterial layer, the distal portion of bacteriocytes contains mucus granules, a well-defined nucleus surrounded by endoplasmic reticulum, mitochondria, and lysosomes. Lysosomal degradation of bacteria was apparent in mussels from all sites in which membrane whorls were visible within secondary lysosomes (Figure 3.9).

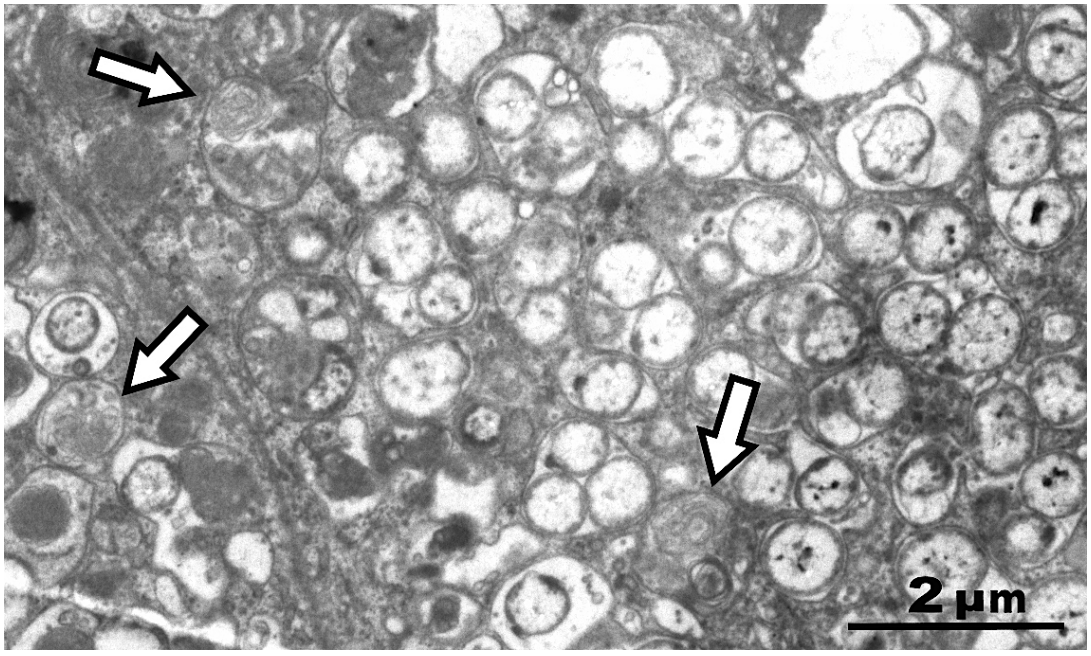

Figure 3.9. Ultrathin section through Champagne mussel gill. Arrows indicate degrading bacteria in secondary lysosomes.

Intercalary cells also contained a large nucleus, endoplasmic reticulum, mucus granules and mitochondria. These cells are the least common of the two epithelial cell types and are interspersed intermittently between bacteriocytes (Figure 3.8 b.). In comparison to bacteriocytes, intercalary cells are quite small. Often, their ciliated apical surface cannot be seen because they are fully enclosed by neighbouring bacteriocytes.

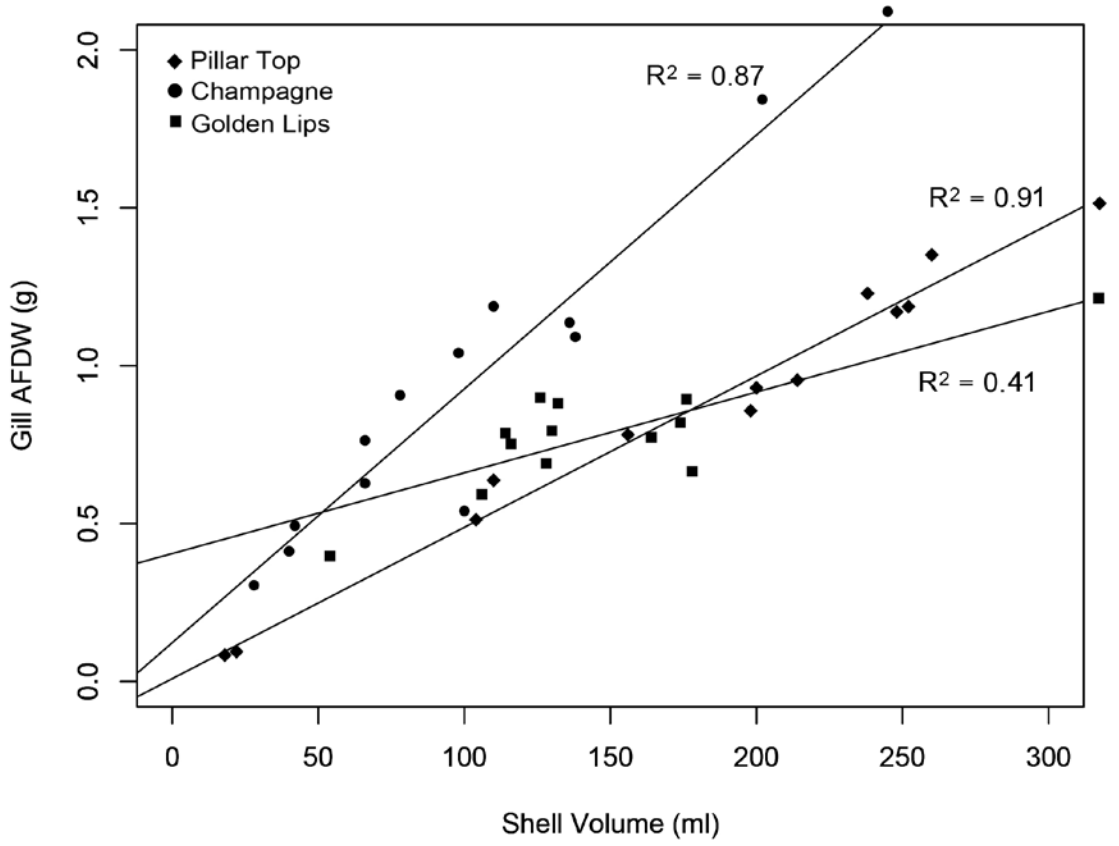

Figure 3.10. The relationship between gill AFDW and shell volume in *B. septemdierum* from Pillar Top, Champagne and Golden Lips.

Bathymodiolus septemdierum displays significant variability in bacterial layer thickness and symbiont abundance among our collection sites and across the literature as summarized in Table 3.3; mussels from Champagne showed the deepest layer reported. The overall gill structure and organelle composition within bacteriocyte and intercalary

cells is, however, markedly similar to other members of the genus (Fiala-Médioni et al., 2002; Fisher et al., 1987). The similarity between the symbiont abundances and GCI of mussels from each site used in TEM from the present study is also noteworthy; Champagne mussels have the highest symbiont abundance and GCI, while Pillar Top and Golden Lips mussels have relatively low symbiont abundances and gill condition indices (Figure 3.10).

Table 3.3. Summary of all available data on *B. septemdierum* gill microscopy including: site location, depth, and symbiont abundances. * indicates data retrieved only from a single figure in the publication. Following Breusing et al. 2015, we accept the Fiji and Indian Ridge mussels as conspecific with those in the Izu-Bonin-Mariana region.

Source	**Location**	**Depth (m)**	**Symbionts per vacuole**	**~ Bacterial Layer Thickness (μm)**
This study	Champagne, NW Eifuku, Mariana Arc	1,605	1-12	25
This study	Golden Lips, NW Eifuku, Mariana Arc	1,604	1-5	12
This study	Pillar Top, NW Eifuku, Mariana Arc	1,561	1-5	12
Dubilier et al. (1998)	LHOS, North Fiji Back Arc Basin	1,850	1	2*
Dubilier et al. (1998)	LHOS, North Fiji Back Arc Basin	1,850	1-12	8*
McKiness and Cavanaugh (2005)	Central Indian Ridge	2450–3300	1-13*	20*
Fujiwara et al. (2000)	Myojin Knoll, Izu-Bonin Arc	1,289	1-6*	12*

Discussion

Shell Condition

The high pCO_2 waters at Northwest Eifuku significantly restrict shell deposition in *Bathymodiolus septemdierum*. At a given shell volume, NW Eifuku shells weigh about half that of shells from Nifonea, ABE and Tui Malila. These results are markedly similar to the findings of Tunnicliffe et al. (2009) who report that mussel shell thickness and daily growth increments are almost half that of shells from mussels collected on the Tongan Arc and in Lau Basin where $\Omega >> 1$ and pH values were 7.87 and 8.42, respectively.

The mussel shell is composed of three layers: an outer organic periostracum, a layer of calcite, and an inner aragonite layer. The low calcite and aragonite saturation states at NW Eifuku ($\Omega \sim 0.01$; Tunnicliffe et al., 2009) reflect a limited availability to both mineral forms of $CaCO_3$ and may contribute to the poorer shell condition observed in these mussels. Moreover, when faced with such energy-demanding stressors, some marine bivalves exhibit significant biological control over the structural integrity of the shell. For example, Melzner et al. (2011) exposed the *M. edulis* to four seawater pCO_2 treatments (39, 142, 240, 405 Pa) and two food algae treatments (310–350 cells ml^{-1}, 1600–2000 cells ml^{-1}) over a seven-week period. They report inner shell (aragonite) dissolution in mussels at all pCO_2 treatments in the low food group, but only find inner shell dissolution at the two highest pCO_2 treatments in the high food group. These findings indicate that the integrity of the inner shell is coupled to the organism's energy budget and, under stressful conditions, mussels likely allocate energy towards vital processes other than shell maintenance.

Although collection sites at NW Eifuku are no more than 100 m apart, calcification is variable (Figure 3.2). Shells from Pillar Top, Champagne, and Near Fouling maintain a relatively consistent W: V relationship over time, suggesting microhabitat conditions are relatively consistent, albeit unfavourable for shell growth. Shells from Golden Lips display a lower W: V ratio at volumes >50 ml, which may indicate a less stable, and even more stressful microhabitat, in the past.

While shell deposition is possible for NW Eifuku mussels despite low Ω and increased calcification costs, an intact periostracum is essential, as any damage to this protective layer would lead to complete shell dissolution in such acidic conditions (Tunnicliffe et al. 2009). The absence of predatory crabs at NW Eifuku is crucial for maintaining an intact periostracum. The presence of predatory crabs at Lau Basin and Nifonea Ridge is evident in several repair scars on shell surfaces from predatory attack and may encourage increased calcification for protection, especially in ABE mussels where shell deposition is high compared to body mass (Figure 3.4).

Body Condition

Mussels show condition index differences across collection sites suggesting that there is an intricate relationship between the physiological response and microhabitat condition. Despite the extremely acidic conditions at Champagne and Near Fouling, mussels maintain a CI comparable to sites with no evidence of high CO_2. High concentrations of hydrogen sulphide accompany CO_2-rich vent fluids; based on previous measurements, Near Fouling mussels are exposed to sulphide concentrations of 101 μM/l, and we estimate sulphide concentrations at Champagne and to be approximately

155 μM/l (Tunnicliffe et al., 2009). We suggest that the pH stress imposed on mussels is partly mitigated by sufficient sulphide availability for symbiotic autotrophs, and by energy diversion from shell maintenance. In contrast, the poor condition index of Golden Lips mussels suggests that the discrepancy between energy supply and demand is greater for these mussels than those at other sites likely due to the stress of high CO_2, and inadequate sulphide availability, as implied by poor GCI in these mussels. Shell condition results corroborate that, over time, Golden Lips mussels inhabit the poorest microhabitat of our collections. Pillar Top mussels display a low CI, but bad weather prevented ROV recovery shortly after collection resulting in a two-day retention of Pillar Top mussels at 1000 m before they could be preserved shipboard. Removed from all sulphide, we speculate that these two days negatively affected condition index since mussels were still alive upon surfacing. The CI we report in these mussels may therefore be deceptively low. The natural conditions of Pillar Top are characterized by a pH ranging between 6.98 and 7.00 and an estimated sulphide concentration of <1 μM/l (Tunnicliffe et al., 2009). Though energy availability may be limited, there are lower maintenance costs associated with the less acidic pH. Mussels from Champagne, Pillar Top and Golden Lips were collected in December when gonadal index, and ultimately the mass of reproductive tissues, was highest. While body condition has been found to correlate positively to the mass of reproductive tissues in some marine bivalves, mussels in low quality habitats may produce fewer gametes due to limited energy reserves (Cardoso et al., 2007). Given the poor microhabitat conditions at Golden Lips and the delayed gametogenesis, we suggest that mussels have a relatively low fecundity, and therefore gonadal mass does not

contribute substantially to CI. In contrast, the healthy condition of Champagne mussels is probably partly facilitated by a relatively high fecundity and ripe gametes.

Perhaps none of the collections returned mussels with maximum potential condition. The CI of Nifonea mussels is similar to that of Champagne and Near Fouling though there is no evidence ofhigh CO_2. About 57% of Nifonea mussels hosted parasitic scale worms (*Branchipolynoe sp)* within the mantle cavity - some mussels with as many as four worms. To date, three species of parasitic scale worm have been identified within the mantle cavity of Bathymodiolus mussels (*B. seepensis*, *B. symmytilida*, and *B. pettiboneae*), some of which ingest mussel tissue as a source of nutrition (Britayev et al., 2003; Britayev et al., 2007; Takahashi et al., 2012). The presence of parasitic scale worms may have affected the CI of Nifonea mussels.

The temperature from the Lau Basin collection (max 15.3°C) is notably higher than that of NW Eifuku collections (~2.6°C) suggesting that thermal stress may be responsible for the relatively low CI in ABE mussels. ABE mussels were collected from a mixed aggregation of *B. septemdierum* and the vent snail, *Ifremeria nautilei,* which occur close to vent emissions, and at temperatures significantly higher than homogenous aggregations of *B. septemdierum* (Podowski et al., 2010). Mixed aggregations of these two species indicate that *B. septemdierum* is surviving near its upper thermal tolerance (Podowski et al., 2010) and several studies report that thermal stress can reduce the condition of marine bivalves. For example, Lagade & Muley (2014) report a significant decline in the condition index of two clam species (*Katelysia opima* and *Meretrix meretrix*) after exposure to elevated temperatures (35°C) for eight days. However, higher sulphide concentrations (0 to 131 μM/l; Podowski et al., 2010) can accompany mixed

aggregations of *Bathymodiolus* and *Ifremeria* that may mitigate temperature effects on CI. However, Beinart et al. (2015) report no carbon fixation in mussels at sulphide concentrations of 350 μM/l, which may further reduce CI.

Several studies on *Bathymodiolus* species relate body condition to habitat. *Bathymodiolus thermophilus* inhabiting regions of highly active venting (and higher sulphide concentrations) have a greater abundance of thiotrophic symbionts within the gills, a higher chemoautotrophic carbon content in their tissues, and ultimately a higher CI than mussels in regions of less active venting (Fisher et al., 1988). Smith (1985) observed the highest condition index and mussel density in *B. thermophilus* at the Galapagos Rift closest to vent effluent, where the nutritive quality and influences of symbiotic bacteria are likely greater. Nix et al. (1995) find a positive relationship between methane concentration and the condition index of the seep-mussel, *Bathymodiolus childressi* that harbours methanotrophic endosymbionts. Similarly, *B. childressi* mussel beds located in seep sites dominated by brine have higher methane and lower toxic sulfide concentrations, little crude oil, and mussels with a relatively faster growth rate and better condition indices than seep sites more distant from brine (Smith et al., 2000; Bergquist et al., 2004). Riou et al. (2010) find that a pulse of particulate matter from surface production augments the condition index of *Bathymodious azoricus.*

Bathymodiolus septemdierum has a broad biogeographic distribution and appears resilient to a wide range of vent conditions that vary on both spatial and temporal scales. This species persists at high densities even when CI is low compared to other *Bathymodiolus* species (Table 3.4.). The highest condition indices of mussels from our study (Champagne, Near Fouling and Nifonea) are less than half those reported in some

B. childressi populations (Smith et al., 2000; Dattagupta et al., 2004; Bergquist et al., 2004) and lower than most *B. thermophilus* (Smith, 1985; Smith et al., 2000) and *B. azoricus* (Riou et al., 2010) populations. Beinart et al. (2015) show carbon fixation by endosymbionts in *B. septemdierum* gills did not occur when sulphide concentrations were too high (350 μM/l), while relatively high condition indices are observed in *B. childressi* at methane concentrations of ~10, 000 μM/l (Nix et al., 1995). The contrast between *B. childressi* and *B. septemdierum* condition indices may result from the efficiency of methanotrophs at high methane concentrations. Differences between *B. azoricus* and *B. septemdierum* may be related to the flexible feeding regime of *B. azoricus*, which can derive energy from suspension-feeding, methanotrophic symbionts, and thiotrophic symbionts (Pond et al., 1998). This mixotrophic lifestyle enables *B. azoricus* to better tolerate habitat variation by switching resource when necessary.

In conclusion, our results indicate that stress can present in many forms and is reflected in body condition. Bathymodioline mussels can withstand a wide range of environmental stressors including extremely high pCO_2 conditions, thermal stress and parasitic infection - especially when energy availability is sufficient.

Gill Condition

In theory, the gill condition index of chemosynthetic mussels serves as proxy for symbiont abundance, which is regulated by environmental sulphide concentration. It has been well established that the chemistry at vent environments is the main driver for the abundance of thiotrophic endosymbionts, as shown in a number of deep-sea bivalves. For example, Dufour and Felbeck (2006) report that symbiont abundance is significantly

reduced in clams (*Thyasira flexuosa*) maintained under low sulphide conditions relative to those in high sulphide conditions. More recently, Fujinoki et al. (2012) find lower symbiont abundances in *B. septemdierum* mussels collected from a low sulphide site (0.29 μM/l) relative to a site with slightly higher concentrations (12.03 μM/l).

The GCI of *B. septemdierum* varies considerably across our collection sites. Mussels from Champagne, Near Fouling and Nifonea have significantly higher gill condition indices than mussels from Pillar Top, Golden Lips and ABE. The GCI results closely reflect the CI results, indicating that healthy gills - and high sulphide concentrations - coincide with a healthy body. Riou et al. (2010) report similar findings in *B. azoricus,* where the CI and GCI were determined from specimens collected from the Menez Gewn vent field on several occasions throughout a one-year period. The collection with the lowest CI corresponds with the lowest GCI. However, the highest GCI of mussels from our study (Champagne, Near Fouling and Nifonea) are less than half those reported in some *B. azoricus* collections. Differences between the GCI of these species may be attributed to the dual symbiosis in *B. azoricus* that may contribute to healthier gills.

Electron microscopy analysis of *B. septemdierum* gills corroborates our GCI results. Mussels from Champagne have a much higher symbiont abundance than Pillar Top and Golden Lips, displayed both by the number of symbionts per vacuole and by the thickness of the bacterial layer. Mussels from Champagne have the thickest bacterial layer (~25 μm), and potentially the highest symbiont abundance reported in this species thus far. In contrast, Dubilier et al. (1998) report the lowest symbiont abundance in *B. septemdierum* where mussels from the North Fiji Basin harbour only a single symbiont

per vacuole and have a ~2 μm thick bacterial layer. Differences in symbiont abundance between populations, and even across microhabitats, suggest that symbionts are highly sensitive to environmental sulphide concentration.

The gill ultrastructure of *B. septemdierum* from NW Eifuku is comparable to other populations and other bathymodioline mussels with only a few differences. For example, intercalary cells are not common in *B. septemdierum* compared to other members of the genus. In *B. thermophilus* intercalary cells alternate between bacteriocytes (Fisher et al., 1987) suggesting a more ciliated external surface in *B. thermophilus* than in *B. septemdierum.* A smaller proportion of intercalary cells is consistent with the ultraoligotrophic nature of the Marianas region, in which *B. septemdierum* may rely less suspension-feeding and more on endosymbionts for nutrition.

While several environmental variables negatively affect the overall condition of vent mussels, optimal sulphide availability appears to be the mitigating factor. Enhanced energy uptake - moderated by symbiont abundance and environmental sulphide - can increase an organism's resilience to environmental stressors and make the organism more robust to changes in condition index.

Table 3.4. Ranges of methane concentration, sulphide concentration, water content, and condition indices in *Bathymodiolus* species. ND: not detectable; - ; not available; subscripts indicates estimated values from the respective publications, 1) Tunnicliffe et al. (2009), 2) Podowski et al. (2010); 3) Sarradin et al. (1999).

Author	**Species**	**Symbiont Type T= thiotrophic M= methanotrophic**	**Site**	**Location**	**Depth (m)**	**Sulphide (µM/l)**	**Methane (µM/l)**	**%Water Weight**	**CI (Total Soft Tissue dry weight in g/ shell volume in ml)**	**CI (Total Soft Tissue AFDW in g/ shell volume in ml)**
This study	*B. septemdierum*	Thiotrophic	Pillar Top	NW Eifuku, Mariana Arc	1,561	$<1_1$	__	91.4 ±1.3	0.027 ± 0.004	0.025 ± 0.004
This study	*B. septemdierum*	Thiotrophic	Champagne	NW Eifuku, Mariana Arc	1,605	155_1	__	89.7 ± 2.1	0.048 ± 0.010	0.045 ± 0.009
This study	*B. septemdierum*	Thiotrophic	Golden Lips	NW Eifuku, Mariana Arc	1,606	n/a	__	92.7 ± 1.7	0.025 ± 0.006	0.023 ± 0.006
This study	*B. septemdierum*	Thiotrophic	Near Fouling	NW Eifuku, Mariana Arc	1,576	101_1	__	n/a	0.044 ± 0.007	0.042 ± 0.007
This study	*B. septemdierum*	Thiotrophic	Nifonea	Nifonea Ridge, Vanuatu	1,900	n/a	__	n/a	0.048 ± 0.012	0.045 ± 0.011
This study	*B. septemdierum*	Thiotrophic	ABE	East Lau Spreading Centre, Lau Basin	2,130	$0\text{-}131_2$	__	n/a	0.038 ± 0.007	0.034 ± 0.019
Smith (1985)	*B. thermophilus*	Thiotrophic	Mussel Bed, Central	Galapagos Rift	2,490	ND	__	84.1 ± 2.2	0.057 ± 0.011	__
Smith (1985)	*B. thermophilus*	Thiotrophic	Mussel Bed, Peripheral	Galapagos Rift	2,490	ND	__	90.1 ± 1.8	0.010 ± 0.003	__
Fisher et al., (1988)	*B. thermophils*	Thiotrophic	Rose Garden, Central Clump	Galapagos Rift	__	0-325	__	79.1 ± 1.4	0.060 ± 0.008	__
Fisher et al., (1988)	*B. thermophils*	Thiotrophic	Rose Garden, Peripheral Site	Galapagos Rift	__	0-35	__	78 ± 1.3	0.056 ± 0.008	__

Fisher et al., (1988)	*B. thermophils*	Thiotrophic	Rose Garden, Peripheral Site 2	Galapagos Rift	__	0-8	__	80.3 ± 1.9	0.046 ± 0.006	__
Dattagupta et al., (2004)	*B. childressi*	Methanotrophic	Brine Pool NR1	Green Canyon, Gulf of Mexico	650	__	42-626[3]	84.3 ± 3.2	__	0.10 ± 0.03
Dattagupta et al., (2004)	*B. childressi*	Methanotrophic	GC 234	Green Canyon, Gulf of Mexico	540	__	__	87.5 ± 2.7	__	0.06 ± 0.02
Dattagupta et al., (2004)	*B. childressi*	Methanotrophic	Bush Hill (BH)	Green Canyon, Gulf of Mexico	540-580	__	__	92.2 ± 1.6	__	0.04 ± 0.012
Nix et al., (1995)	*B. childressi*	Methanotrophic	Bush Hill (GC 184/185)	Green Canyon, Gulf of Mexico	540-580	ND	0-22	90.5 ± 1.3	0.051 ± 0.010	__
Nix et al., (1995)	*B. childressi*	Methanotrophic	GC 234	Green Canyon, Gulf of Mexico	540	6746-7956	72-10744	89.3 ± 2.84	0.062 ± 0.020	__
Nix et al., 1995	*B. childressi*	Methanotrophic	GC 272	Green Canyon, Gulf of Mexico	730	ND	2-4	90.0 ± 1.5	0.056 ± 0.011	__
Smith et al., (2000)	*B. childressi*	Methanotrophic	Brine Pool NR1, Inner Zone	Green Canyon, Gulf of Mexico	650	ND	136-2197	82.5 ± 1.8	__	0.12 ± 0.02
Smith et al., (2000)	*B. childressi*	Methanotrophic	Brine Pool NR1, Middle Zone	Green Canyon, Gulf of Mexico	650	<500	100-432	84.6 ± 1.0	__	0.10 ± 0.01
Smith et al., (2000)	*B. childressi*	Methanotrophic	Brine Pool NR1, Outer Zone	Green Canyon, Gulf of Mexico	650	>13000	35-799	83.9 ± 1.9	__	0.11 ± 0.02
Riou et al., (2010)	*B. azoricus*	Thiotrophic and methanotrophic	PP30/PP31	Menez Gwen vent field, Mid-Atlantic Ridge	817	62[3]	100[3]	__	0.051-0.099	__
Bergquist et al., (2004)	*B. childressi*	Methanotrophic	Bush Hill (P1)	Green Canyon, Gulf of Mexico	540-580	1, 0, 4, 0, 0	38, 0, 3, 0, 0	~81.2, 84.1, 84.0, 88.1, 92.3	__	__
Bergquist et al., (2004)	*B. childressi*	Methanotrophic	GC 234 (P2)	Green Canyon, Gulf of Mexico	540	1, 0	0, 35	~87.5, 86.3	__	__

Bergquist et al., (2004)	*B. childressi*	Methanotrophic	Brine Pool NR1 (B1)	Green Canyon, Gulf of Mexico	650	0, 42, 100, 1	19, 794, 1483, 433	87.5, 85.0, 80.7, 80.2	__	__
Bergquist et al., (2004)	*B. childressi*	Methanotrophic	Brine Pool 2 (B2)	Garden Banks, Gulf of Mexico	670	0	452	87.0	__	__

Literature Cited

Addadi, L., Raz, S., & Weiner, S. (2003). Taking advantage of disorder: amorphous calcium carbonate and its roles in biomineralization. *Advanced Materials*, *15*(12), 959–970. http://doi.org/10.1002/adma.200300381

Bayne, B. L., & Thompson, R. J. (1970). Some physiological consequences of keeping *Mytilus edulis* in the laboratory. *Helgolander Wissenschaftliche Meeresuntersuchungen*, *552*, 526–552.

Beinart, R. A, Gartman, a, Sanders, J. G., Luther, G. W., & Girguis, P. R. (2015). The uptake and excretion of partially oxidized sulfur expands the repertoire of energy resources metabolized by hydrothermal vent symbioses. *Proceedings. Biological Sciences / The Royal Society*, *282*(1806), 20142811. http://doi.org/10.1098/rspb.2014.2811

Bergquist, D. C., Fleckenstein, C., Szalai, E. B., Knisel, J., & Fisher, C. R. (2004). Environment drives physiological variability in the cold seep mussel *Bathymodiolus childressi*. *Limnology and Oceanography*, *49*(3), 706–715.

Boron, W. F. (2004). Regulation of intracellular pH. *Advances in Physiology Education*, *28*(1-4), 160–79. http://doi.org/10.1152/advan.00045.2004

Britayev, T. A., Krylova, E. M., Martin, D., Von Cosel, R., & Asksiu, T. (2003). Symbiont – host interaction in the association of the scale worm *Branchipolynoe aff. seepensis* (Polychaeta: Polynoidae) with the hydrothermal mussel, *Bathymodiolus spp*. *International Research: Biological Studies*, *12*(2), 13–16.

Britayev, T. A., Martin, D., Krylova, E. M., von Cosel, R., & Aksiuk, T. S. (2007). Life-history traits of the symbiotic scale-worm *Branchipolynoe seepensis* and its relationships with host mussels of the genus *Bathymodiolus* from hydrothermal vents. *Marine Ecology*, *28*(1), 36–48. http://doi.org/10.1111/j.1439-0485.2007.00152.x

Cardoso, Joana FMF, Dekker, R., & Witte, Johannes IJ, Van der Veer, H. (2007). Is reproductive failure responsible for reduced recruitment of intertidal *Mytilus edulis L*. in the western Dutch Wadden Sea? *Senckenbergiana maritima*, *37*(2), 83-92.

Caro, A., Gros, O., Got, P., De Wit, R., & Troussellier, M. (2007). Characterization of the population of the sulfur-oxidizing symbiont of *Codakia orbicularis* (Bivalvia, Lucinidae) by single-cell analyses. *Applied and Environmental Microbiology*, *73*(7), 2101–2109. http://doi.org/10.1128/AEM.01683-06

Crosby, M., & Gale, L. (1990). A review and evalutaion of bivalve condition index methodologies with a suggested standard method. *Journal of Shellfish Research, 9*(1), 233–237.

Dattagupta, S., Bergquist, D. C., Szalai, E. B., & Fisher, C. R. (2004). Tissue carbon, nitrogen, and sulfur stable isotope turnover in transplanted *Bathymodiolus childressi* mussels: Relation to growth and physiological condition, *49*(4), 1144–1151.

Distel, D. L., Lee, H. K., & Cavanaugh, C. M. (1995). Intracellular coexistence of methano- and thioautotrophic bacteria in a hydrothermal vent mussel. *Proceedings of the National Academy of Sciences, 92*, 9598–9602.

Dubilier, N., Windoffer, R., & Giere, O. (1998). Ultrastructure and stable carbon isotope composition of the hydrothermal vent mussels from the North Fiji Basin, western Pacific. *Marine Ecological Progress Series, 165,* 187-193.

Dufour, S. C. (2005). Gill anatomy and the evolution of symbiosis in the bivalve family Thyasiridae. *Biological Bulletin, 208*, 200–212.

Dufour, S., & Felbeck, H. (2006). Symbiont abundance in thyasirids (Bivalvia) is related to particulate food and sulphide availability. *Marine Ecology Progress Series*, *320*, 185–194. http://doi.org/10.3354/meps320185

Duperron, S. (2010). *The Vent and Seep Biota*. (S. Kiel, Ed.) (Vol. 33, pp. 137–167). Dordrecht: Springer Netherlands. http://doi.org/10.1007/978-90-481-9572-5 *Microbiology Ecology*, *63*(3), 338–49. http://doi.org/10.1111/j.1574-6941.2008.00438.x

Feely, R. A., Sabine, C. L., Lee, K., Berelson, W., Kleypas, J., Fabry, V. J., & Millero, F. J. (2004). Impact of anthropogenic CO_2 on the $CaCO_3$ system in the oceans. *Science, 305*, 362-366.

Fiala-Médioni, A., McKiness, Z., Dando, P., Boulegue, J., Mariotti, A., Alayse-Danet, A., Robinson, J. & Cavanaugh, C. (2002). Ultrastructural, biochemical, and immunological characterization of two populations of the mytilid mussel *Bathymodiolus azoricu*s from the Mid-Atlantic Ridge: evidence for a dual symbiosis. *Marine Biology*, *141*(6), 1035–1043. http://doi.org/10.1007/s00227-002-0903-9

Fisher, C., Childress, J., Arp, A., Brooks, J. M., Distel, D., Favuzzi, J. A., … Soto, T. (1988). Microhabitat variation in the hydrothermal vent mussel, *Bathymodiolus thermophilus*, at the Rose Garden vent on the Galapagos Rift. *Deep Sea Research Part A. Oceanographic Research Papers*, *35*(10-11), 1769–1791. http://doi.org/10.1016/0198-0149(88)90049-0

Fisher, C., Childress, J., Oremland, R., & Bidigare, R. (1987). The importance of methane and thiosulfate in the metabolism of the bacterial symbionts of two deep-sea mussels. *Marine Biology, 71*, 59–71.

Fujinoki, M., Koito, T., Nemoto, S., Kitada, M., Yamaguchi, Y., Hyodo, S., … Inoue, K. (2011). Comparison of the amount of thiotrophic symbionts in the deep-sea mussel *Bathymodiolus septemdierum* under different sulfide levels using fluorescent *in situ* hybridization. *Fisheries Science, 78*(1), 139–146. http://doi.org/10.1007/s12562-011-0419-7

Gaston, G. R., Bartlett, J. H. W., Mcallister, A. P., & Heard, R. W. (1996). Biomass variations of estuarine macrobenthos preserved in ethanol and formalin. *Estuaries, 19*(3), 674–679.

Gazeau, F., Quiblier, C., Jansen, J. M., Gattuso, J.-P., Middelburg, J. J., & Heip, C. H. R. (2007). Impact of elevated CO_2 on shellfish calcification. *Geophysical Research Letters, 34*(7), L07603. http://doi.org/10.1029/2006GL028554

Grieshaber, M.K., Volkel, S. (1998) Animal adaptations for tolerance and exploitation of poisonous sulfide. *Annual Review of Physiology. 60*, 33–53. doi:10.1146/annurev.physiol.60.1.33

Hall-Spencer, J. M., Rodolfo-Metalpa, R., Martin, S., Ransome, E., Fine, M., Turner, S. M., … Buia, M.-C. (2008). Volcanic carbon dioxide vents show ecosystem effects of ocean acidification. *Nature, 454*(7200), 96–99. http://doi.org/10.1038/nature07051

Hüning, A. K., Melzner, F., Thomsen, J., Gutowska, M. a., Krämer, L., Frickenhaus, S., … Lucassen, M. (2013). Impacts of seawater acidification on mantle gene expression patterns of the Baltic Sea blue mussel: implications for shell formation and energy metabolism. *Marine Biology, 160*(8), 1845–1861. http://doi.org/10.1007/s00227-012-1930-9

Jannasch, H. (1995). Microbial interactions with hydrothermal fluids. In American Geophysical Union (Ed.), *Seafloor Hydrothermal Systems: Physical, chemical, biological, and geological interactions* (ed. S. E. , pp. 273–296). Washington, DC.

Kádár, E., Bettencourt, R., Costa, V., Santos, R. S., Lobo-da-Cunha, A., & Dando, P. (2005). Experimentally induced endosymbiont loss and re-acquirement in the hydrothermal vent bivalve *Bathymodiolus azoricus*. *Journal of Experimental Marine Biology and Ecology, 318*(1), 99–110. http://doi.org/10.1016/j.jembe.2004.12.025

Lagade, V., & Muley, D. (2014). Effect of short term temperature on physiological body indices of two estuarine venerid clams *Katelysia opima* and *Meretrix meretrix* (Mollusca: Bivalvia). *Journal of Ecophysiology and Occupational Health. 14*(3,4), 167–174. http://doi.org/10.15512/joeoh/2014/v14i3

Lannig, G., Eilers, S., Pörtner, H. O., Sokolova, I. M., & Bock, C. (2010). Impact of ocean acidification on energy metabolism of oyster, *Crassostrea gigas*- Changes in metabolic pathways and thermal response. *Marine Drugs*, *8*(8), 2318–39. http://doi.org/10.3390/md8082318

Lupton, J., Butterfield, D., Lilley, M., Olson, E., Baker, E., Roe, K., & Greene, R. (2006). Submarine venting of liquid carbon dioxide on a Mariana Arc volcano. *Geochemisty, Geophysics, Geosystems*, http://doi.org/10.1029/2005GC001152

Melzner, F., Stange, P., Trübenbach, K., Thomsen, J., Casties, I., Panknin, U., … Gutowska, M. A. (2011). Food supply and seawater pCO_2 impact calcification and internal shell dissolution in the blue mussel *Mytilus edulis*. *PloS One*, *6*(9), e24223. http://doi.org/10.1371/journal.pone.0024223

Mercado-Silva, N. (2005). Condition index of the eastern oyster, *Crassostrea virginica* (Gmelin, 1791) in Sapelo Island Georgia - Effects of site, position on bed and pea crab parasitism. *Journal of Shellfish Research, 24*(1), 121–126.

Michaelidis, B., Ouzounis, C., Paleras, A., & Pörtner, H. O. (2005). Effects of long-term moderate hypercapnia on acid – base balance and growth rate in marine mussels *Mytilus galloprovincialis. Marine Ecological Progress Series, 293*, 109–118.

Nelson, D. C., Hagen, K. D., & Edwards, D. B. (1995). The gill symbiont of the hydrothermal vent mussel *Bathymodiolus thermophilus* is a psychrophilic, chemoautotrophic, sulfur bacterium. *Marine Biology, 121*(3), 487–495. http://doi.org/10.1007/BF00349457

Nix, E. R., Fisher, C. R., Vodenichar, J., & Scott, K. M. (1995). Physiological ecology of a mussel with methanotrophic endosymbionts at three hydrocarbon seep sites in the Gulf of Mexico. *Marine Biology*, *122*(4), 605–617. http://doi.org/10.1007/BF00350682

Orr, J. C., Fabry, V. J., Aumont, O., Bopp, L., Doney, S. C., Feely, R. A., … Yool, A. (2005). Anthropogenic ocean acidification over the twenty-first century and its impact on calcifying organisms. *Nature*, *437*(7059), 681–686. http://dx.doi.org/10.1038/nature04095

Podowski, E., Ma, S., Luther, G., Wardrop, D., & Fisher, C. (2010). Biotic and abiotic factors affecting distributions of megafauna in diffuse flow on andesite and basalt along the Eastern Lau Spreading Center, Tonga. *Marine Ecology Progress Series, 418*, 25–45. http://doi.org/10.3354/meps08797

Pond, D. W., Bell, M. V, Dixon, D. R., Fallick, A. E., Segonzac, M., & Sargent, J. R. (1998). Stable-carbon-isotope composition of fatty aids in hydrothermal vent mussels containing methanotrophic and thiotrophic bacterial endosymbionts. *Applied and Environmental Microbiology, 64*(1), 370–375.

Rheault RB, R. M. (1996). Food-limited growth and condition index in the eastern oyster, *Crassostrea virginica* (Gmelin 1791), and the bay scallop, *Argopecten irradians irradians*, *Journal of Shellfish Research*, *15*(2), 271–283.

Ries, J. B., Cohen, a. L., & McCorkle, D. C. (2009). Marine calcifiers exhibit mixed responses to CO_2-induced ocean acidification. *Geology*, *37*(12), 1131–1134. http://doi.org/10.1130/G30210A.1

Riou, V., Duperron, S., Halary, S., Dehairs, F., Bouillon, S., Martins, I., … Serrão Santos, R. (2010). Variation in physiological indicators in *Bathymodiolus azoricus* (Bivalvia: Mytilidae) at the Menez Gwen Mid-Atlantic Ridge deep-sea hydrothermal vent site within a year. *Marine Environmental Research*, *70*(3-4), 264–71. http://doi.org/10.1016/j.marenvres.2010.05.008

Sarradin, P., Caprais, J., Riso, R., Kerouel, R., & Aminot, A. (1999). Chemical environment of the hydrothermal mussel communities in the Lucky Strike and Menez Gwen vent fields, Mid Atlantic Ridge. *Cahiers De Biologie Marine*, *40*, 93–104.

Smith, E. B., Scott, K. M., Nix, E. R., Korte, C., & Fisher, C. R. (2000). Growth and condition of seep mussels (*Bathymodiolus childressi*) at a Gulf of Mexico brine pool. *Ecology*, *81*(9), 2392. http://doi.org/10.2307/177462

Smith, K. L. (1985). Deep-sea hydrothermal vent mussels: nutritional state and distribution at the Galapagos Rift. *Ecology*, *66*(3), 1067–1080. http://doi.org/10.2307/1940566

Sokolova, I. M., Frederich, M., Bagwe, R., Lannig, G., & Sukhotin, A. a. (2012). Energy homeostasis as an integrative tool for assessing limits of environmental stress tolerance in aquatic invertebrates. *Marine Environmental Research*, *79*, 1–15. http://doi.org/10.1016/j.marenvres.2012.04.003

Takahashi, Y., Sasaki, Y., Chikaraishi, Y., Tsuchiya, M., Watanabe, H., Asahida, T., … Fujikura, K. (2012). Does the symbiotic scale-worm feed on the host mussel in deep-sea vent fields? *Research of Organic Geochemisrty*, *26*, 23–26.

Thomsen, J., Gutowska, M.A., Saphörster, J., Heinemann, A., Fietzke, J., et al. (2010) Calcifying invertebrates succeed in a naturally CO_2-rich coastal habitat but are threatened by high levels of future acidification. *Biogeosciences*, *7*, 3879–3891.

Thomsen, J., Haynert, K., Wegner, K. M., & Melzner, F. (2015). Impact of seawater carbonate chemistry on the calcification of marine bivalves. *Biogeosciences*, *12*(14), 4209–4220. http://doi.org/10.5194/bg-12-4209-2015

Thomsen, J., & Melzner, F. (2010). Moderate seawater acidification does not elicit long-term metabolic depression in the blue mussel *Mytilus edulis*. *Marine Biology*, *157*(12), 2667–2676. http://doi.org/10.1007/s00227-010-1527-0

Tunnicliffe, V., Davies, K. T. A., Butterfield, D. A., Embley, R. W., Rose, J. M., & Jr, W. W. C. (2009). Survival of mussels in extremely acidic waters on a submarine volcano. *Nature Geoscience*, *2*(5), 344–348. http://doi.org/10.1038/ngeo500

Chapter 4 : General Conclusion

Introduction

Given the rapidly acidifying nature of our present oceans, it is becoming increasingly important to determine the ecological consequences of physiological stress. When habitat quality declines, metabolic adjustments are made in an effort to support basal maintenance costs, often at the expense of an organism's growth and reproduction (Sokolova et al., 2012). In the long-term, reductions in growth and reproduction can effectively diminish the survival of the species, which may ultimately have consequences for the entire community. Throughout this thesis, I show that the overall health of hydrothermal vent mussels (*Bathymodiolus septemdierum*) is determined by the complex interplay of chemical, physical and biological factors that vary on both spatial and temporal scales. I suggest that mussels are more resilient to stressors such as high pCO_2 when hydrogen sulphide concentration is sufficient, and that energy budget adjustments may be made to maximize fitness.

Major Outcomes

In Chapter 2, I establish the basic reproductive characteristics of *B. septemdierum.* Maturation size differs between sexes: males reaching sexual maturity at smaller sizes than females. Mussels are functionally dioecious, though I observed protogynous hermaphroditism in thermally stressed mussels. I suggest that female to male sex change may be a strategy to maximize reproductive output. Male mussels tend to dominate when environmental conditions are poor because producing eggs is energetically more expensive than producing sperm (Russell-Hunter, 1979). While this is the first report of

protogyny in any *Bathymodiolus* species, protandrous hermaphroditism has previously been observed in several species including *B. septemdierum* (Le Pennec & Beninger, 1997). Therefore, my findings provide evidence that sex change direction is variable and is likely influenced by environmental conditions. I also provide evidence that gamete development is consistent with the proposed annual cycle of other *Bathymodiolus* species, with some variability exhibited across collection sites. I found no evident effect of pH on reproductive condition in *B. septemdierum,* though I was not able to assess fecundity, which can be adversely affected by stressful conditions in some marine organisms (e.g. Bayne et al., 1983; Kurihara, 2008).

In Chapter 3, I show that shell deposition is significantly restricted in mussels surviving in low pH conditions. I used a volumetric condition index (CI) to investigate the physiological response of *B. septemdierum* to habitat quality, and found that high pCO_2, thermal stress, and parasitic infection may negatively affect CI. However, I suggest that mussels are more resilient to stressors when energy availability is sufficient. My gill microscopy and gill condition index (GCI) results show that healthy gills often accompany a healthy body. Previous work has demonstrated that chemosynthetic mussels can increase the abundance of symbiotic bacteria in the gills when environmental sulphide concentrations are favourable (Dufour & Felbeck, 2006; Fujinoki et al., 2011). Gonadal mass has been shown to correlate positively with CI in marine bivalves (Cardoso et al., 2007), though I was not able to assess its relative contribution to CI in *B. septemdierum*. The gonadal mass of mussels at sulphide-rich habitats may contribute significantly to CI as gametogenesis progresses and gametes become mature, while

mussels from sulphide-poor sites may produce fewer gametes due to limited energy reserves, effectively reducing their contribution to the organism's CI.

Big Picture

The vent mussel, *Bathymodiolus septemdierum*, is a dominant member of the macrofauna at many hydrothermal vent sites in the western Pacific and Indian Ocean (Breusing et al., 2015). The biogeographic distribution of *B. septemdierum* is among the broadest of all hydrothermal vent fauna, suggesting a substantial resilience to a wide range of vent conditions. At Northwest Eifuku volcano, mussels are exposed to extremely acidic conditions that reduce availability of carbonate ions, probably increase calcification costs, and induce excess CO_2 in body fluids and tissues. In order to restore acid-base balance, mussels remove excess H^+ from the intra- and extra-cellular compartments of the body and accumulate bicarbonate (Seibel & Walsh, 2003; Pörtner et al., 2004; Fabry et al., 2008). These processes are made possible by energy-dependent protein carriers like proton ATPases that mediate active ion exchange across epithelial membranes (Seibel & Walsh, 2003; Pörtner et al., 2004; Fabry et al., 2008). Enhanced energy uptake, facilitated by high symbiont abundances and high environmental sulphide concentrations, can mitigate some of the excess costs associated with acid-base regulation. When energy availability is insufficient, lipid and carbohydrate stores are utilized to supplement energy requirements, thereby diminishing a mussel's overall condition and potentially decreasing reproductive output. Energy may also be diverted from calcification in support of fitness-sustaining processes during periods of pH stress (Thomsen & Melzner, 2010). The overall findings from this thesis are summarized in Figure 4.1.

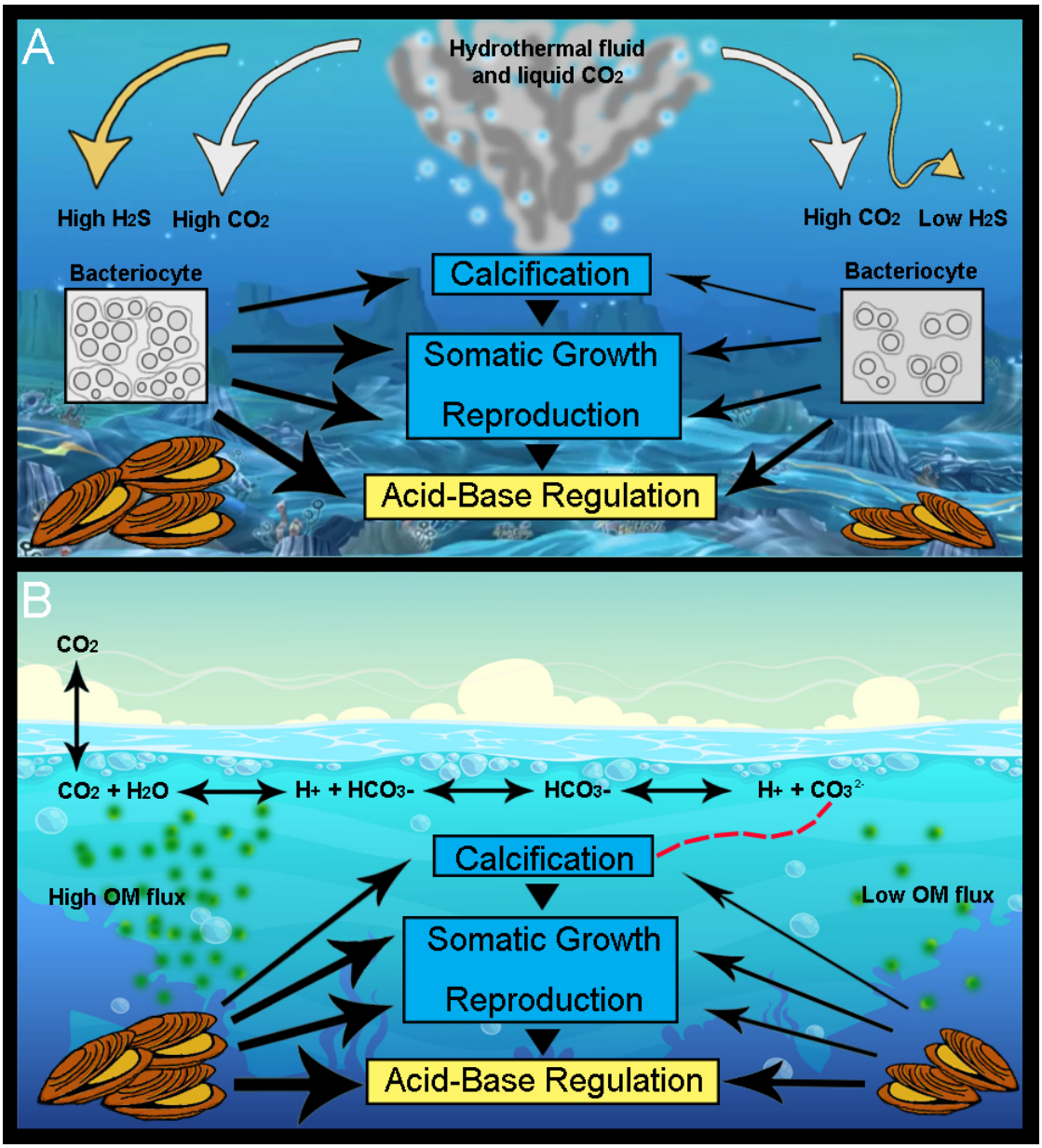

Figure 4.1. a) A depiction of the effects of high CO_2 concentration on the energy budget of hydrothermal vent mussels. The effects of high CO_2 concentration can be minimized by sufficient energy supply. High hydrogen sulphide (H_2S) concentrations increase symbiont abundance, which provides mussels with more energy to allocate to processes such as calcification, somatic growth, reproduction, and acid-base regulation, relative to low H_2S concentrations. b) A depiction of our findings from a hydrothermal vent setting translated to coastal mussels faceted with ocean acidification. The weight of single sided arrows indicates the intensity of CO_2, H_2S and energy flux (black single-sided arrows). Arrowheads between biological processes represent potential energy flow from the least vital (calcification) to most vital (acid-base regulation) biological process. Acid-base regulation is in yellow because it was not directly tested in this thesis. Organic matter is abbreviated as OM, and dashed red line represents the use of CO_3^{2-} in calcification.

The distribution and survival of *Bathymodiolus septemdierum* at hydrothermal vent environments is determined by chemical, physical and biological factors that vary on small spatial and temporal scales. Given the complex and dynamic nature of hydrothermal vents, habitat conditions may frequently deviate from optimal. Environmental conditions are considered suboptimal if an organism needs to increase energy expenditure on maintenance, defense or repair, which often occurs at the expense of an organism's energy reserves (Lannig et al., 2010; Sokolova et al., 2012). While the extent of stress tolerance is flexible and can be shifted by adaptation or acclimatization, mussels can withstand suboptimal conditions as long as basal metabolic requirements are satisfied. The results from this thesis reveal some factors that may affect the distribution limits of *B. septemdierum* within a hydrothermal vent environment.

My results suggest that energy availability is a dominant factor in determining the degree of tolerance demonstrated by mussels to environmental stressors. The sulphide-oxidizing symbionts in *B. septemdierum* gills require a minimal level of sulphide exposure to ensure healthy growth and reproduction of their mussel host, and this level will vary according to the energy requirements imposed on mussels from other environmental factors. Sulphide availability ultimately defines the 'outer' distribution limit, or the maximum distance mussels can survive from vent emissions. The 'inner' distribution limit, or the minimum distance to vent emissions mussels can tolerate may be influenced by temperature, sulphide concentration and/or CO_2 concentration. Mussels collected from a mixed aggregation of *Ifremaria nautilei* and *Bathymodiolus septemdierum,* occur close to vent emissions, and at temperatures significantly higher than homogenous aggregations of *B. septemdierum.* I report that mussels living at a

maximum temperature of 15.3°C in a mixed aggregation display a poor physiological condition and protogynous hermaphroditism, suggesting there may be some degree of thermal stress imposed on these mussels. Podowski et al. (2010) suggest that *B. septemdierum* is limited to regions where vent fluids do not exceed ~20°C. Moreover, Beinart et al. (2015) show carbon fixation by symbionts in *B. septemdierum* gills did not occur when sulphide concentrations were too high (350 μM/l), and sulphide concentrations tend to increase with proximity to high temperature venting. At Northwest Eifuku, mussels were not collected nor observed in regions where pH<5, suggesting that proximity to CO_2-rich vent fluids may also limit the 'inner' distribution limit of *B. septemdierum.* The cost of prolonged or frequent exposure to pH<5 on calcification and acid-base regulation may be too severe for mussels to tolerate regardless of sulphide availability.

Bathymodiolus septemdierum proves an exceptional model to illustrate how a shell-forming organism may adapt to withstand the stress of an acidic environment. Short-term laboratory ocean acidification experiments often provide insight into the initial responses of organisms to increased CO_2 concentrations. Information from *B. septemdierum* with prolonged survival in a naturally acidic environment may better inform models of future responses (Hall-Spencer et al., 2008) since ocean acidification is not a short-term stressor. Bathymodioline mussels are closely related to shallow water mytilids (Distel et al., 2000). Therefore, the adaptations observed in *B. septemdierum* to life at a CO_2 vent, including reduced calcification, and potential energy budget adjustments to maximize body growth and reproduction, may reflect adaptations we expect to observe in shallow water mytilids as the surface ocean becomes progressively

more acidic. Grasping a complete understanding of an organism's energy budget is necessary in order to make predictions about stress tolerance and survival in response to CO_2-driven acidification caused by anthropogenic emissions or CO_2 vents.

Future Directions

This study highlights the importance of considering habitat characteristics carefully when formulating species responses to ocean acidification. An organism's response to an environmental stressor can vary across populations, and may be influenced by stress intensity, stress duration, energy availability, and supplementary stressors. In the future, investigating the interaction of all potential environmental factors acting on an organism's energy budget will provide the most comprehensive understanding of an organism's response to ocean acidification.

Ideally, long-term data from natural populations will prove most accurate in predicting future responses of marine organisms to ocean acidification. CO_2-vents provide excellent *in situ* conditions for studying acidification because the complex interaction between chemical, physical and biological factors is difficult to replicate in a laboratory setting, especially for extended periods of time. However, the difficulty and cost associated with deep-sea research, presented some obstacles throughout this thesis including limited samples and water chemistry data. The reproductive cycle of *B. septemdierum,* and the pH effects on reproduction, should be further investigated with more frequent sampling throughout the year, from both low pH and control (seawater pH) sites. Future work should also focus on addressing the fecundity of *B. septemdierum* from low pH and control collection sites as reproductive output can be negatively affected by high pCO_2. Though I was able to establish trends in body and gill condition based on

estimated sulphide concentrations, future work is required with more precise water chemistry to develop a more complete understanding of the relationship between environmental stressors, sulphide concentration, symbiont abundance and condition index.

I demonstrate that low pH conditions at NW Eifuku significantly restrict shell growth in *B. septemdierum.* Shell deposition is possible despite low $CaCO_3$ saturation states and increased calcification costs, but an intact periostracum is essential, as any damage to this protective layer would lead to complete shell dissolution in such acidic conditions (Tunnicliffe et al., 2009). Due to time constraints, I was unable to investigate if mussels allocate additional energy to periostracum formation during periods of pH stress. Hüning et al. (2013) report that *Mytilus edulis* can increase tyrosinase expression in the mantle tissue in response to elevated pCO_2; tyrosinase is an enzyme associated with periostracum formation. Calcifying animals without a periostracum are considered more vulnerable to ocean acidification than those protected by an organic layer (Ries et al., 2009; Lischka et al., 2010; (Rodolfo-Metalpa et al., 2011). Therefore, determining if enhanced periostracum formation in *B. septemdierum* is an adaptation used to tolerate extremely acidic conditions should provide some insight on the strategy coastal mussels may utilize in response to future ocean acidification.

In addition to being an excellent model species to investigate the consequences of ocean acidification, *B. septemdierum* is a foundation species at several hydrothermal vent sites. An imminent threat to *B. septemdierum* communities is the industrial interest for the mining of seafloor massive sulphide (SMS) deposits commonly associated with hydrothermal vents. SMS deposits are areas of hard substratum rich in base metal and

sulphide content, along with exploitable concentrations of gold and silver (Boschen et al., 2013). Although SMS mining has been an interest for decades, very little is known about how it will affect biological communities. I suggest that future work focus on understanding how mussels will tolerate the stress of nearby mining, and how the vent community may respond if mussel growth, reproduction or survival is reduced. As a foundation species, gaining knowledge the stress tolerance of *B. septemdierum* is a first step, and a critical piece for the complete understanding of hydrothermal vent ecology.

Literature Cited

Bayne, B. L., Salkeld, P. N., Worrall, C. M. (1983). Reproductive effort and value in different populations of the marine mussel, *Mytilus edulis L*. *Oecologia*, *59*, 18–26.

Bayne, B. L., Salkeld, P. N., Worrall, C. M. (1983). Reproductive effort and value in different populations of the marine mussel, *Mytilus edulis L*. *Oecologia*, *59*, 18–26.

Beinart, R. A, Gartman, a, Sanders, J. G., Luther, G. W., & Girguis, P. R. (2015). The uptake and excretion of partially oxidized sulfur expands the repertoire of energy resources metabolized by hydrothermal vent symbioses. *Proceedings. Biological Sciences / The Royal Society*, *282*(1806), 20142811. http://doi.org/10.1098/rspb.2014.2811

Boschen, R. E., Rowden, a. a., Clark, M. R., & Gardner, J. P. A. (2013). Mining of deep-sea seafloor massive sulfides: A review of the deposits, their benthic communities, impacts from mining, regulatory frameworks and management strategies. *Ocean & Coastal Management*, *84*, 54–67. http://doi.org/10.1016/j.ocecoaman.2013.07.005

Breusing, C., Johnson, S., Tunnicliffe, V., & Vrijenhoek, R. (2015). Population structure and connectivity in Indo-Pacific deep-sea mussels of the *Bathymodiolus septemdierum* complex. *Conservation Genetics*, 1–16. http://doi.org/10.1007/s10592-015-0750-0

Cardoso, Joana FMF, Dekker, R., & Witte, Johannes IJ, Van der Veer, H. (2007). Is reproductive failure responsible for reduced recruitment of intertidal *Mytilus edulis L*. in the western Dutch Wadden Sea? *Senckenbergiana maritima*, *37*(2), 83-92.

Distel, D., Baco, A., Chuang, E., Morrill, W., Cavanaugh, C., Smith, C. (2000) Do mussels take wooden steps to deep-sea vents? *Nature 403*, 725–726.

Dufour, S., & Felbeck, H. (2006). Symbiont abundance in thyasirids (Bivalvia) is related to particulate food and sulphide availability. *Marine Ecology Progress Series*, *320*, 185–194. http://doi.org/10.3354/meps320185

Fabry, V. J., Seibel, B. A., Feely, R. A., & Orr, J. C. (2008). Impacts of ocean acidification on marine fauna and ecosystem processes. *Journal of Marine Science, 65*(3), 414-432.

Fujinoki, M., Koito, T., Nemoto, S., Kitada, M., Yamaguchi, Y., Hyodo, S., … Inoue, K. (2011). Comparison of the amount of thiotrophic symbionts in the deep-sea mussel *Bathymodiolus septemdierum* under different sulfide levels using fluorescent *in situ* hybridization. *Fisheries Science, 78*(1), 139–146. http://doi.org/10.1007/s12562-011-0419-7

Hall-Spencer, J. M., Rodolfo-Metalpa, R., Martin, S., Ransome, E., Fine, M., Turner, S. M., … Buia, M.-C. (2008). Volcanic carbon dioxide vents show ecosystem effects of ocean acidification. *Nature*, *454*(7200), 96–99. http://doi.org/10.1038/nature07051

Hüning, A. K., Melzner, F., Thomsen, J., Gutowska, M. a., Krämer, L., Frickenhaus, S., … Lucassen, M. (2012). Impacts of seawater acidification on mantle gene expression patterns of the Baltic Sea blue mussel: implications for shell formation and energy metabolism. *Marine Biology*, *160*(8), 1845–1861. http://doi.org/10.1007/s00227-012-1930-9

Kurihara, H. (2008). Effects of CO_2-driven ocean acidification on the early developmental stages of invertebrates. *Marine Ecology Progress Series*, *373*, 275–284. http://doi.org/10.3354/meps07802

Lannig, G., Eilers, S., Pörtner, H. O., Sokolova, I. M., & Bock, C. (2010). Impact of ocean acidification on energy metabolism of oyster, *Crassostrea gigas*- Changes in metabolic pathways and thermal response. *Marine Drugs*, *8*(8), 2318–39. http://doi.org/10.3390/md8082318

Le Pennec, M. & Beninger, P. G. (1997). Ultrastructural characteristics of spermatogenesis in three species of deep-sea hydrothermal vent mytilids. *Canadian Journal of Zoology*, *75*(2), 308–316. http://doi.org/10.1139/z97-039

Lischka, S., Büdenbender, J., Boxhammer, T., & Riebesell, U. (2010). Impact of ocean acidification and elevated temperatures on early juveniles of the polar shelled pteropod *Limacina helicina*: mortality, shell degradation, and shell growth. *Biogeosciences Discussions*, *7*(6), 8177–8214. http://doi.org/10.5194/bgd-7-8177-2010.

Podowski, E., Ma, S., Luther, G., Wardrop, D., & Fisher, C. (2010). Biotic and abiotic factors affecting distributions of megafauna in diffuse flow on andesite and basalt along the Eastern Lau Spreading Center, Tonga. *Marine Ecology Progress Series*, *418*, 25–45. http://doi.org/10.3354/meps08797

Portner, H. O., Langenbuch, M., & Reipschlager, A. (2004). Biological impact of elevated ocean CO_2 concentrations: lessons from animal physiology and earth history. *Journal of Oceanography*, *60*(4), 705–718. http://doi.org/10.1007/s10872-004-5763-0

Ries, J. B., Cohen, a. L., & McCorkle, D. C. (2009). Marine calcifiers exhibit mixed responses to CO_2-induced ocean acidification. *Geology*, *37*(12), 1131–1134. http://doi.org/10.1130/G30210A.1

Rodolfo-Metalpa, R., Houlbreque, F., Tambutte, E., Boisson, F., Baggini, C., Patti, F. P., … Hall-Spencer, J. M. (2011). Coral and mollusc resistance to ocean acidification

adversely affected by warming. *Nature Climate Change*, *1*(6), 308–312. http://dx.doi.org/10.1038/nclimate1200

Russell-Hunter, W. D. (1979). *A Life of Invertebrates*. *The Quarterly Review of Biology* (Vol. 54). New York: Macmillan Publishing Company. http://doi.org/10.1086/411368

Seibel, B. a., & Walsh, P. w. (2003). Biological impacts of deep-sea carbon dioxide injection inferred from indices of physiological performance. *Journal of Experimental Biology*, *206*(4), 641–650. http://doi.org/10.1242/jeb.00141

Sokolova, I. M., Frederich, M., Bagwe, R., Lannig, G., & Sukhotin, A. a. (2012). Energy homeostasis as an integrative tool for assessing limits of environmental stress tolerance in aquatic invertebrates. *Marine Environmental Research*, *79*, 1–15. http://doi.org/10.1016/j.marenvres.2012.04.003

Thomsen, J., & Melzner, F. (2010). Moderate seawater acidification does not elicit long-term metabolic depression in the blue mussel *Mytilus edulis*. *Marine Biology*, *157*(12), 2667–2676. http://doi.org/10.1007/s00227-010-1527-0

Tunnicliffe, V., Davies, K. T. A., Butterfield, D. A., Embley, R. W., Rose, J. M., & Jr, W. W. C. (2009). Survival of mussels in extremely acidic waters on a submarine volcano. *Nature Geoscience*, *2*(5), 344–348. http://doi.org/10.1038/ngeo500

APPENDIX A: Supplementary Figures for Chapter 3

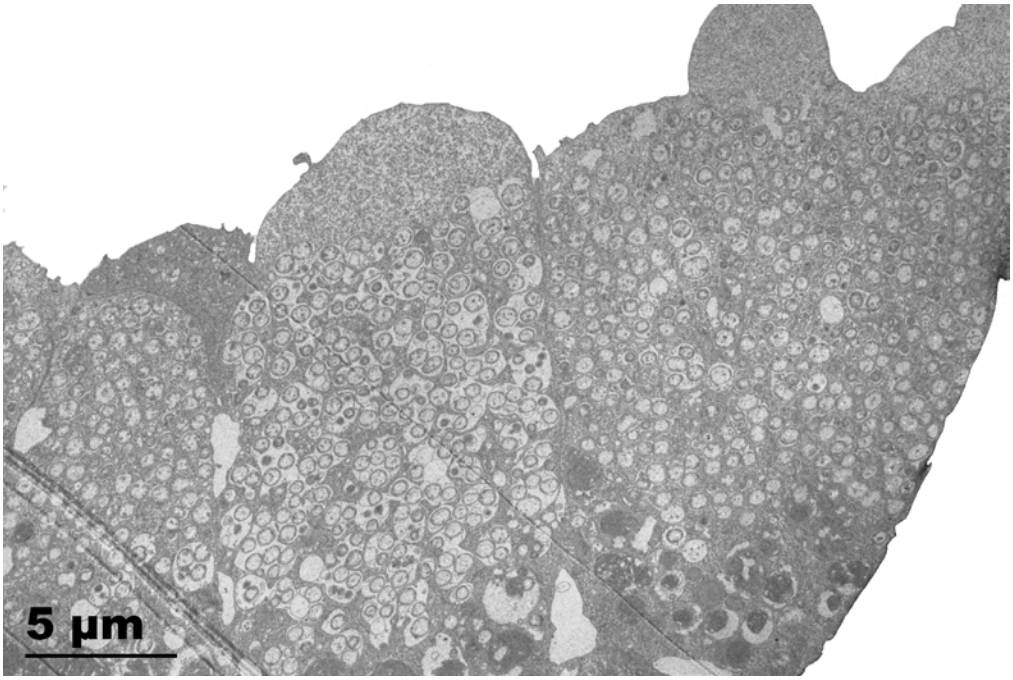

Figure A.1. Ultrathin cross section through Champagne mussel gill.

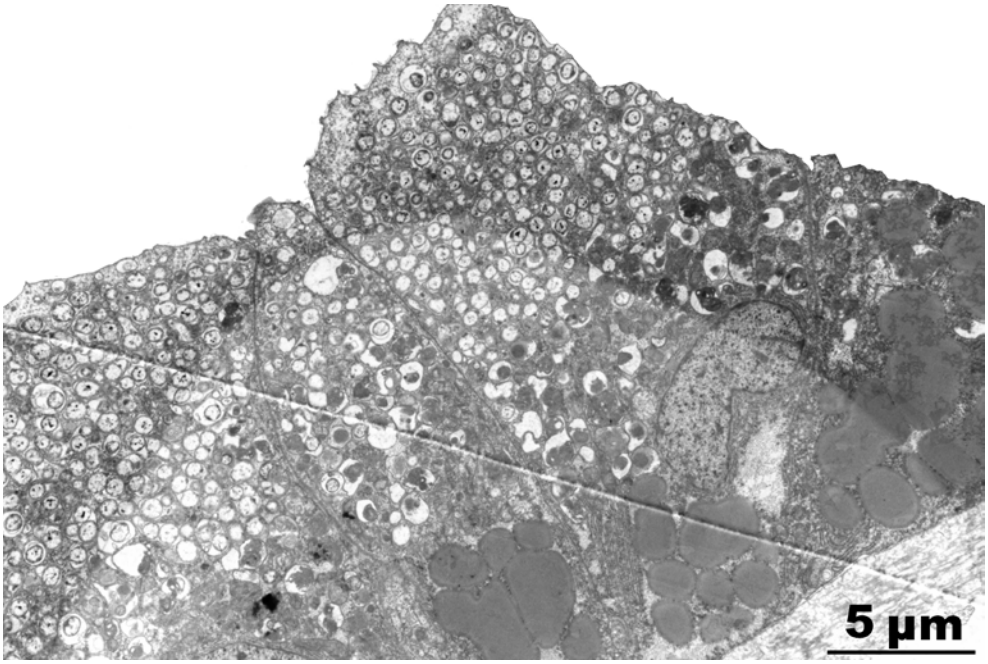

Figure A.2. Ultrathin cross section through Golden Lips mussel gill.

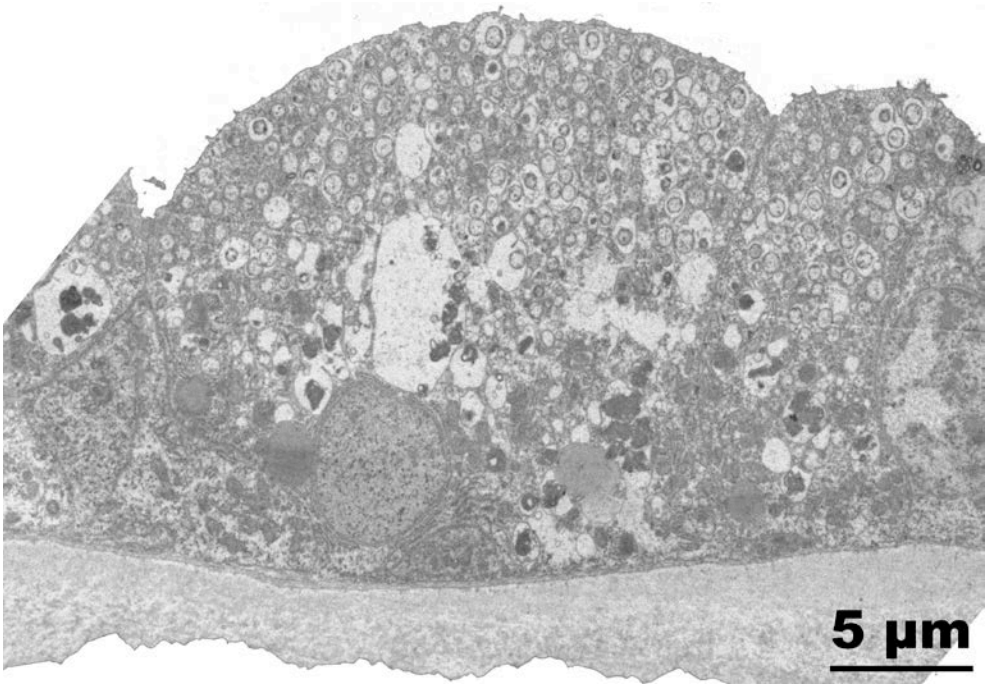

Figure A.3. Ultrathin cross section through Golden Lips mussel gill.

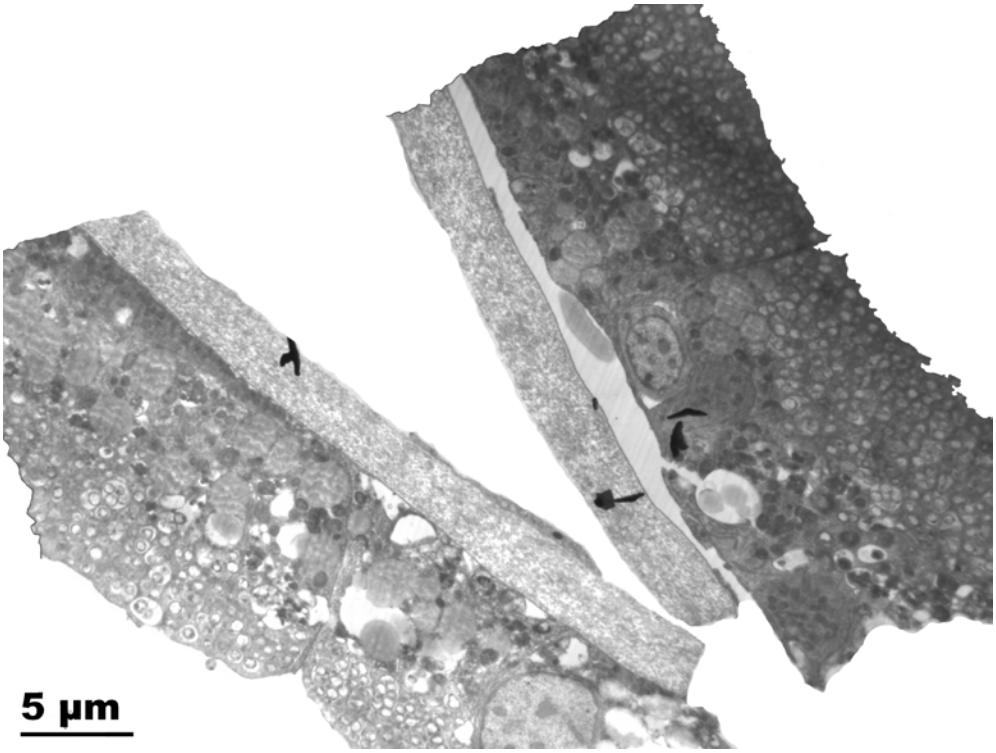

Figure A.4. Ultrathin cross section through Golden Lips mussel gill.

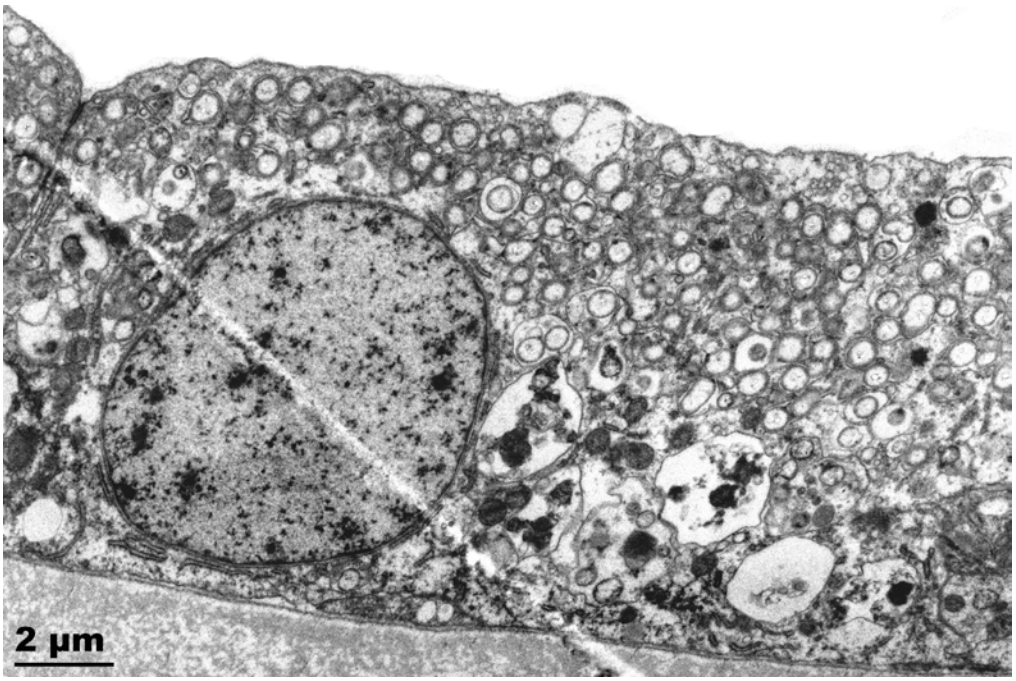

Figure A.5. Ultrathin cross section through Pillar Top mussel gill.

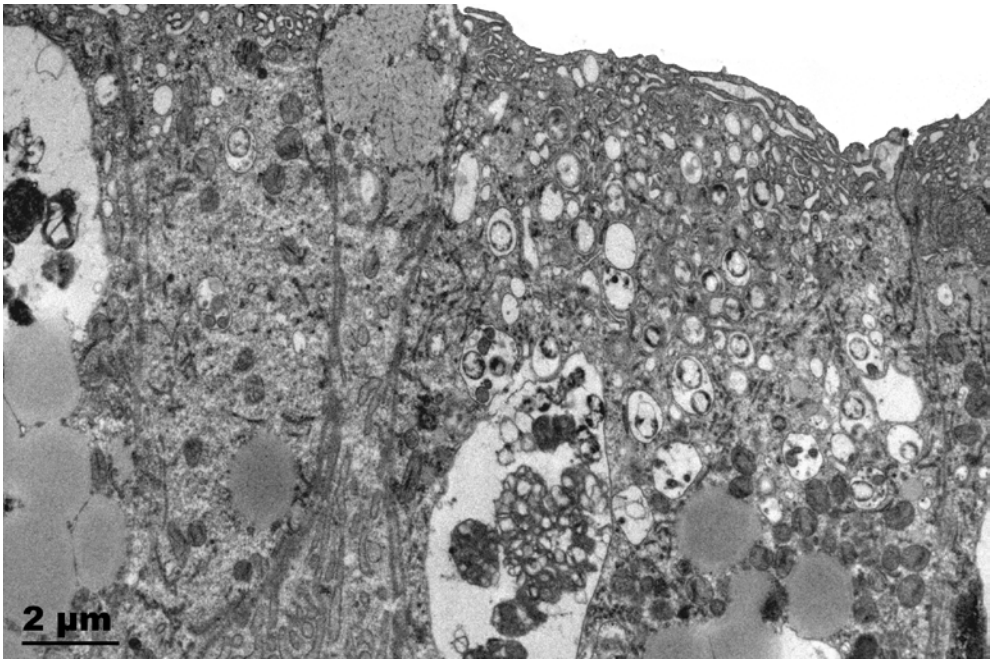

Figure A.6. Ultrathin cross section through Pillar Top mussel gill.

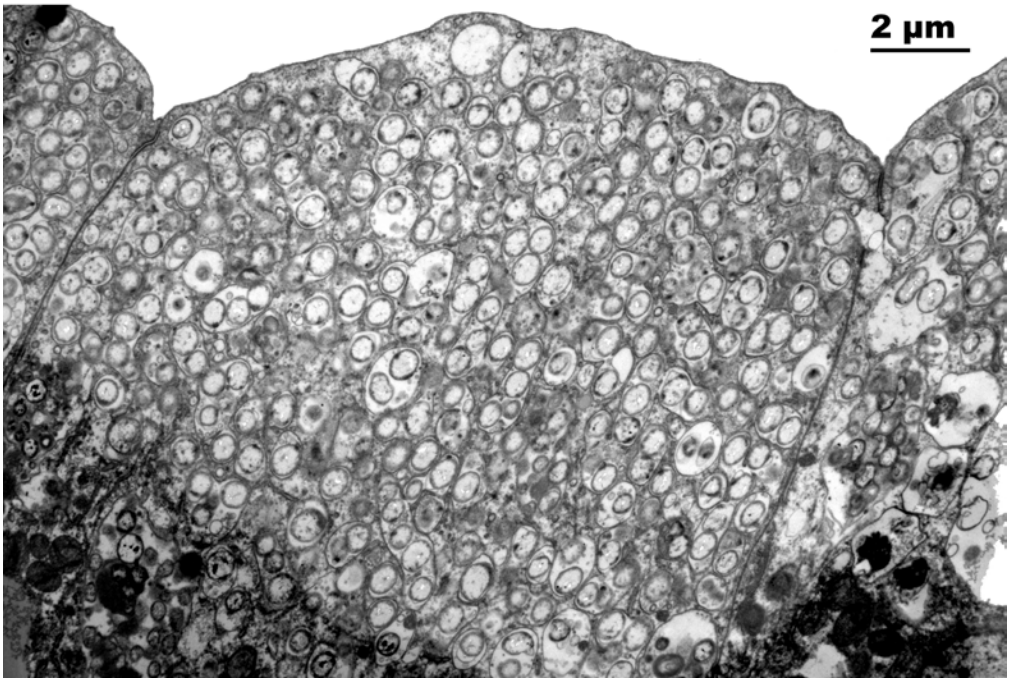

Figure A.7. Ultrathin cross section through Pillar Top mussel gill.

APPENDIX B: Thesis Data

Pillar Top Data

Location and Site	Date of Collection	Dive	Sample Number	Sex (m/f)
N.W. Eifuku, Pillar Top	December 6, 2014	J798-mB37	13-1	Female
N.W. Eifuku, Pillar Top	December 6, 2014	J798-mB37	13-2	Female
N.W. Eifuku, Pillar Top	December 6, 2014	J798-mB37	13-3	Female
N.W. Eifuku, Pillar Top	December 6, 2014	J798-mB37	13-4	Female
N.W. Eifuku, Pillar Top	December 6, 2014	J798-mB37	13-5	Female
N.W. Eifuku, Pillar Top	December 6, 2014	J798-mB37	13-6	Female
N.W. Eifuku, Pillar Top	December 6, 2014	J798-mB37	13-7	Female
N.W. Eifuku, Pillar Top	December 6, 2014	J798-mB37	13-8	Female
N.W. Eifuku, Pillar Top	December 6, 2014	J798-mB37	13-9	Female
N.W. Eifuku, Pillar Top	December 6, 2014	J798-mB37	13-10	Female
N.W. Eifuku, Pillar Top	December 6, 2014	J798-mB37	13-11	Female
N.W. Eifuku, Pillar Top	December 6, 2014	J798-mB37	13-12	Female
N.W. Eifuku, Pillar Top	December 6, 2014	J798-mB37	13-13	Female
N.W. Eifuku, Pillar Top	December 6, 2014	J798-mB37	13-14	Female
N.W. Eifuku, Pillar Top	December 6, 2014	J798-mB37	13-15	Male
N.W. Eifuku, Pillar Top	December 6, 2014	J798-mB37	13-16	Male
N.W. Eifuku, Pillar Top	December 6, 2014	J798-mB37	13-17	Male
N.W. Eifuku, Pillar Top	December 6, 2014	J798-mB37	13-18	Male
N.W. Eifuku, Pillar Top	December 6, 2014	J798-mB37	13-19	Male
N.W. Eifuku, Pillar Top	December 6, 2014	J798-mB37	13-20	Male
N.W. Eifuku, Pillar Top	December 6, 2014	J798-mB37	13-21	Male
N.W. Eifuku, Pillar Top	December 6, 2014	J798-mB37	13-22	Male
N.W. Eifuku, Pillar Top	December 6, 2014	J798-mB37	13-23	Male
N.W. Eifuku, Pillar Top	December 6, 2014	J798-mB37	13-24	Male
N.W. Eifuku, Pillar Top	December 6, 2014	J798-mB37	13-25	Male
N.W. Eifuku, Pillar Top	December 6, 2014	J798-mB37	13-26	N/a (frozen)
N.W. Eifuku, Pillar Top	December 6, 2014	J798-mB37	13-27	N/a (frozen)
N.W. Eifuku, Pillar Top	December 6, 2014	J798-mB37	13-28	N/a (frozen)
N.W. Eifuku, Pillar Top	December 6, 2014	J798-mB37	13-29	N/a (frozen)
N.W. Eifuku, Pillar Top	December 6, 2014	J798-mB37	13-30	N/a (frozen)
N.W. Eifuku, Pillar Top	December 6, 2014	J798-mB37	13-31	N/a (frozen)
N.W. Eifuku, Pillar Top	December 6, 2014	J798-mB37	13-32	N/a (frozen)
N.W. Eifuku, Pillar Top	December 6, 2014	J798-mB37	13-33	N/a (frozen)

Pillar Top Reproductive Stages (Gametogenesis)			
MALES		**FEMALES**	
Sample #	**Stage**	**Sample #**	**Stage**
13-18	5	13-1	4
13-20	4	13-3	5
13-17	5	13-4	5
13-15	5	13-6	5
13-16	5	13-2	5
13-19	5	13-9	5

Pillar Top Oocyte Diameters					
Sample 13-3	Sample 13-4	Sample 13-6	Sample 13-2	Sample 13-1	Sample 13-9
45.83	50.37	41.23	37.47	38.83	40.25
37.35	50.55	53.27	45.25	33.91	41.83
47.99	40.35	33.87	35.78	23.87	43.82
46.00	32.50	42.85	38.96	33.91	38.37
42.43	48.58	34.48	41.67	35.78	37.42
34.29	42.05	43.68	38.16	25.00	31.81
38.34	40.69	33.91	45.57	32.40	36.74
32.94	36.00	30.98	45.17	35.50	40.58
31.30	39.60	38.95	42.00	37.42	46.48
44.16	44.50	33.05	42.81	28.57	39.50
36.33	41.29	40.00	39.94	34.64	47.24
42.85	30.98	36.74	32.73	27.13	42.43
35.31	41.57	42.43	41.57	40.80	40.80
44.72	36.74	40.99	50.20	36.52	39.89
45.61	34.48	43.75	52.50	30.33	42.26
35.31	47.12	34.47	46.21	33.05	36.95
30.59	35.21	44.96	39.97	36.33	39.19
46.90	42.00	37.15	41.83	45.61	42.85
45.28	45.91	41.23	46.90	37.15	43.63
44.50	47.92	40.40	43.13	28.37	34.07
50.79	46.73	42.66	26.08	39.95	36.74
38.08	39.37	41.95	36.40	34.64	36.74
38.83	38.42	38.17	38.50	35.36	43.36
42.77	43.43	32.76	36.06	32.00	39.42
36.12	39.99	40.62	39.50	34.64	34.47
36.51	47.49	46.00	37.82	41.83	44.72

44.16	41.29	40.69	38.88	42.43	33.41
39.69	34.21	43.01	41.83	41.35	39.80
28.84	45.83	32.40	38.42	45.46	44.79
39.55	42.21	40.00	45.52	38.73	40.25
43.75	39.34	41.29	44.72	44.72	40.50
39.60	44.00	40.25	43.99	33.44	49.11
37.35	33.99	54.99	36.78	38.73	42.33
38.68	48.06	40.40	43.71	37.99	51.96
46.28	39.47	44.70	47.43	39.38	36.22
39.05	43.63	42.77	44.27	43.13	41.89
40.50	44.27	33.94	43.95	37.42	36.33
37.42	44.36	51.09	39.97	40.12	49.84
43.87	45.28	47.05	31.45	34.64	34.50
29.73	32.00	36.52	40.25	39.60	35.78
49.51	51.62	42.85	40.62	42.25	43.86
39.57	45.52	50.79	46.28	39.37	38.79
38.34	34.64	40.99	29.50	35.50	28.46
43.43	33.05	33.67	34.48	47.67	40.62
46.73	33.54	43.87	47.43	31.50	45.72
40.12	46.48	41.35	39.37	34.86	46.09
30.00	43.47	49.07	42.43	43.36	35.92
47.33	40.93	40.93	45.61	45.50	41.02
47.75	45.89	43.01	46.50	31.86	48.99
40.99	32.25	43.27	36.74	36.40	37.55
42.21	38.68	55.50	42.05	45.83	47.96
38.24	39.24	44.28	41.57	28.98	31.02
43.90	48.29	34.50	46.54	40.47	44.90
41.47	41.83	42.66	42.33	42.43	40.99
34.47	42.81	40.00	37.35	33.82	48.77
51.50	42.90	41.71	36.06	32.33	35.21
35.47	38.34	34.28	36.95	40.25	43.63
38.08	32.50	47.43	42.66	43.87	36.33
45.57	39.34	44.72	50.82	39.87	42.14
36.22	56.44	39.99	32.86	43.45	37.95
32.94	39.76	33.23	34.41	34.86	42.50
43.37	48.48	40.00	41.29	39.24	37.15
41.00	52.23	44.72	34.21	45.99	36.06
42.36	41.18	34.86	47.33	36.74	34.47
40.62	37.23	44.99	34.21	36.41	37.52
44.90	41.13	44.18	46.90	32.00	47.02
39.55	34.96	37.95	37.42	29.00	34.07
43.47	39.99	41.89	43.01	34.50	42.71
37.99	37.95	38.34	44.36	30.98	53.85

47.90	49.36	49.50	46.67	39.50	45.99
31.50	40.15	47.33	30.46	28.72	38.96
28.98	42.90	37.76	47.24	34.64	39.60
37.42	42.81	42.00	37.15	40.30	47.18
36.41	42.90	42.43	34.50	26.46	36.50
30.98	47.33	11.40	45.61	28.98	46.48
35.33	44.09	37.42	33.67	42.00	40.12
38.73	29.58	40.56	42.36	34.06	31.40
38.83	48.19	44.67	36.06	35.00	43.27
30.20	40.80	34.79	44.82	35.78	33.00
36.33	42.66	30.50	34.64	30.33	39.97
39.57	50.20	43.86	37.15	43.82	44.50
34.21	43.47	42.25	46.33	39.23	33.76
29.73	37.08	40.99	38.89	26.50	31.61
34.99	44.02	27.71	39.37	35.36	47.99
47.29	32.00	38.99	41.02	31.86	40.82
40.00	39.55	41.50	36.99	29.70	47.90
50.20	37.00	43.63	27.50	36.50	43.01
46.48	45.83	46.09	38.08	46.50	50.00
33.44	36.33	38.73	47.33	31.08	40.56
45.30	40.80	49.07	37.83	27.84	38.73
42.05	42.85	40.00	44.48	34.86	34.07
43.47	43.13	46.90	45.83	47.62	44.72
42.00	45.11	53.07	41.89	38.97	37.09
31.86	44.27	46.13	29.17	35.24	34.99
46.83	46.31	44.27	42.43	39.69	37.55
35.36	42.85	45.61	49.79	25.10	32.86
29.73	53.36	40.12	46.00	31.11	44.82
37.47	42.90	47.62	47.33	34.64	40.00
36.52	34.06	42.43	40.50	42.85	40.30
43.45	40.53	41.47	39.60	38.79	29.95
44.50	42.43	42.85	40.30	48.74	33.99
43.86	39.12	51.91	39.12	36.74	42.90
46.48	31.00	40.91	35.92	30.50	45.89
36.00	40.62	50.73	38.11	40.25	36.74
41.82	40.99	46.65	46.00	40.00	39.37
38.11	35.92	43.00	55.10	42.36	31.43
43.90	44.72	42.05	41.47	41.13	47.75
36.95	32.86	46.28	41.95	30.00	42.43
36.08	33.05	29.39	46.04	35.92	34.06
29.98	44.79	42.14	32.86	38.73	39.38
45.23	46.90	40.12	37.55	34.41	32.40
45.61	35.62	42.90	43.82	28.98	38.37

39.19	43.00	40.62	42.00	39.37	46.28
47.73	37.75	41.23	45.28	42.71	39.50
40.91	39.99	42.43	40.79	28.98	44.83
36.74	41.18	47.74	37.79	34.90	38.37
46.90	32.25	45.61	42.71	39.80	34.94
46.28	35.72	37.95	42.00	27.84	46.31
38.37	40.12	35.57	32.53	32.86	47.62
44.50	44.50	37.35	44.09	29.58	42.43

Pillar Top Sample Number	Shell Length (mm)	Shell Height (mm)	Shell Width (mm)	Shell Volume (mL) *both valves	Shell Weight (g) *both valves	Body Wet Weight (g)
13-1	126.3	52.9	21.5	176	19.36	57.12
13-2	125.5	51.2	22.0	188	20.24	64.98
13-3	118.0	48.0	19.3	144	17.00	48.1
13-4	140.0	54.0	21.9	222	25.52	61.24
13-5	139.0	50.1	30.5	252	27.34	79.43
13-6	142.0	51.2	29.0	264	25.68	76.66
13-7	129.9	51.3	22.0	200	17.34	49.43
13-8	132.7	45.0	26.5	186	19.28	50.66
13-9	117.5	46.6	21.0	148	17.66	45.57
13-10	129.0	54.5	23.0	214	22.66	76.27
13-11	124.0	52.0	23.0	198	21.04	56.48
13-12	136.0	57.0	25.0	238	29.1	86.35
13-13	120.0	54.0	21.7	156	21.28	53.56
13-14	137.0	58.2	28.0	260	26.76	75.82
13-15	142.0	56.0	24.0	248	29.22	85.19
13-16	100.5	45.0	18.0	94	10.66	30.37
13-17	83.8	48.9	13.5	60	7.88	26.86
13-18	77.0	36.5	13.0	58	7.48	22.36
13-19	79.0	38.0	12.0	62	7.14	21.63
13-20	51.0	20.5	7.0	20	3.20	5.40
13-21	138.2	58.0	25.0	248	23.80	78.9
13-22	99.5	41.0	12.2	104	10.06	33.27
13-23	102.0	45.0	16.5	110	11.08	40.16
13-24	52.0	27.0	7.0	22	3.36	6.52
13-25	51.4	24.9	5.5	18	2.66	4.47
13-26	138.5	54.9	24.8	238	24.98	N/a
13-27	124.0	50.0	22.5	186	20.18	N/a
13-28	118.5	52.0	19.5	166	19.50	N/a
13-29	138.0	54.5	23.0	206	24.42	N/a

13-30	120.0	53.2	19.0	164	19.68	N/a
13-31	94.0	41.0	14.0	78	9.72	N/a
13-32	95.0	41.5	15.0	94	11.20	N/a
13-33	100.0	44.0	16.5	110	11.22	N/a

Pillar Top Sample Number	Gill Dry Weight (g)	Total Body Dry Weight (g)	Gill Ash Weight (g)	Total Body Ash Weight (g)	Gill Condition Index	Total Body Condition Index	% Water Weight
13-5	1.2807	5.7862	0.0936	0.3418	0.0047	0.0216	92.71
13-7	1.0132	4.8696	0.0832	0.3313	0.0047	0.0227	90.14
13-10	1.0487	5.5282	0.0946	0.4969	0.0045	0.0235	92.75
13-11	0.6027	4.1979	0.0452	0.2233	0.0028	0.0201	92.56
13-12	1.3094	5.9150	0.0804	0.3103	0.0052	0.0235	93.15
13-13	0.8503	4.3963	0.0688	0.2564	0.0050	0.0265	91.79
13-14	1.4963	5.8065	0.1451	0.3824	0.0052	0.0209	92.34
13-21	1.2697	7.2780	0.0992	0.6162	0.0047	0.0269	90.77
13-22	0.5491	3.3794	0.0369	0.2421	0.0049	0.0302	89.84
13-23	0.6894	3.8084	0.0521	0.2878	0.0058	0.0320	90.51
13-24	0.1037	0.6094	0.0090	0.0518	0.0043	0.0253	90.65
13-25	0.0921	0.4943	0.0086	0.0460	0.0046	0.0249	88.94

Champagne Data

Location and Site	Date of Collection	Dive	Sample Number	Sex (m/f)
N.W. Eifuku, Champagne	December 14, 2014	J799-mB36	36-1	Female
N.W. Eifuku, Champagne	December 14, 2014	J799-mB36	36-2	Female
N.W. Eifuku, Champagne	December 14, 2014	J799-mB36	36-3	Male
N.W. Eifuku, Champagne	December 14, 2014	J799-mB36	36-4	Male
N.W. Eifuku, Champagne	December 14, 2014	J799-mB36	36-5	Male
N.W. Eifuku, Champagne	December 14, 2014	J799-mB36	36-6	Male
N.W. Eifuku, Champagne	December 14, 2014	J799-mB36	36-7	Female
N.W. Eifuku, Champagne	December 14, 2014	J799-mB36	36-8	Male
N.W. Eifuku, Champagne	December 14, 2014	J799-mB36	36-9	Female
N.W. Eifuku, Champagne	December 14, 2014	J799-mB36	36-10	Female
N.W. Eifuku, Champagne	December 14, 2014	J799-mB36	36-11	Male
N.W. Eifuku, Champagne	December 14, 2014	J799-mB36	36-12	Male
N.W. Eifuku, Champagne	December 14, 2014	J799-mB36	36-13	Female
N.W. Eifuku, Champagne	December 14, 2014	J799-mB36	36-14	Female

N.W. Eifuku, Champagne	December 14, 2014	J799-mB36	36-15	Male
N.W. Eifuku, Champagne	December 14, 2014	J799-mB36	36-16	Female
N.W. Eifuku, Champagne	December 14, 2014	J799-mB36	36-17	Female
N.W. Eifuku, Champagne	December 14, 2014	J799-mB36	36-18	Male
N.W. Eifuku, Champagne	December 14, 2014	J799-mB36	38-19	Male
N.W. Eifuku, Champagne	December 14, 2014	J799-mB36	36-20	Male
N.W. Eifuku, Champagne	December 14, 2014	J799-mB36	36-21	Male
N.W. Eifuku, Champagne	December 14, 2014	J799-mB36	36-22	Female
N.W. Eifuku, Champagne	December 14, 2014	J799-mB36	36-23	Female
N.W. Eifuku, Champagne	December 14, 2014	J799-mB36	36-24	Male
N.W. Eifuku, Champagne	December 14, 2014	J799-mB36	36-25	Male
N.W. Eifuku, Champagne	December 14, 2014	J799-mB36	36-26	N/a (frozen)
N.W. Eifuku, Champagne	December 14, 2014	J799-mB36	36-27	N/a (frozen)
N.W. Eifuku, Champagne	December 14, 2014	J799-mB36	36-28	N/a (frozen)
N.W. Eifuku, Champagne	December 14, 2014	J799-mB36	36-29	N/a (frozen)
N.W. Eifuku, Champagne	December 14, 2014	J799-mB36	36-30	N/a (frozen)
N.W. Eifuku, Champagne	December 14, 2014	J799-mB36	36-31	N/a (frozen)
N.W. Eifuku, Champagne	December 14, 2014	J799-mB36	36-32	N/a (frozen)
N.W. Eifuku, Champagne	December 14, 2014	J799-mB36	36-33	N/a (frozen)
N.W. Eifuku, Champagne	December 14, 2014	J799-mB36	36-34	N/a (frozen)
N.W. Eifuku, Champagne	December 14, 2014	J799-mB36	36-35	N/a (frozen)
N.W. Eifuku, Champagne	*April 10, 2004*	*R791-J208*	*No label 1*	*Female*
N.W. Eifuku, Champagne	*April 10, 2004*	*R791-J208*	*No label 2*	*Female*
N.W. Eifuku, Champagne	*April 10, 2004*	*R791-J208*	*No label 3*	*Female*
N.W. Eifuku, Champagne	*April 12, 2004*	*R793-J199*	*No label 4*	*Male*

Champagne Reproductive Stages (Gametogenesis)

MALES		**FEMALES**	
Sample #	**Stage**	**Sample #**	**Stage**
36-8	5	36-10	4
36-25	5	36-2	5
36-3	5	36-7	5
36-18	5	36-23	5
36-11	5	36-16	5
36-19	5	36-1	4

Champagne Oocyte Circular Equivalents					
Sample 36-7	Sample 36-1	Sample 36-23	Sample 36-2	Sample 36-16	Sample 36-10
39.34	44.50	36.52	45.17	35.41	37.09
47.12	33.63	31.84	42.43	46.48	41.23
36.28	38.34	44.90	42.71	40.79	38.96
34.07	50.53	37.82	41.67	39.94	50.56
48.43	41.47	42.90	45.90	42.43	37.76
38.37	51.22	45.83	46.00	44.16	42.40
39.50	37.76	38.47	35.36	36.74	48.74
46.04	36.74	43.59	45.03	42.00	38.47
48.00	40.99	38.41	37.23	34.90	43.37
46.86	35.31	44.02	37.34	48.37	33.67
35.69	42.53	51.09	42.81	37.35	43.01
42.33	37.95	54.77	28.77	39.12	39.42
37.42	39.80	42.05	39.55	50.60	45.30
39.12	48.17	42.43	39.12	44.72	38.34
47.12	46.72	47.92	42.25	44.88	30.41
51.58	43.01	34.47	47.49	48.77	40.42
44.16	36.74	43.13	34.21	46.48	43.87
42.25	44.72	33.67	30.94	46.73	37.95
46.04	32.86	45.03	43.99	41.57	38.88
38.54	44.67	36.33	47.15	46.21	37.76
50.62	36.33	45.30	42.90	36.00	40.00
32.86	40.99	43.13	43.95	42.05	39.97
39.80	40.56	44.00	36.06	40.62	41.23
47.33	34.64	36.88	44.70	38.73	54.26
27.50	37.95	35.24	52.87	39.94	45.52
33.44	42.95	47.56	43.00	41.02	51.58
41.89	33.99	39.91	43.59	34.86	31.08
33.00	38.54	39.76	37.42	48.91	41.47
40.79	35.21	42.66	51.44	43.30	47.33
40.25	35.36	45.23	40.53	40.25	42.90
39.55	38.18	39.80	42.95	39.50	46.48
37.95	42.43	50.35	29.39	40.00	34.96
43.82	40.12	42.95	45.50	44.90	42.40
47.00	38.42	39.69	43.43	38.34	48.99
31.94	39.50	37.42	35.71	48.63	34.86
37.95	52.44	46.90	34.64	40.25	35.00
46.65	38.50	47.91	45.28	52.15	34.64
32.45	45.83	33.67	43.47	39.50	50.35

46.37	35.21	40.50	52.44	36.74	43.95
43.95	46.73	44.02	45.28	42.00	40.15
43.82	46.43	43.36	52.25	49.48	33.17
46.95	43.99	38.78	37.88	35.07	53.57
35.33	42.14	46.37	43.43	46.13	34.94
49.50	36.93	40.62	36.88	44.27	56.92
34.58	47.33	43.07	39.19	41.83	50.20
32.86	48.28	42.00	48.40	43.36	46.50
42.78	47.91	47.49	38.34	42.95	26.12
46.95	47.33	44.50	53.72	38.34	49.44
36.93	30.50	48.43	41.81	43.82	41.13
35.57	49.50	44.72	50.20	45.83	36.95
35.78	37.88	47.62	44.88	41.95	50.91
35.50	32.40	36.33	43.95	37.08	45.96
45.28	42.66	40.00	44.90	37.09	49.96
42.43	34.28	34.50	48.79	35.50	52.25
39.69	41.57	32.40	47.01	41.11	40.56
42.00	31.18	48.74	40.00	39.60	32.65
40.25	45.17	43.50	36.00	37.34	44.16
40.25	40.69	49.85	40.12	43.24	42.43
41.42	42.71	47.75	41.95	30.74	44.50
39.23	40.80	43.99	43.24	45.83	47.74
43.01	41.00	35.92	40.69	40.62	32.86
41.99	40.00	42.43	47.96	43.01	33.67
44.99	39.80	42.85	36.92	50.00	34.99
41.95	47.00	40.15	47.97	41.95	43.01
38.99	45.30	50.79	42.90	34.21	42.71
39.42	41.47	36.88	48.19	47.18	50.16
41.57	44.27	45.61	44.82	35.78	51.96
44.99	46.04	44.27	42.78	47.43	38.34
31.46	53.05	36.92	54.91	27.50	39.89
35.21	29.80	35.07	50.73	44.27	45.43
44.72	44.72	44.90	37.95	39.50	31.86
44.50	47.43	40.56	40.82	27.93	37.34
40.56	50.00	48.93	32.50	50.52	40.99
32.86	44.16	36.66	36.66	41.47	40.50
45.61	37.67	49.64	35.72	31.75	44.18
43.59	46.62	38.08	38.47	39.91	40.12
45.91	38.54	45.92	40.99	41.41	32.31
44.28	47.75	40.69	38.17	47.37	40.12
40.00	28.72	33.50	38.57	49.04	47.49
44.27	31.94	46.58	35.50	47.48	47.74
42.90	42.36	43.07	47.18	41.83	39.69

37.88	37.99	38.97	43.82	46.09	49.75
46.32	42.00	40.62	35.21	39.69	39.19
45.17	45.91	39.50	33.82	44.41	45.28
43.86	45.46	35.50	48.74	40.25	40.80
43.82	37.04	39.97	43.13	41.11	34.64
33.54	46.86	48.19	39.42	34.25	33.44
43.47	35.50	43.13	36.33	29.66	46.90
48.06	32.94	35.92	45.54	43.44	40.00
40.21	44.88	47.24	51.62	52.68	35.07
43.82	30.98	39.20	49.50	38.96	37.15
41.47	43.36	42.00	52.92	44.16	43.59
42.81	38.46	35.71	48.37	45.83	42.90
44.72	45.54	33.82	43.36	43.71	51.38
41.29	50.20	42.25	38.46	43.13	40.99
28.37	36.03	44.16	46.43	40.35	44.27
36.78	43.07	38.57	39.95	30.33	36.52
44.72	39.50	31.94	52.87	36.88	40.25
42.77	39.69	40.25	29.66	35.65	42.43
38.88	44.54	39.50	40.69	49.14	55.99
45.83	42.36	35.07	49.42	43.37	30.03
34.58	35.50	47.33	39.55	38.79	36.51
37.23	33.94	43.37	46.90	40.82	38.54
34.64	41.23	53.98	45.46	40.12	52.80
41.83	47.74	40.00	45.83	38.34	39.50
40.15	29.39	38.73	44.41	44.27	36.99
32.94	43.13	37.95	42.99	32.86	46.50
47.96	48.79	31.75	48.63	40.91	44.18
52.44	41.86	41.64	36.06	25.98	52.92
40.00	47.91	44.88	50.75	43.71	35.71
28.64	33.05	49.11	42.85	44.54	41.95
39.37	42.43	42.05	39.34	41.82	42.33
39.69	44.00	33.41	33.20	41.71	29.98
29.17	32.03	40.62	41.13	40.99	40.12
37.82	44.50	34.96	45.44	41.95	30.98
46.15	38.73	42.60	37.95	39.24	29.58
32.17	37.47	41.29	39.69	42.43	41.95
41.13	40.12	34.86	46.09	48.99	34.06
32.40	42.90	39.19	35.50	42.14	44.72
46.28	40.00	34.21	50.52	43.44	37.34

Champagne Sample Number	Shell Length (mm)	Shell Height (mm)	Shell Width (mm)	Shell Volume (mL) *both valves	Shell Weight (g) *both valves	Body Wet Weight (g)
36-1	102.5	44.5	19.5	122	12.38	43.01
36-2	118.5	52.0	24.0	202	20.58	79.81
36-3	99.9	43.0	16.5	104	11.98	48.71
36-4	88.0	37.0	15.0	66	8.58	33.51
36-5	60.0	29.0	9.0	28	4.50	15.95
36-6	100.0	50.0	15.0	110	12.06	51.37
36-7	76.0	33.5	12.6	54	5.70	25.15
36-8	103.0	44.0	18.0	116	12.58	54.71
36-9	99.0	42.5	16.0	98	10.16	40.02
36-10	81.0	38.0	12.0	54	7.30	25.45
36-11	106.0	50.9	20.0	142	15.90	66.15
36-12	66.5	32.5	9.5	30	5.80	18.20
36-13	93.0	43.5	14.9	78	9.88	34.66
36-14	83.0	39.0	13.0	66	7.92	30.14
36-15	55.5	24.0	7.0	20	3.36	11.12
36-16	110.0	52.0	20.0	160	13.70	62.45
36-17	102.9	46.5	21.0	138	13.48	51.56
36-18	85.0	36.5	14.0	68	9.12	N/a
38-19	72.0	37.0	10.5	42	7.46	33.97
36-20	73.0	32.5	10.0	40	6.68	21.86
36-21	96.5	44.0	15.5	100	11.08	46.06
36-22	105.5	46.5	18.0	136	13.78	51.71
36-23	73.5	32.5	13.5	52	6.62	22.19
36-24	76.5	37.0	14.0	66	7.74	28.93
36-25	65.5	33.0	8.0	32	5.48	17.76
36-26	N/a	N/a	N/a	N/a	N/a	N/a
36-27	100.5	51.0	16.0	98	13.72	38.14
36-28	91.0	42.0	14.5	86	10.06	N/a
36-29	81.0	38.0	12.0	32	4.35	N/a
36-30	96.0	43.0	17.0	47	5.7	N/a
36-31	91.0	40.5	14.0	39	4.31	N/a
36-32	85.0	39.0	12.8	31	4.05	N/a
36-33	101.0	46.5	15.5	52	5.68	N/a
36-34	82.2	35.0	12.0	28	3.52	N/a
36-35	77.5	37.2	12.5	34	3.97	N/a
No label 1	*91.7*	*45.0*	*31.0*	N/a	N/a	N/a
No label 2	*94.7*	*42.5*	*31.0*	N/a	N/a	N/a

No label 3	*90.2*	*43.0*	*30.5*	N/a	N/a	N/a
No label 4	*39.0*	*29.0*	*10.0*	N/a	N/a	N/a

Champagne Sample Number	Gill Dry Weight (g)	Total Body Dry Weight (g)	Gill Ash Weight (g)	Total Body Ash Weight (g)	Gill Condition Index	Total Body Condition Index	% Water Weight
36-2	1.9956	10.6389	0.1524	0.5591	0.0091	0.0499	86.66
36-4	0.6673	3.5383	0.0395	0.2260	0.0095	0.0502	89.44
36-5	0.3332	1.5775	0.0284	0.1197	0.0109	0.0521	90.10
36-6	1.2659	5.2464	0.0777	0.4029	0.0108	0.0440	89.78
36-9	1.1130	4.4685	0.0725	0.2257	0.0106	0.0433	88.83
36-13	0.9797	4.3551	0.0731	0.2304	0.0116	0.0529	87.43
36-14	0.8310	4.0068	0.0676	0.2369	0.0116	0.0571	86.70
36-17	1.1592	5.0894	0.0678	0.2294	0.0079	0.0352	90.12
38-19	0.5353	2.4424	0.0422	0.1857	0.0117	0.0537	92.81
36-20	0.4435	1.9442	0.0310	0.1395	0.0103	0.0451	91.10
36-21	0.5796	3.2030	0.0394	0.2266	0.0054	0.0298	93.04
36-22	1.2686	4.6045	0.1319	0.3562	0.0084	0.0312	91.09

Golden Lips Data

Location and Site	Date of Collection	Dive	Sample Number	Sex (m/f)
N.W. Eifuku, Golden Lips	December 14, 2014	J799-mB38	38-1	Female
N.W. Eifuku, Golden Lips	December 14, 2014	J799-mB38	38-2	Male
N.W. Eifuku, Golden Lips	December 14, 2014	J799-mB38	38-3	Male
N.W. Eifuku, Golden Lips	December 14, 2014	J799-mB38	38-4	Male
N.W. Eifuku, Golden Lips	December 14, 2014	J799-mB38	38-5	Male
N.W. Eifuku, Golden Lips	December 14, 2014	J799-mB38	38-6	Female
N.W. Eifuku, Golden Lips	December 14, 2014	J799-mB38	38-7	Female
N.W. Eifuku, Golden Lips	December 14, 2014	J799-mB38	38-8	Female
N.W. Eifuku, Golden Lips	December 14, 2014	J799-mB38	38-9	Female
N.W. Eifuku, Golden Lips	December 14, 2014	J799-mB38	38-10	Female
N.W. Eifuku, Golden Lips	December 14, 2014	J799-mB38	38-11	Female
N.W. Eifuku, Golden Lips	December 14, 2014	J799-mB38	38-12	Female
N.W. Eifuku, Golden Lips	December 14, 2014	J799-mB38	38-13	Female
N.W. Eifuku, Golden Lips	December 14, 2014	J799-mB38	38-14	Female
N.W. Eifuku, Golden Lips	December 14, 2014	J799-mB38	38-15	Female
N.W. Eifuku, Golden Lips	December 14, 2014	J799-mB38	38-16	Female
N.W. Eifuku, Golden Lips	December 14, 2014	J799-mB38	38-17	Female

N.W. Eifuku, Golden Lips	December 14, 2014	J799-mB38	38-18	Female
N.W. Eifuku, Golden Lips	December 14, 2014	J799-mB38	38-19	Female
N.W. Eifuku, Golden Lips	December 14, 2014	J799-mB38	38-20	Male
N.W. Eifuku, Golden Lips	December 14, 2014	J799-mB38	38-21	Female
N.W. Eifuku, Golden Lips	December 14, 2014	J799-mB38	38-22	Male
N.W. Eifuku, Golden Lips	December 14, 2014	J799-mB38	38-23	Female
N.W. Eifuku, Golden Lips	December 14, 2014	J799-mB38	38-24	Female
N.W. Eifuku, Golden Lips	December 14, 2014	J799-mB38	38-25	Female
N.W. Eifuku, Golden Lips	December 14, 2014	J799-mB38	38-26	Female
N.W. Eifuku, Golden Lips	December 14, 2014	J799-mB38	38-27	Female
N.W. Eifuku, Golden Lips	December 14, 2014	J799-mB38	38-28	Female
N.W. Eifuku, Golden Lips	December 14, 2014	J799-mB38	38-29	Female
N.W. Eifuku, Golden Lips	December 14, 2014	J799-mB38	38-30	Male
N.W. Eifuku, Golden Lips	December 14, 2014	J799-mB38	38-31	N/a (frozen)
N.W. Eifuku, Golden Lips	December 14, 2014	J799-mB38	38-32	N/a (frozen)
N.W. Eifuku, Golden Lips	December 14, 2014	J799-mB38	38-33	N/a (frozen)
N.W. Eifuku, Golden Lips	December 14, 2014	J799-mB38	38-34	N/a (frozen)
N.W. Eifuku, Golden Lips	December 14, 2014	J799-mB38	38-35	N/a (frozen)
N.W. Eifuku, Golden Lips	December 14, 2014	J799-mB38	38-36	N/a (frozen)
N.W. Eifuku, Golden Lips	December 14, 2014	J799-mB38	38-37	N/a (frozen)
N.W. Eifuku, Golden Lips	December 14, 2014	J799-mB38	38-38	N/a (frozen)
N.W. Eifuku, Golden Lips	December 14, 2014	J799-mB38	38-39	N/a (frozen)
N.W. Eifuku, Golden Lips	December 14, 2014	J799-mB38	38-40	N/a (frozen)
N.W. Eifuku, Golden Lips	December 14, 2014	J799-mB38	38-41	N/a (frozen)
N.W. Eifuku, Golden Lips	December 14, 2014	J799-mB38	38-42	N/a (frozen)
N.W. Eifuku, Golden Lips	December 14, 2014	J799-mB38	38-43	N/a (frozen)
N.W. Eifuku, Golden Lips	December 14, 2014	J799-mB38	38-44	N/a (frozen)
N.W. Eifuku, Golden Lips	December 14, 2014	J799-mB38	38-45	N/a (frozen)

Golden Lips Reproductive Stages (Gametogenesis)

MALES		**FEMALES**	
Sample #	**Stage**	**Sample #**	**Stage**
38-30	6	38-27	4
38-3	4	38-8	4
38-17	3	38-7	4
38-24	3	38-1	3
38-4	4	38-26	3
38-5	3		
38-2	4		

Golden Lips Oocyte Circular Equivalent				
Sample 38-1	Sample 38-8	Sample 38-27	Sample 38-7	Sample 38-26
37.79	45.00	28.28	28.57	33.82
48.66	45.37	28.28	28.91	27.39
31.18	42.66	32.86	32.88	36.74
34.21	42.90	29.58	43.50	20.49
32.12	32.86	28.98	19.90	26.40
28.28	36.00	43.82	23.37	28.58
39.50	50.82	31.08	34.58	41.11
44.96	36.95	27.13	29.58	44.50
39.80	42.00	42.85	22.98	24.37
42.66	35.21	38.83	33.23	30.33
47.90	38.78	25.42	31.18	30.00
45.37	44.43	20.78	30.71	23.81
43.90	25.38	27.35	45.17	29.58
23.98	47.33	33.27	37.35	23.92
39.37	40.56	36.08	20.90	26.51
45.28	37.68	24.37	42.43	22.91
29.85	35.89	26.51	26.27	43.82
27.39	31.37	41.57	32.65	30.41
32.86	46.48	30.17	13.42	32.40
46.31	32.25	19.36	26.00	27.11
30.59	37.42	29.73	26.93	28.46
35.21	32.50	30.59	35.78	32.40
30.41	24.49	22.98	38.37	38.78
30.17	41.26	31.98	20.78	47.12
45.03	26.08	28.98	36.51	29.39
42.14	45.72	33.05	19.90	29.00
44.50	32.40	20.98	39.24	31.00
26.50	27.11	30.03	40.69	25.69
38.42	50.20	29.80	32.86	26.46
20.00	36.22	29.58	26.40	32.45
38.79	45.44	27.28	30.59	34.29
45.17	29.39	24.66	28.72	28.28
34.64	38.83	18.76	39.24	25.69
39.24	34.99	28.37	32.65	26.72
41.95	32.03	46.48	23.24	34.86
39.24	27.55	29.39	24.49	31.81
22.36	39.24	40.40	22.91	28.98
25.46	48.37	27.71	33.82	31.08
22.36	26.27	26.00	34.41	33.17

39.60	41.67	39.38	26.00	30.59
34.70	43.43	24.90	47.12	30.76
38.24	48.44	22.65	32.40	23.98
33.41	43.44	40.21	33.44	30.17
47.33	40.00	27.75	37.95	20.98
40.40	26.94	25.46	30.40	32.86
56.23	39.60	33.05	27.57	38.73
31.18	27.11	32.31	33.00	32.94
48.99	39.50	29.50	28.84	38.26
40.62	27.46	28.98	26.83	42.40
22.65	34.21	30.33	21.00	32.86
30.85	41.57	34.29	38.08	22.05
33.91	36.22	27.11	43.01	28.28
42.77	47.83	21.35	22.05	28.28
25.10	35.21	29.58	27.50	32.76
47.37	19.97	32.86	41.83	25.50
22.80	36.74	25.26	26.46	27.00
45.17	36.93	33.50	37.04	33.47
28.57	48.93	30.59	25.92	30.50
28.84	34.77	39.99	24.92	25.98
40.99	37.55	28.00	31.62	36.00
27.93	21.42	37.95	20.49	32.79
35.50	37.95	27.39	33.47	30.17
44.88	43.44	23.92	32.50	30.59
36.74	28.77	28.84	36.00	34.64
36.12	22.27	36.47	35.50	22.91
34.00	35.00	35.50	42.66	21.21
43.86	35.10	26.93	31.18	20.78
36.51	34.96	28.00	31.46	31.75
28.25	42.45	23.00	37.47	24.49
35.50	49.60	41.95	24.68	28.57
27.28	48.54	40.12	30.71	36.22
40.56	36.50	23.07	39.12	22.98
28.72	36.33	32.40	31.86	29.22
43.50	25.30	24.08	29.85	27.93
26.83	41.47	30.00	30.85	37.95
29.39	47.73	32.50	26.70	26.08
38.57	37.76	24.45	30.17	43.75
44.67	29.58	22.80	40.25	40.12
36.00	32.86	39.95	30.85	23.24
38.17	43.59	34.90	28.77	25.00
37.47	36.33	43.82	35.78	40.69
42.43	42.06	21.35	38.54	35.50

26.32	38.46	24.45	32.86	24.82
51.44	47.96	24.68	38.97	30.94
35.07	44.12	26.50	44.90	42.85
52.80	44.89	35.94	45.61	29.29
28.14	40.95	21.98	41.41	25.00
45.72	40.56	21.79	27.35	31.50
43.99	46.73	33.63	46.04	38.88
34.00	28.93	33.47	28.46	28.72
34.64	34.21	26.50	24.08	37.82
25.30	36.88	29.85	35.33	30.17
33.99	29.80	22.80	22.80	44.27
39.12	36.33	27.46	33.47	27.50
28.28	48.06	30.50	35.99	28.28
47.96	40.80	35.21	43.01	21.21
31.43	44.02	24.37	43.27	24.39
20.62	43.43	31.75	40.21	28.98
51.03	19.08	20.49	38.00	28.46
55.00	40.00	20.78	32.94	27.11
47.90	34.48	22.98	26.46	23.66
36.66	31.75	23.07	24.98	22.05
28.91	34.94	29.46	30.98	38.95
44.70	40.99	35.47	42.36	30.00
21.79	40.25	26.72	34.50	32.40
39.55	40.56	35.99	30.66	24.49
45.90	29.29	27.71	24.39	35.99
36.37	35.65	39.37	43.87	27.93
29.39	38.34	42.90	29.00	50.62
45.83	43.82	29.33	34.99	26.46
25.81	35.72	32.45	31.40	32.40
25.92	40.91	43.24	20.15	24.27
25.10	34.58	22.23	41.23	23.32
24.49	33.44	26.32	39.24	24.33
32.16	43.47	32.86	36.41	26.08
35.00	37.95	26.93	16.31	37.50
18.71	35.41	24.00	31.46	26.00
32.86	44.50	27.22	31.62	37.09
54.00	45.37	34.07	43.44	33.87
24.68	41.42	30.71	25.10	29.29

Golden Lips Sample Number	Shell Length (mm)	Shell Height (mm)	Shell Width (mm)	Shell Volume (mL) *both valves	Shell Weight (g) *both valves	Body Wet Weight (g)
38-1	110.0	53.0	17.0	136	12.98	52.31
38-2	112.0	47.0	19.8	154	15.54	45.93
38-3	124.0	50.0	24.0	184	16.88	51.76
38-4	91.0	42.0	16.0	74	11.88	25.76
38-5	84.7	38.4	15.0	72	11.76	26.32
38-6	119.5	53.0	20.0	188	11.26	53.97
38-7	106.6	48.5	18.0	126	14.22	50.99
38-8	124.5	54.0	19.0	186	15.50	55.55
38-9	106.0	48.5	16.0	128	13.68	26.16
38-10	108.5	46.0	15.5	116	11.34	37.73
38-11	118.0	48.0	20.0	176	12.92	52.74
38-12	103.0	46.7	17.2	114	10.46	52.27
38-13	105.5	47.0	17.0	126	14.10	44.65
38-14	110.0	49.0	12.0	132	12.78	43.11
38-15	119.0	49.5	15.0	132	13.16	47.82
38-16	114.0	53.5	19.5	164	18.56	54.42
38-17	122.0	50.0	22.0	174	18.80	58.90
38-18	120.5	47.8	18.7	152	15.42	54.09
38-19	98.8	43.0	12.0	106	7.00	36.80
38-20	78.5	35.0	12.5	54	10.02	21.69
38-21	110.5	50.5	19.0	144	16.62	48.99
38-22	120.5	48.5	20.0	160	16.58	60.51
38-23	103.0	48.5	17.0	130	17.92	44.24
38-24	102.0	45.0	20.5	124	9.34	50.93
38-25	113.0	50.5	19.0	162	15.32	61.04
38-26	122.5	50.0	21.9	190	19.42	48.89
38-27	93.0	41.9	15.0	90	12.16	27.72
38-28	119.5	51.0	22.0	178	19.44	62.18
38-29	117.0	50.0	19.0	150	18.10	N/a
38-30	98.0	44.0	17.0	106	8.60	29.60
38-31	100	42.0	20.0	118	10.86	N/a
38-32	111	50.0	18.0	126	14.42	38.27
38-33	69	33.0	8.9	36	4.26	40.39
38-34	119	47.0	16.0	132	16.54	12.77
38-35	113	48.0	21.0	164	14.94	45.03
38-36	116	50.0	21.0	168	12.40	42.63
38-37	107	48.6	17.0	116	14.76	46.30
38-38	124	52.5	21.0	176	18.44	36.02

38-39	113	52.8	18.5	134	16.16	45.98
38-40	128.9	51.8	21.0	196	21.84	46.12
38-41	104	51.0	16.9	118	14.08	68.78
38-42	100	45.5	14.6	100	12.14	38.06
38-43	124	56.0	20.2	190	19.34	35.53
38-44	105.5	49.5	15.0	112	13.86	60.03
38-45	85.5	40.0	12.8	70	8.18	37.67

Golden Lips Sample Number	Gill Dry Weight (g)	Total Body Dry Weight (g)	Gill Ash Weight (g)	Total Body Ash Weight (g)	Gill Condition Index	Total Body Condition Index	% Water Weight
36-2	1.9956	10.6389	0.1524	0.5591	0.0091	0.0499	86.6697
36-4	0.6673	3.5383	0.0395	0.2260	0.0095	0.0502	89.4411
36-5	0.3332	1.5775	0.0284	0.1197	0.0109	0.0521	90.1097
36-6	1.2659	5.2464	0.0777	0.4029	0.0108	0.0440	89.7870
36-9	1.1130	4.4685	0.0725	0.2257	0.0106	0.0433	88.8343
36-13	0.9797	4.3551	0.0731	0.2304	0.0116	0.0529	87.4348
36-14	0.8310	4.0068	0.0676	0.2369	0.0116	0.0571	86.7060
36-17	1.1592	5.0894	0.0678	0.2294	0.0079	0.0352	90.1292
38-19	0.5353	2.4424	0.0422	0.1857	0.0117	0.0537	92.8101
36-20	0.4435	1.9442	0.0310	0.1395	0.0103	0.0451	91.1061
36-21	0.5796	3.2030	0.0394	0.2266	0.0054	0.0298	93.0460
36-22	1.2686	4.6045	0.1319	0.3562	0.0084	0.0312	91.0955

Near Fouling Data

Location and Site	Date of Collection	Dive	Sample Number	Sex (m/f)
N.W. Eifuku, Near Fouling	April 10, 2004	R792-J178	1	Male
N.W. Eifuku, Near Fouling	April 10, 2004	R792-J178	2	Female
N.W. Eifuku, Near Fouling	April 10, 2004	R792-J178	3	Female
N.W. Eifuku, Near Fouling	April 10, 2004	R792-J178	4	Male
N.W. Eifuku, Near Fouling	April 10, 2004	R792-J178	5	Male
N.W. Eifuku, Near Fouling	April 10, 2004	R792-J178	6	Female
N.W. Eifuku, Near Fouling	April 10, 2004	R792-J178	7	Female
N.W. Eifuku, Near Fouling	April 10, 2004	R792-J178	8	Male
N.W. Eifuku, Near Fouling	April 10, 2004	R792-J178	9	Female
N.W. Eifuku, Near Fouling	April 10, 2004	R792-J178	10	Female

N.W. Eifuku, Near Fouling	April 10, 2004	R792-J178	11	Male
N.W. Eifuku, Near Fouling	April 10, 2004	R792-J178	12	Female
N.W. Eifuku, Near Fouling	April 10, 2004	R792-J178	13	Female
N.W. Eifuku, Near Fouling	April 10, 2004	R792-J178	14	Female
N.W. Eifuku, Near Fouling	April 10, 2004	R792-J178	15	Male
N.W. Eifuku, Near Fouling	April 10, 2004	R792-J178	16	Female
N.W. Eifuku, Near Fouling	April 10, 2004	R792-J178	17	Female
N.W. Eifuku, Near Fouling	April 10, 2004	R792-J178	18	Female
N.W. Eifuku, Near Fouling	April 10, 2004	R792-J178	19	Female
N.W. Eifuku, Near Fouling	April 10, 2004	R792-J178	20	Female
N.W. Eifuku, Near Fouling	April 10, 2004	R792-J178	21	Female
N.W. Eifuku, Near Fouling	April 10, 2004	R792-J178	22	Female
N.W. Eifuku, Near Fouling	April 10, 2004	R792-J178	23	Female
N.W. Eifuku, Near Fouling	April 10, 2004	R792-J178	24	Female
N.W. Eifuku, Near Fouling	April 10, 2004	R792-J178	25	Female
N.W. Eifuku, Near Fouling	April 10, 2004	R792-J178	26	Female
N.W. Eifuku, Near Fouling	April 10, 2004	R792-J178	27	Female
N.W. Eifuku, Near Fouling	April 10, 2004	R792-J178	28	Female
N.W. Eifuku, Near Fouling	April 10, 2004	R792-J178	29	Female
N.W. Eifuku, Near Fouling	April 10, 2004	R792-J178	30	Female
N.W. Eifuku, Near Fouling	April 12, 2004	R793-J199	*No label 1*	Male

Near Fouling Reproductive Stages (Gametogenesis)			
MALES		**FEMALES**	
Sample #	**Stage**	**Sample #**	**Stage**
15	3	10	3
1	3	9	3
4	2	7	2
8	3	2	3
11	2	3	2
No label 1	3	6	2

Near Fouling Oocyte Circular Equivalents					
Sample 2	Sample 3	Sample 6	Sample 7	Sample 9	Sample 10
39.80	25.92	45.17	37.79	55.48	43.71
32.47	34.06	35.94	22.76	38.47	41.13
31.94	28.28	25.00	33.63	40.42	37.09
38.73	40.66	27.75	32.31	36.28	23.45

24.49	22.63	40.62	39.89	38.00	40.62
29.39	22.98	29.33	39.42	28.98	27.28
41.35	27.96	35.67	39.12	30.40	34.32
29.58	29.80	30.98	25.50	38.68	27.84
51.77	25.79	31.37	35.99	23.69	32.00
38.73	26.50	24.04	26.38	40.00	39.57
29.66	40.31	31.62	42.90	33.91	5.74
30.85	35.21	17.89	33.54	33.94	38.34
30.85	37.95	31.30	33.32	41.67	21.91
39.42	33.88	33.32	27.71	27.50	34.47
25.69	39.17	42.78	34.00	35.57	28.98
29.24	29.56	21.45	27.98	26.46	26.46
37.95	26.93	31.18	40.35	29.29	21.02
25.69	29.33	33.50	28.53	37.67	37.15
26.83	33.32	26.27	34.00	39.42	28.39
26.83	40.25	27.57	35.72	35.07	41.23
37.15	43.71	41.70	30.41	29.15	36.41
33.47	32.86	35.78	22.45	27.96	28.46
26.27	30.30	36.06	29.66	27.22	36.78
34.21	25.69	24.25	28.50	38.11	34.87
28.14	34.64	23.45	30.59	32.40	28.93
31.62	30.05	30.41	40.12	31.00	28.14
38.34	30.59	28.14	37.55	34.47	22.98
31.84	38.88	29.58	27.11	42.58	36.66
30.00	35.78	39.69	42.06	31.22	27.39
29.58	28.77	39.55	32.86	37.47	34.21
34.06	31.62	40.89	30.59	32.86	35.24
44.16	32.50	33.00	27.13	23.37	41.23
37.42	44.16	27.87	40.95	21.79	42.33
31.22	28.28	35.36	31.84	31.84	31.94
31.62	30.82	30.00	38.88	34.25	29.80
20.12	31.45	43.90	36.74	35.21	38.08
41.82	32.88	37.88	32.86	43.36	31.75
32.94	29.39	23.87	42.71	44.72	38.37
37.82	35.36	28.64	37.42	45.17	18.44
32.56	25.92	26.72	37.04	37.42	33.87
20.49	28.00	42.43	29.50	36.33	43.82
33.17	30.41	30.94	45.44	35.87	36.78
26.70	20.40	33.87	34.86	40.40	40.00
35.50	35.33	30.00	36.12	21.42	37.15
39.80	30.00	34.25	37.52	36.66	27.20
44.27	30.66	33.05	37.95	31.94	21.79
35.67	37.15	30.59	29.85	37.95	34.50

19.77	29.95	33.27	25.69	46.48	39.95
37.23	39.24	30.00	35.33	36.33	30.40
19.08	25.46	30.98	38.34	27.71	38.08
29.29	32.62	41.42	44.27	27.11	38.54
22.91	39.57	33.99	24.08	26.38	20.45
25.10	35.24	26.72	30.30	45.73	30.33
25.98	31.46	31.94	42.81	30.00	42.90
28.72	33.47	46.73	27.96	25.38	43.59
26.32	41.13	36.74	39.50	41.13	35.87
33.76	28.84	39.89	34.48	39.12	23.92
34.58	41.35	26.83	31.40	26.50	27.28
26.12	34.29	33.57	39.00	38.79	28.84
34.21	49.80	32.65	35.33	37.09	26.83
36.08	25.30	27.93	42.71	35.94	36.74
24.45	35.24	25.83	27.57	35.87	24.49
38.54	26.46	36.06	33.41	29.15	32.86
28.14	27.04	33.32	30.98	35.62	33.99
27.39	29.66	33.47	30.94	42.36	39.12
37.88	41.23	44.09	34.99	40.12	40.35
22.80	20.07	39.12	23.56	26.83	33.94
37.08	33.67	42.90	38.78	40.95	37.76
40.12	34.96	23.62	40.99	30.71	21.45
27.11	26.83	23.32	44.43	38.37	41.95
32.40	30.30	21.91	38.99	32.45	38.52
31.81	34.07	34.99	30.74	30.82	27.75
30.98	35.50	26.12	31.94	47.43	39.89
25.08	28.64	26.50	36.88	41.83	35.00
24.74	30.00	42.58	34.99	38.68	26.27
24.08	35.92	47.35	35.50	25.98	30.40
27.39	44.02	30.46	37.00	31.75	33.50
31.61	34.41	37.52	27.93	41.41	26.87
36.33	27.98	36.84	35.69	34.96	30.33
38.73	26.87	35.65	24.39	28.28	39.12
41.42	32.03	32.03	32.25	35.92	32.65
34.07	35.50	36.52	30.41	42.43	39.97
30.17	34.29	21.91	34.47	27.39	35.89
22.20	36.00	28.14	37.95	36.37	27.13
37.15	37.15	35.50	33.23	25.98	31.30
26.27	31.30	28.46	34.77	37.42	31.22
30.74	35.41	48.37	42.21	48.54	41.57
51.96	25.42	28.64	33.47	38.68	46.28
24.66	42.33	35.87	30.41	32.65	20.20
27.98	33.91	34.64	35.50	32.76	30.94

26.27	34.58	38.34	33.76	29.50	25.26
33.76	25.30	25.81	34.48	32.03	34.32
28.14	28.98	34.06	41.83	14.07	35.47
47.70	31.61	35.94	28.28	46.73	33.88
29.85	38.34	46.48	33.63	34.21	39.89
24.49	33.91	25.10	27.71	27.46	26.72
25.10	28.46	44.88	36.78	41.81	35.78
45.17	39.37	35.21	30.30	39.76	39.94
31.46	29.33	27.39	42.21	39.80	39.12
39.12	29.56	27.84	31.22	26.83	25.83
35.10	32.31	26.83	38.68	30.17	29.66
27.50	24.49	46.13	32.86	28.57	30.17
25.69	26.83	46.28	31.40	42.60	34.21
35.10	29.66	39.57	39.42	26.53	33.17
24.90	27.96	32.86	27.55	32.62	24.49
40.00	28.98	24.49	30.50	25.10	25.83
35.33	34.58	26.46	36.88	36.74	39.12
30.00	29.95	37.00	32.76	32.76	33.47
27.13	29.93	23.32	29.46	40.62	28.84
24.49	39.50	26.83	23.47	42.60	27.96
48.17	34.48	29.15	44.50	30.17	30.94
26.46	25.50	32.98	38.34	40.95	38.68
32.12	36.88	43.50	36.08	33.32	21.56
25.38	36.74	24.49	31.40	30.41	31.18
28.28	37.76	21.42	26.94	40.62	27.93
34.48	21.02	23.98	40.35	28.39	26.50
37.42	33.44	33.17	42.25	26.93	34.64
28.72	32.17	27.87	51.77	35.50	33.32
33.67	30.41	37.09	23.66	42.90	26.83
28.14	32.25	25.79	36.06	37.34	36.28

Near Fouling Sample Number	Shell Length (mm)	Shell Height (mm)	Shell Width (mm)	Shell Volume (mL) *both valves	Shell Weight (g) *both valves
1	87.0	38.0	21.0	N/a	N/a
2	N/a	N/a	N/a	N/a	N/a
3	126.0	53.0	27.0	N/a	N/a
4	119.0	52.0	24.0	N/a	N/a
5	N/a	N/a	N/a	N/a	N/a
6	133.0	52.0	27.0	200	24.86
7	136.0	49.5	23.0	N/a	N/a

8	157.0	59.0	30.0	N/a	N/a
9	125.0	51.0	24.0	N/a	N/a
10	N/a	N/a	N/a	N/a	N/a
11	149.0	64.0	28.5	N/a	N/a
12	123.0	49.0	22.0	138	19.14
13	134.5	57.0	23.5	N/a	N/a
14	146.0	52.0	24.0	222	27.65
15	120.0	51.0	25.5	N/a	N/a
16	101.0	42.0	20.0	84	10.51
17	125.0	41.0	24.5	142	18.40
18	121.0	47.0	24.0	146	18.99
19	133.5	58.0	26.0	N/a	N/a
20	121.0	49.5	25.0	154	19.32
21	129.0	46.0	23.5	156	21.80
22	133.0	54.5	25.0	164	20.50
23	114.0	46.0	22.5	112	16.13
24	131.0	53.0	25.0	168	21.71
25	146.0	57.5	30.5	248	32.08
26	134.0	56.0	21.0	N/a	N/a
27	130.0	54.5	25.0	N/a	N/a
28	123.0	47.0	27.0	158	21.38
29	85.0	37.0	16.0	50	7.32
30	84.0	36.5	15.5	56	8.92
No label 1	29.0	15.0	8.0	N/a	N/a

Near Fouling Sample Number	Gill Dry Weight (g)	Total Body Dry Weight (g)	Gill Ash Weight (g)	Total Body Ash Weight (g)	Gill Condition Index	Total Body Condition Index
6	1.8883	6.7954	0.1522	0.4231	0.0087	0.0319
12	1.4973	5.9835	0.1032	0.3142	0.0101	0.0411
14	1.9400	8.8441	0.1411	0.5488	0.0081	0.0374
16	0.8292	4.0199	0.0519	0.1883	0.0093	0.0456
17	1.5090	5.2978	0.1151	0.3334	0.0098	0.0350
18	1.4454	7.0730	0.0925	0.3828	0.0093	0.0458
20	0.9910	4.9322	0.1128	0.3292	0.0057	0.0299
21	1.3890	6.3528	0.1206	0.4218	0.0081	0.0380
22	1.7323	7.0020	0.1191	0.5042	0.0098	0.0396
23	1.2938	6.1773	0.0962	0.3390	0.0107	0.0521
24	1.2107	6.7509	0.0851	0.3306	0.0067	0.0382
25	2.1833	11.0916	0.1558	0.6768	0.0082	0.0420
28	1.6453	6.8877	0.0993	0.3512	0.0097	0.0414

29	0.4457	2.7698	0.0265	0.1026	0.0084	0.0533
30	0.5197	3.0312	0.0367	0.1632	0.0086	0.0512

Nifonea Data

Location and Site	Date of Collection	Dive	Sample Number	Sex (m/f)	Parasites in Body Cavity
Nifonea, Vanuatu	July 22, 2013	SO229-060-06-01	1	Female	No
Nifonea, Vanuatu	July 22, 2013	SO229-060-06-01	2	Male	No
Nifonea, Vanuatu	July 22, 2013	SO229-077-01-01	3	Male	Yes
Nifonea, Vanuatu	July 22, 2013	SO229-077-01-01	4	Male	Yes
Nifonea, Vanuatu	July 22, 2013	SO229-077-01-01	5	Female	Yes
Nifonea, Vanuatu	July 22, 2013	SO229-077-01-01	6	Female	Yes
Nifonea, Vanuatu	July 22, 2013	SO229-077-01-01	7	Male	Yes
Nifonea, Vanuatu	July 22, 2013	SO229-077-01-01	8	Female	No
Nifonea, Vanuatu	July 22, 2013	SO229-077-01-01	9	Female	No
Nifonea, Vanuatu	July 22, 2013	SO229-077-01-01	10	Male	Yes
Nifonea, Vanuatu	July 22, 2013	SO229-077-01-01	11	Female	No
Nifonea, Vanuatu	July 22, 2013	SO229-077-01-01	12	Male	Yes
Nifonea, Vanuatu	July 22, 2013	SO229-077-01-01	13	Female	No
Nifonea, Vanuatu	July 22, 2013	SO229-027-06-01	14	Female	Yes
Nifonea, Vanuatu	July 22, 2013	SO229-027-06-01	15	Male	No
Nifonea, Vanuatu	July 22, 2013	SO229-027-06-01	16	Female	Yes
Nifonea, Vanuatu	July 22, 2013	SO229-027-06-01	17	Female	Yes
Nifonea, Vanuatu	July 22, 2013	SO229-027-06-01	18	Male	Yes
Nifonea, Vanuatu	July 22, 2013	SO229-027-06-01	19	Male	No
Nifonea, Vanuatu	July 22, 2013	SO229-027-06-01	20	Female	No
Nifonea, Vanuatu	July 22, 2013	SO229-027-06-01	21	Female	Yes
Nifonea, Vanuatu	July 22, 2013	SO229-027-06-01	22	Male	No
Nifonea, Vanuatu	July 22, 2013	SO229-027-06-01	23	Male	Yes

Nifonea Sample Number	Shell Length (mm)	Shell Height (mm)	Shell Width (mm)	Shell Volume (mL) *both valves	Shell Weight (g) *both valves
1	94.5	45.0	19.0	N/a	N/a
2	117.0	58.0	24.0	N/a	N/a
3	88.0	40.5	16.0	68	16.54
4	87.5	41.5	18.0	70	17.20
5	114.0	56.0	21.0	146	33.09

6	105.0	53.5	21.5	124	22.55
7	87.0	42.0	15.0	64	16.84
8	123.5	55.5	22.5	182	36.68
9	101.0	47.0	18.5	94	22.36
10	120.5	68.0	21.0	168	35.59
11	101.5	54.0	20.0	100	24.27
12	114.0	61.0	22.0	164	32.67
13	100.0	51.0	19.3	N/a	N/a
14	137.0	60.0	24.5	218	43.44
15	135.0	64.0	26.0	210	44.02
16	123.0	61.5	25.0	N/a	N/a
17	113.5	52.0	25.3	138	29.96
18	119.0	56.5	24.0	N/a	N/a
19	91.0	41.5	40.0	N/a	N/a
20	113.0	52.0	20.5	130	26.42
21	125.5	59.0	23.0	154	35.42

Nifonea Sample Number	**Gill Dry Weight (g)**	**Total Body Dry Weight (g)**	**Gill Ash Weight (g)**	**Total Body Ash Weight (g)**	**Gill Condition Index**	**Total Body Condition Index**
3	0.8529	4.4837	0.0542	0.2460	0.0117	0.0623
4	0.6258	3.1895	0.0459	0.2064	0.0083	0.0426
5	1.5224	8.8741	0.1020	0.3961	0.0097	0.0581
6	0.7671	4.0647	0.0508	0.2156	0.0058	0.0310
7	0.6668	3.8926	0.0452	0.2501	0.0097	0.0569
8	1.8311	8.4325	0.1160	0.3827	0.0094	0.0442
9	0.8876	3.9576	0.0664	0.2242	0.0087	0.0397
10	0.9158	7.0433	0.0668	0.4071	0.0051	0.0395
11	0.6674	3.4080	0.0405	0.1674	0.0063	0.0324
12	0.8833	5.5411	0.0527	0.3570	0.0051	0.0316
14	2.0866	12.7829	0.1673	0.6129	0.0088	0.0558
15	1.5662	11.0624	0.1245	0.4288	0.0069	0.0506
17	1.1318	5.9157	0.1027	0.3783	0.0075	0.0401
20	1.1422	4.8281	0.0766	0.2588	0.0082	0.0351
21	1.1629	9.9057	0.0864	0.6638	0.0070	0.0600

Lau Basin Data

Location and Site	Date of Collection	Dive	Sample Number	Depth (m)	Sex (m/f)
TM1, Tui Malila, Lau Basin	22-Apr-16	1928-5	1	1888	Male
TM1, Tui Malila, Lau Basin	22-Apr-16	1928-5	2	1888	Male
TM1, Tui Malila, Lau Basin	22-Apr-16	1928-5	3	1888	Male
TM1, Tui Malila, Lau Basin	22-Apr-16	1928-5	4	1888	Male
TM1, Tui Malila, Lau Basin	22-Apr-16	1928-5	5	1888	Male
ABE, Lau Basin	26-Apr-16	1931	46	2130	Hermaphrodite/male
ABE, Lau Basin	26-Apr-16	1931	40	2130	Hermaphrodite/male
ABE, Lau Basin	26-Apr-16	1931	32	2130	Female
ABE, Lau Basin	26-Apr-16	1931	44	2130	Female
ABE, Lau Basin	26-Apr-16	1931	34	2130	Male
ABE, Lau Basin	26-Apr-16	1931	29	2130	Male
ABE, Lau Basin	26-Apr-16	1931	38	2130	Male
ABE, Lau Basin	26-Apr-16	1931	43	2130	Male
ABE, Lau Basin	26-Apr-16	1931	37	2130	Male
ABE, Lau Basin	26-Apr-16	1931	35	2130	Hermaphrodite/male
ABE, Lau Basin	26-Apr-16	1931	31	2130	Hermaphrodite/male
ABE, Lau Basin	26-Apr-16	1931	47	2130	Male
ABE, Lau Basin	26-Apr-16	1931	50	2130	Male
ABE, Lau Basin	26-Apr-16	1931	28	2130	Male
ABE, Lau Basin	26-Apr-16	1931	49	2130	Male

ABE Reproductive Stages (Gametogenesis)

MALES		FEMALES	
Sample #	**Stage**	**Sample #**	**Stage**
38	2	32	2
50	2	44	3
3	3		
28	3		
37	3		
29	1		

ABE Oocyte Circular Equivalents	
Sample 32	Sample 44
26.46	10.95
34.47	46.48
20.07	39.89
28.72	37.50
42.85	7.94
35.36	21.98
28.46	32.79
36.99	14.83
53.67	18.03
35.50	35.89
49.60	37.35
35.24	31.11
34.77	30.17
16.88	32.17
19.44	31.46
46.00	46.50
35.99	27.98
19.05	44.50
27.75	53.10
31.46	35.10
24.37	27.93
28.53	23.69
20.00	12.85
25.50	22.36
19.90	28.72
50.20	33.47
48.63	33.32
23.66	29.24
28.98	23.24
18.76	25.04
42.25	34.77
30.00	18.44
19.34	19.90
42.66	43.47
37.42	44.67
29.85	33.94
28.62	36.33
22.80	24.08
21.49	41.83

16.31	30.59
39.50	37.95
18.76	33.05
46.90	36.00
41.42	40.89
29.50	34.50
8.77	30.40
18.44	24.49
51.38	32.40
34.47	26.15
49.44	24.00
33.05	25.98
32.12	26.00
20.17	34.21
16.73	30.50
43.87	29.50
39.47	21.42
18.11	29.50
40.25	10.49
35.50	21.21
26.12	41.50
31.45	39.42
26.27	38.34
35.87	31.62
45.28	20.49
28.28	38.73
31.62	43.43
25.51	21.91
29.56	23.49
28.72	28.72
32.17	37.42
35.07	20.49
25.69	33.91
28.98	24.45
36.92	34.47
24.37	38.52
34.90	24.25
37.15	22.23
29.46	44.90
14.83	32.86
26.32	20.49
12.85	37.47
37.95	25.04

45.48	33.32
31.46	23.87
34.90	36.12
30.50	30.17
16.88	37.50
18.44	24.08
9.54	28.28
9.95	27.35
36.37	49.44
41.67	18.89
42.58	32.86
22.36	23.24
21.35	43.47
25.51	28.50
28.00	13.42
32.86	41.18
21.49	29.93
28.98	28.91
25.30	21.49
45.83	45.92
42.58	44.50
42.43	23.98
10.00	19.34
23.87	36.33
14.28	43.44
38.95	21.98
40.00	12.49
22.49	32.45
21.49	19.97
30.98	38.47
50.30	32.86
35.99	25.08
22.58	42.95
42.99	44.09
45.48	20.78
37.09	12.41
16.61	21.21
14.49	13.96

ABE Sample Number	Shell Length (mm)	Shell Height (mm)	Shell Width (mm)	Shell Volume (mL) *both valves	Shell Weight (g) *both valves
1	59.5	33.0	11.0	24	4.55
2	76.0	40.0	16.0	52	8.97
3	72.0	43.0	14.0	54	8.06
4	57.0	33.5	11.0	22	4.77
5	43.0	24.5	8.0	10	3.25
46	101.5	48.5	119.0	104	12.74
40	101.0	50.5	50.0	112	13.08
32	88.5	45.0	18.0	86	10.83
44	94.5	49.0	18.5	92	11.47
34	97.5	49.0	18.5	88	11.01
29	96.5	48.0	18.0	94	11.62
38	116.0	56.0	23.5	150	16.31
43	82.0	45.0	15.0	54	9.11
37	108.0	53.0	21.5	114	15.34
35	85.0	40.5	17.0	62	8.14
31	81.5	41.0	18.0	64	11.50
47	N/a	N/a	N/a	N/a	N/a
50	86.0	44.0	16.5	70	10.15
28	106.0	56.0	20.0	132	17.30
49	94.0	45.5	16.5	78	11.53

ABE Sample Number	Gill Dry Weight (g)	Total Body Dry Weight (g)	Gill Ash Weight (g)	Total Body Ash Weight (g)	Gill Condition Index	Total Body Condition Index
40	0.6604	3.3972	0.0838	0.3309	0.0051	0.0274
34	0.7553	4.1769	0.0760	0.3866	0.0077	0.0431
29	0.5840	4.2987	0.0678	0.3057	0.0055	0.0425
43	0.3793	2.5933	0.0524	0.3649	0.0061	0.0413
37	0.7047	3.7172	0.0928	0.6485	0.0054	0.0269
35	0.4826	2.7150	0.0660	0.2926	0.0067	0.0391
50	0.3281	2.3918	0.0481	0.2444	0.0040	0.0307
28	0.7166	3.7182	0.0919	0.3249	0.0047	0.0257
49	0.4429	2.6602	0.0696	0.3158	0.0048	0.0301